UDK 621.3:(53+54+621+66)(05)(497.1)=00 ISSN 0352-9045

INFORMACIJE MIDEM 4 ○ 2000

Strokovno društvo za mikroelektroniko elektronske sestavne dele in materiale

Strokovna revija za mikroelektroniko, elektronske sestavne dele in materiale
Journal of Microelectronics, Electronic Components and Materials

INFORMACIJE MIDEM, LETNIK 30, ŠT. 4(96), LJUBLJANA, december 2000

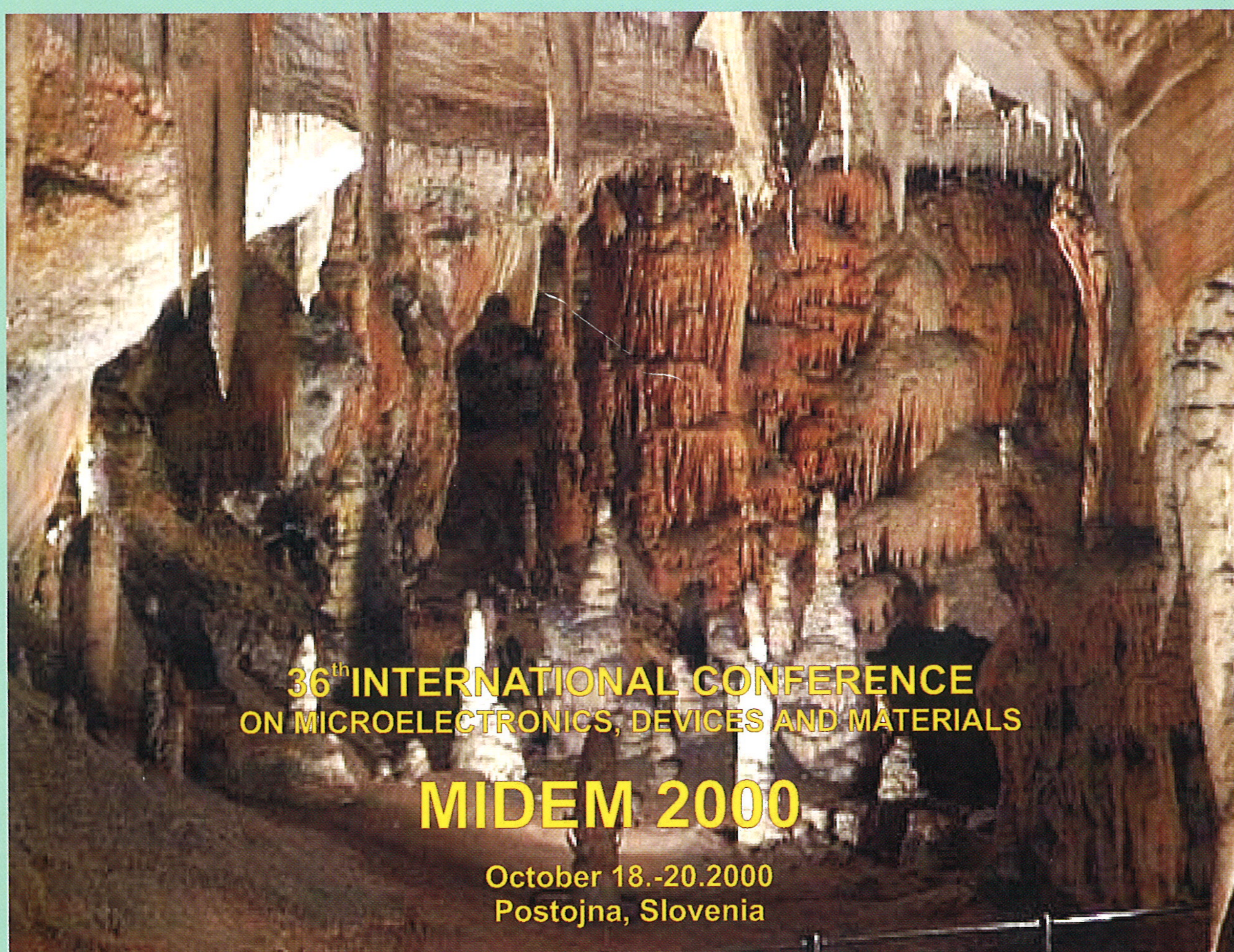

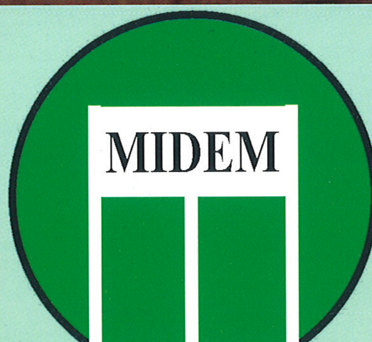

DRUŠTVO-SOCIETY

Slovenia Chapter

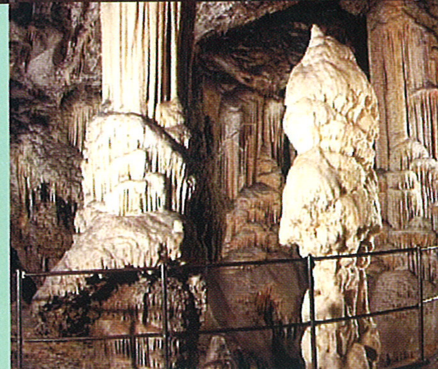

UDK 621.3:(53+54+621+66)(05)(497.1)=00 ISSN 0352-9045

INFORMACIJE **MIDEM** 4 ○ 2000

INFORMACIJE MIDEM LETNIK 30, ŠT. 4(96), LJUBLJANA, DECEMBER 2000

INFORMACIJE MIDEM VOLUME 30, NO. 4(96), LJUBLJANA, DECEMBER 2000

Revija izhaja trimesečno (marec, junij, september, december). Izdaja strokovno društvo za mikroelektroniko, elektronske sestavne dele in materiale - MIDEM.
Published quarterly (march, june, september, december) by Society for Microelectronics, Electronic Components and Materials - MIDEM.

Glavni in odgovorni urednik
Editor in Chief
Dr. Iztok Šorli, dipl.ing.,
MIKROIKS d.o.o., Ljubljana

Tehnični urednik
Executive Editor
Dr. Iztok Šorli, dipl.ing.,
MIKROIKS d.o.o., Ljubljana

Uredniški odbor
Editorial Board
Doc. dr. Rudi Babič, dipl.ing., Fakulteta za elektrotehniko, računalništvo in informatiko Maribor
Dr.Rudi Ročak, dipl.ing., MIKROIKS d.o.o., Ljubljana
mag.Milan Slokan, dipl.ing., MIDEM, Ljubljana
Zlatko Bele, dipl.ing., MIKROIKS d.o.o., Ljubljana
Dr. Wolfgang Pribyl, Austria Mikro Systeme International AG, Unterpremstaetten
mag. Meta Limpel, dipl.ing., MIDEM, Ljubljana
Miloš Kogovšek, dipl.ing., Ljubljana
Prof. Dr. Marija Kosec, dipl. ing., Inštitut Jožef Stefan, Ljubljana

Časopisni svet
International Advisory Board
Prof. dr. Slavko Amon, dipl.ing., Fakulteta za elektrotehniko, Ljubljana,
PREDSEDNIK - PRESIDENT
Prof. dr. Cor Claeys, IMEC, Leuven
Dr. Jean-Marie Haussonne, EIC-LUSAC, Octeville
Dr. Marko Hrovat, dipl.ing., Inštitut Jožef Stefan, Ljubljana
Prof. dr. Zvonko Fazarinc, dipl.ing., CIS, Stanford University, Stanford
† Prof. dr. Drago Kolar, dipl.ing., Inštitut Jožef Stefan, Ljubljana
Dr. Giorgio Randone, ITALTEL S.I.T. spa, Milano
Prof. dr. Stane Pejovnik, dipl.ing., Fakulteta za kemijo in kemijsko tehnologijo, Ljubljana
Dr. Giovanni Soncini, University of Trento, Trento
Prof.dr. Janez Trontelj, dipl.ing., Fakulteta za elektrotehniko, Ljubljana
Dr. Anton Zalar, dipl.ing., ITPO, Ljubljana
Dr. Peter Weissglas, Swedish Institute of Microelectronics, Stockholm

Naslov uredništva
Headquarters
Uredništvo Informacije MIDEM
Elektrotehniška zveza Slovenije
Dunajska 10, 1000 Ljubljana, Slovenija
tel.: + 386 (0)1 51 12 221
fax: + 386 (0)1 51 12 217
e-mail: Iztok.Sorli@guest.arnes.si
http://paris.fe.uni-lj.si/midem/journal.htm

Letna naročnina znaša 12.000,00 SIT, cena posamezne številke je 3000,00 SIT. Člani in sponzorji MIDEM prejemajo Informacije MIDEM brezplačno.
Annual subscription rate is DEM 200, separate issue is DEM 50. MIDEM members and Society sponsors receive Informacije MIDEM for free.

Znanstveni svet za tehnične vede I je podal pozitivno mnenje o reviji kot znanstveno strokovni reviji za mikroelektroniko, elektronske sestavne dele in materiale. Izdajo revije sofinanci rajo Ministrstvo za znanost in tehnologijo in sponzorji društva.
Scientific Council for Technical Sciences of Slovene Ministry of Science and Technology has recognized Informacije MIDEM as scientific Journal for microelectronics, electronic components and materials.
Publishing of the Journal is financed by Slovene Ministry of Science and Technology and by Society sponsors.

Znanstveno strokovne prispevke objavljene v Informacijah MIDEM zajemamo v podatkovne baze COBISS in INSPEC.

Prispevke iz revije zajema ISI® v naslednje svoje produkte: Sci Search®, Research Alert® in Materials Science Citation Index™

Scientific and professional papers published in Informacije MIDEM are assessed into COBISS and INSPEC databases.

The Journal is indexed by ISI® for Sci Search®, Research Alert® and Material Science Citation Index™

Po mnenju Ministrstva za informiranje št.23/300-92 šteje glasilo Informacije MIDEM med proizvode informativnega značaja.

Grafična priprava in tisk / Printed by: BIRO M, Ljubljana

Naklada / Circulation: 1000 izvodov / 1000 issues

Poštnina plačana pri pošti 1102 Ljubljana
Slovenia Taxe Percue

UDK621.3:(53+54+621+66), ISSN0352-9045 Informacije MIDEM 30(2000)4,Ljubljana

VSEBINA / CONTENT

ZNANSTVENO STROKOVNI PRISPEVKI		PROFESSIONAL SCIENTIFIC PAPERS
G.U. Pignatel, M. Boscardin, G.-F. Dalla Betta: Najnovejša dognanja pri razvoju silicijevih detektorjev sevanja v IRST	191	G.U. Pignatel, M. Boscardin, G.-F. Dalla Betta: Recent Developments in Silicon Radiation Detectors at IRST
P. Mach: Diagnosticiranje nelinearnosti tokovno-napetostne karakteristike - teorija in uporaba	199	P. Mach: Diagnostics of Nonlinearity of Current vs. Voltage Characteristics - Theory and Application
A.Zalar: Karakterizacija materialov z Augerjevo elektronsko spektroskopsko (AES) profilno analizo	203	A.Zalar: Materials Characterisation by Auger Electron Spectroscopy Sputter Depth Profiling
J.J. Hren, V.V. Zhirnov, Z. Sitar, G. Wojak: Vrednotenje dielektričnih materialov na merilnih konicah	210	J.J. Hren, V.V. Zhirnov, Z. Sitar, G. Wojak: Characterisation of Dielectrics on the "tips of needles"
H. Bender: Uporaba fokusiranega curka ionov pri analizi adpovedi	216	H. Bender: Application of Focused Ion Beam for Failure Analysis
I. Muševič: Mikroskopija na atomsko silo	223	I. Muševič: Atomic Force Microscopy
N. Daneu, A. Rečnik, S. Bernik: Uporaba metod elektronske mikroskopije za študij inverznih meja v varistorski keramiki na osnovi ZnO	228	N. Daneu, A. Rečnik, S. Bernik: The Application of Electron Microscopy methods in the Study of Inversion Boundaries in ZnO-Based Varistors
KONFERENCA MIDEM 2000 – POROČILO	233	**MIDEM 2000 CONFERENCE REPORT**
ZOISOVA PRIZNANJA		**ZOIS PRIZES**
MED LETOŠNJIMI PREJEMNIKI ZOISOVIH PRIZNANJ STA DVA ČLANA DRUŠTVA MIDEM	235	THIS YEAR'S ZOIS PRIZES WERE AWARDED TO TWO MIDEM MEMBERS
VESTI	237	**NEWS**
KOLEDAR PRIREDITEV	244	**CALENDAR OF EVENTS**
VSEBINA LETNIKA 2000	245	**VOLUME 2000 CONTENT**
MIDEM prijavnica	249	MIDEM Registration Form

Slika na naslovnici: Letošnja konferenca MIDEM 2000 se je odvijala v hotelu Jama v Postojni. Udeleženci konference so ob priložnosti lahko občudovali lepote Postojnske jame.

Front page: MIDEM 2000 Conference was held in hotel Jama, Postojna. One of the evenings, the participants were able to admire beauties of Postojna caves.

36th INTERNATIONAL CONFERENCE ON MICROELECTRONICS, DEVICES AND MATERIALS

and the WORKSHOP on

ANALYTICAL METHODS IN MICROELECTRONICS AND ELECTRONIC MATERIALS

CONFERENCE 2000

Slovenia Section

Slovenia Chapter

October 18. - 20. 2000
Hotel JAMA, Postojna, SLOVENIA

UDK621.3:(53+54+621+66), ISSN0352-9045 Informacije MIDEM 30(2000)4, Ljubljana

RECENT DEVELOPMENTS IN SILICON RADIATION DETECTORS AT IRST

G. U. Pignatel[a], M. Boscardin[b], G.-F. Dalla Betta[b]
[a]Dipartimento di Ingegneria dei Materiali, Universita di Trento, Trento, Italy
[b]IRST, Divisione Microsistemi, Povo, Trento, Italy

INVITED PAPER
MIDEM 2000 CONFERENCE
18.10.00 – 20.10.00, Postojna, Slovenia

Keywords: HEP, High Energy Physics, Si (silicon) radiation detectors, ALICE, A Large Ion Collider Experiments, ATLAS, A Toroidal Lhc ApparatuS, LHC, Large Hadron Colliders, double-sided microstrip detectors, fabrication technology, experimental results

Abstract: In the last few years, the Institute for Research, Science and Technology (IRST) has been involved in a research program, supported by the Italian Institute of Nuclear Physics (INFN), aimed at setting up the technological capabilities for the production of double-sided silicon detectors for high energy physics experiments. We report on the most relevant achievements of this R&D activity, with emphasis on some recent results from the development of detectors oriented to ALICE (A Large Ion Collider Experiment) and ATLAS (A Toroidal LHC ApparatuS) experiments at LHC.

Najnovejša dognanja pri razvoju silicijevih detektorjev sevanja v IRST

Ključne besede: HEP fizika energij visokih, Si detektorji sevanja silicijevi, ALICE eksperimenti v trkalnikih z ioni velikimi, ATLAS aparati z LHC toroidnim, LHC trkalniki hadronski veliki, detektorji na osnovi mikrotrakasti dvostranski, tehnologija izdelave, rezultati eksperimentalni

Izvleček: V zadnjih nekaj letih je IRST (Institute for Research, Science and Technology) vključen v raziskovalni program, ki ga podpira Italijanski institut za jedrsko fiziko (INFN), katerega cilj je razviti tehnološke kapacitete za proizvodnjo dvostranskih silicijevih detektorjev sevanja za uporabo pri fizikalnih poskusih z visokoenergijskimi delci. V tem prispevku podajamo najnovejša dognanja razvojno-raziskovalnega dela s posebnim poudarkom na rezultatih, ki smo jih dobili pri razvoju detektorja za eksperimenta ALICE (A Large Ion Collider Experiment) in ATLAS (A Toroidal LHC ApparatuS) pri LHC

1. Introduction

Silicon radiation detectors have been extensively used as tracking devices in high energy physics experiments for quite a long time. In the last few years, considerable efforts have been dedicated by many research groups to the study and the improvement of the radiation hardness of these detectors in view of their massive application at LHC and for other high luminosity applications /1/. The possibility for these devices to be efficiently operated in very harsh radiation environments for the full lifetime of the experiments has required to cope with new design and processing aspects /2/.

Since 1997, we have been conducting a research program, supported by INFN (Italian National Institute for Nuclear Physics), aimed at setting up the technological capabilities for the production of double-sided microstrip detectors suitable for the challenging demands of the future high energy physics experiments. Within this framework, the main efforts have recently been dedicated to the development of microstrip detectors designed for ALICE, an LHC experiment aimed at the study of heavy ion collisions. Moreover, IRST has also been committed to the fabrication of ATLAS pixel detector prototypes.

In this paper the most relevant achievements of these technological developments will be presented. In particular, the main design and processing issues will be discussed and some selected results from the electrical characterization of microstrip and pixel detectors will be reported.

2. Development of a double-sided microstrip detector technology

Some preliminary results have already been reported at MIDEM Conference /3/, which demonstrated the feasibility of production of double-sided microstrip detectors at IRST. In fact, in spite of the lack of experience in double-side wafer processing, the first prototypes exhibited good electrical characteristics as well as a reasonably low defect rate, not far from the typical figures of high-quality double-sided detectors /4/. Further work has been going on since then, allowing for the fabrication process to be improved in many respects. In particular, two batches of double-sided microstrip detectors (SD2, SD3) were processed, allowing different technological options and design solutions to be evaluated.

Most of the technological development work was conducted using a dedicated wafer layout, consisting of three different microstrip detectors and several test structures. In particular, in order to have a first-hand comparison with detectors fabricated by other manufacturers, a reference detector was designed adopting as a model the layer 1 detectors for the Silicon Vertex Detector of the Babar experiment /5/, which were being

tested at INFN-Trieste. Although this design was not intended for operation in extreme radiation environments, it was deemed appropriate for the evaluation of the technology. This detector, in the following referred to as SB, consists of 384 strips, parallel on both sides of the wafers. The strip length is 5.1 cm, whereas the strip pitch is 50 μm; the strip width is 22 μm on the p-side and 14 μm on the n-side. The overall area occupation of the detector is 2.12×5.64 cm^2 (including the scribe-lines). Strip isolation on the ohmic-side is obtained by means of individual box-shaped p-stops. Strips are biased by poly-Si resistors placed at the opposite ends of alternate strips and all connected to a common metal bias-line. An implanted guard-ring surrounds the detector active area in order to properly shape the electric field and collect the edge leakage current.

Other detector layouts were considered, and several test structures were also present on the wafer, including: (i) standard test structures, intended as general diagnostic devices, among which a diode with guard-ring, gated-diodes and MOS capacitors (with both poly-Si and metal gate), coupling capacitors, Van der Pauw resistors, etc; (ii) dedicated test structures, aimed at the analysis of some particular aspects of the detector design and at radiation tolerance studies.

2.1 Fabrication technology

Detectors were processed at IRST on 100 mm-diameter, FZ, 300-μm-thick, <111>-oriented, n-type silicon wafers, with nominal resistivity of 6 kΩ·cm. The fabrication process can be outlined as follows:

- field oxide growth (wetO_2, 1 μm);
- p^+ (p-side) and n^+ (n-side) strip definition and field-oxide dry etching;
- screen oxide growth (dryO_2, 70 nm);
- p^+ (p-side) and n^+ (n-side) strip implantations;
- n-type scribe-line (p-side) definition, field-oxide dry etching and implantation;
- p-stop (n-side) definition, field-oxide dry etching and implantation;
- main oxide growth (dryO_2, overall thickness 100÷130 nm);
- TEOS deposition (100÷150 nm) for stacked capacitors;
- polysilicon deposition (350 nm), doping by ion implantation, patterning and dopant activation;
- annealing (N_2, 750°C) and TEOS deposition (800 nm);
- contact opening, metallization and sintering.

Some modifications to the above sequence were implemented as process splits, concerning: (i) the etching of the implant windows on the field oxide (dry vs. wet); (ii) additional, high-temperature (1000°C, dry O_2) annealing steps following the main p^+ and n^+ implantations; (iii) different stacking dielectrics for coupling capacitors (SiO_2-TEOS vs. SiO_2-Si_3N_4); (iv) different doses and energies for the implantations; (v) different starting materials (<111> vs. <100> substrates).

Fig. 1 shows a schematic cross section of the double-sided detector structure: as can be seen, the previously described process allows integrated coupling capacitors to be obtained having a recessed structure with a stacked-dielectric insulator (SiO_2-TEOS), aimed at providing both high specific capacitance and good yield /6/. It is also worth noting that a thick oxide (SiO_2-TEOS stacked layer) covers the p-stop regions; since in many detector designs a superposition of the metal pads with the p-stop can occur, this technological feature can be effective in reducing the risk of metal contacts to the p-stops.

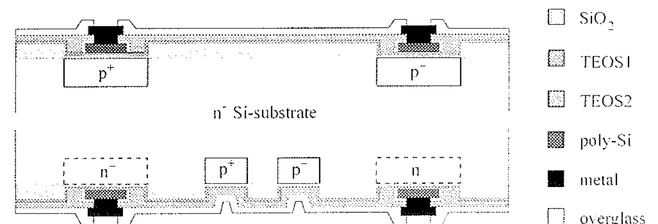

Fig. 1. Schematic cross section of a double-sided detector structure (not to scale).

2.2 Experimental results

The electrical characterization of the microstrip detectors was carried out with a semi-automatic test equipment by using standard procedures. The following measurements were performed on each detector: (i) total leakage current (bias-line & guard-ring); (ii) operating voltage and breakdown voltage; (iii) strip coupling capacitance and interstrip capacitance; (iv) strip (metal) series resistance. Finally, the so-called AC and DC scans were performed by using dedicated probe-cards and the total number of defects was evaluated on each detector. The AC scan consists of measuring the current on the AC pads, so as to check for shorts between adjacent metal lines and for the integrity of coupling capacitors; the DC scan allows to measure other key parameters of individual strips, including leakage current, poly-Si bias resistance and interstrip resistance. The criteria adopted for detector evaluation are representative of the electrical specifications for the detectors to be used in a real high-energy physics experiment and are described in detail in Ref. /5/.

The mean value and the standard deviation of the most relevant electrical parameters measured on the SB detectors from batches SD2 and SD3 are summarized in Table 1. The reported values are all within the considered specifications. A detailed description of the experimental results can be found in /7/. As an example, Fig. 2 shows the distribution of the effective strip bias resistance for all the tested SB detectors from batch SD3. The bias resistance value for most of the strips is included in the range from 6 to 8 MΩ, evidence of adequate process control.

Moreover, the defect rate was considerably reduced with respect to the first prototypes /4/. In fact, the total fraction of inefficient strips is in the order of a few %, with many detectors featuring values close to 1%. It is worth

noting that the incidence of strips with isolated, process-related defects is generally lower than 3 %, whereas the presence of a higher number of defects is to be attributed to accidental mechanical damage of the wafers. The detector quality could be further improved by reducing the number of defects due to lithographical problems, such as shorts between metal and implant lines, and interruptions of strips and p-stops, the latter representing now a significant fraction of the overall number of defects.

Table 1. Main electrical parameters measured on SB detectors.

Parameter	Unit	Mean value	Std. Dev.
Bias line leakage current	nA	165.1	38.1
Guard ring leakage current	nA	16.1	3.4
Breakdown voltage	V	189.0	31.1
Operating voltage	V	29.5	3.3
Coupling capacitance (p-side)	pF/cm	35.1	1.4
Coupling capacitance (n-side)	pF/cm	20.1	1.0
Interstrip capacitance (p-side)	pF/cm	1.13	0.03
Interstrip capacitance (n-side)	pF/cm	1.04	0.02
Poly-Si bias resistance	MΩ	6.7	1.2
Metal resistance	Ω/cm	32.0	1.2

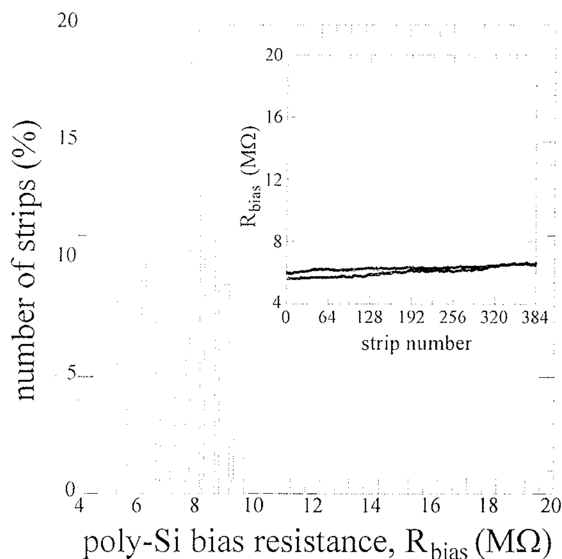

Fig. 2. Distribution of the strip bias resistance for SB detectors, with a typical scan in the inset.

The stability of the leakage currents was also tested at room temperature on a few detectors both on wafer and after dicing. For these measurements, detectors were kept reverse-biased at 80 V, i.e. well beyond the full depletion voltage, for 17 hours or longer. All of the tested detectors exhibited a very stable behavior. As an example, Fig. 3 shows the bias-line and the guard-ring current curves as a function of time for an SB detector after dicing: the variations of the leakage current in the last 2 hours of the measurement were about 0.12% and 0.9% for bias-line and guard-ring, respectively. Similar results were obtained for the other tested detectors, with maximum leakage current variations never exceeding 2.5% in the last 2 hours of the measure-ments. Moreover, no appreciable differences could be observed between undiced and diced detectors.

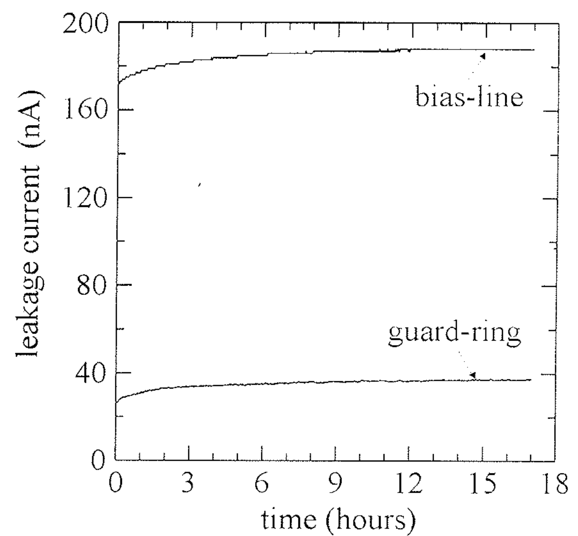

Fig. 3. Bias-line current and guard-ring current vs. time for SB detectors reverse biased at 80V.

3. ALICE microstrip detectors

Within the previously depicted framework, we have recently focused our attention to the development of double-sided, AC-coupled, microstrip detectors oriented to ALICE, an LHC experiment aimed at the study of heavy ion collisions. The Inner Tracking System of ALICE consists of six cylindrical layers of silicon detectors; in particular, the two outermost layers will be equipped with double-sided microstrip detectors /8/.

3.1 Detector design and fabrication

A dedicated wafer layout has been designed, containing the ALICE detector, two "baby" detectors (2.1 x 2.1 mm^2) suitable for beam telescope applications, and several test structures. The layout of the ALICE detector was designed according to the specifications outlined in the TDR /8/. The detector consists of 768 strips, tilted on both sides to obtain a stereoscopic angle of 35 mrad. The strip length (projection on the short edge of the detector) is 40 mm, whereas the strip pitch is 95 μm. As

for the strip width, two different values were adopted on both detector sides in order to evaluate the impact of this parameter on the detector performance. Narrow strips, 30μm and 35μm wide on the p-side and the n-side, respectively, are used in one half of the detector, whereas the other half features wider strips, 50μm and 49μm wide on the p-side and the n-side, respectively. The total detector area, including scribe-lines, is 75 x 42 mm^2.

Since radiation damage is not expected to be of major concern for ALICE, strips are biased by punch-through at both ends, thus avoiding extra processing steps associated to poly-Si resistors. An implanted guard-ring surrounds the bias-line. Strip isolation on the ohmic-side is obtained by means of individual box-shaped p-stops. In the narrow-strip half of the detectors, an additional individual p-stop implant is inserted inbetween the box-shaped p-stops.

Two batches of ALICE detectors were fabricated at IRST. A photograph of a processed wafer is shown in Fig. 4, with the large ALICE detector surrounded by the two telescope detectors and by several test structures. The fabrication technology is the same as outlined in Section 2, apart from the poly-Si related steps, which were not implemented. The only technological split is concerned with the coupling capacitors, which were based on either SiO_2-TEOS or SiO_2-Si_3N_4 stacked layers.

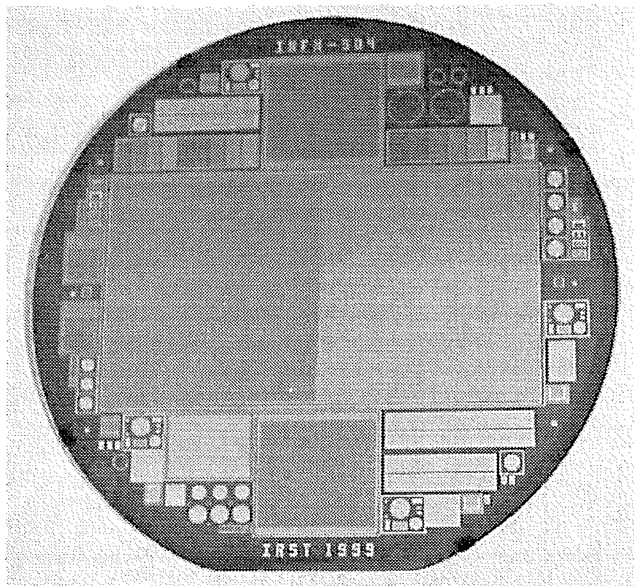

Fig. 4. Photograph of an ALICE microstrip detector wafer (p-side).

3.2 Experimental results

Preliminary measurements on test structures allowed to assess the good quality of the fabrication process. In particular, low leakage current values, in the order of 1nA/cm^2 at full depletion, were measured on 4-mm^2 test diodes with guard-ring: the corresponding values of bulk generation lifetime are about 30 ms. Diode breakdown voltage is generally higher than 200 V. The value of the surface generation velocity, extracted by means of gated diodes, is in the order of 24(3.5) cm/s on wafers employing TEOS(Si_3N_4) for coupling capacitors, corresponding to a surface leakage current density of about 40(6) nA/cm^2.

The electrical characterization of the detectors was carried out at INFN-Trieste. The total leakage current of the detectors (bias-line & guard-ring) were measured first, confirming the low values measured on test structures: in particular, the bias-line current was typically in the order of 500 nA at full depletion, whereas the guard-ring current was lower than 15 nA. The AC and DC scans were performed at an operating voltage of 40V by using dedicated probe-cards. The electrical specifications reported in /8/ were adopted as criteria for the detector evaluation.

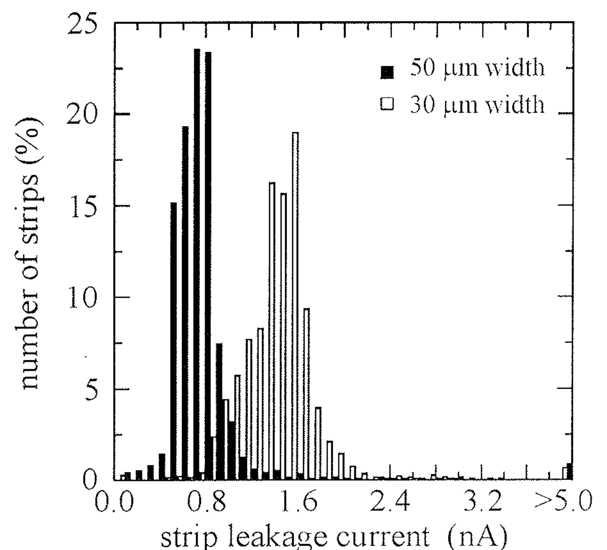

Fig. 5. Distribution of the strip leakage current for ALICE detectors.

Fig. 5 shows the distribution of the strip leakage current of all the tested detectors; two distinct groups of strips having different leakage current values can be observed, corresponding to the two different strip width values. As a matter of fact, due to a non negligible contribution from surface generation, strips featuring a lower width/pitch ratio are characterized by a higher leakage current /7/. The same difference between the two halves of the detectors in terms of leakage current can also be observed in Fig. 6, showing a typical scan of this parameter. However, the average value of the strip leakage current is well below 2 nA in both cases (see Table 2, referring to detectors featuring a SiO_2-Si_3N_4 stacked insulator for coupling capacitors), and only a small fraction of the strips, lower than 1%, exceeds the specification value (5 nA). The interstrip resistance and the equivalent resistance of the punch-through bias structure were also extracted from DC scans, the resulting values largely exceeding the minimum values required by the specifications.

Fig. 7 shows a typical scan of coupling capacitors: the current measured on good capacitors, biased at a voltage of 20 V across the dielectric, is lower than 100

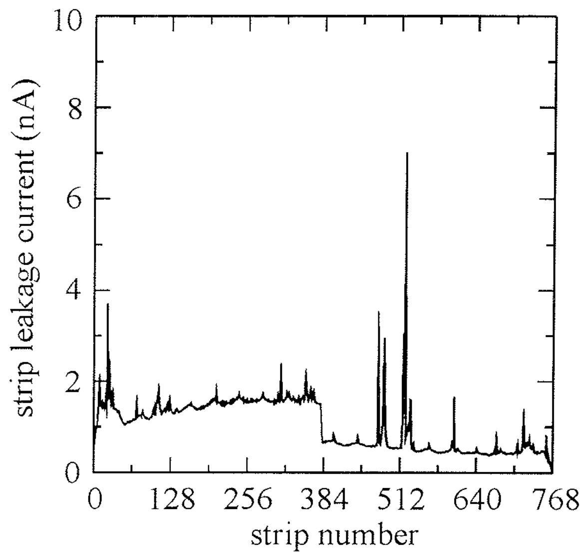

Fig. 6. Typical scan of the strip leakage current on the p-side of an ALICE detector.

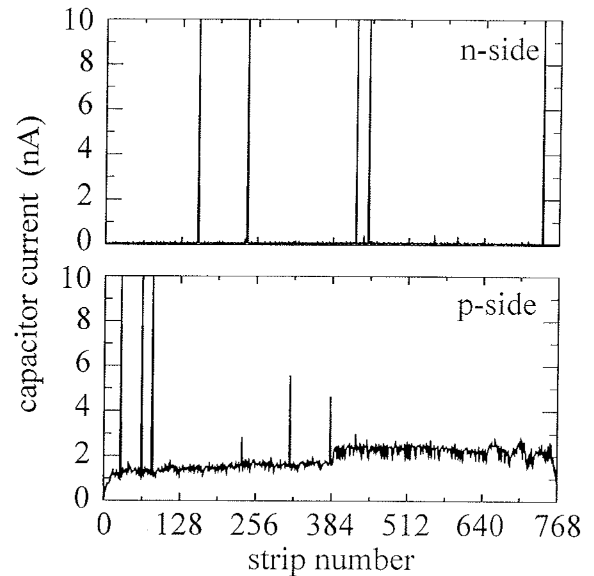

Fig. 7. Typical scan of the coupling capacitor current on the p-side and the n-side of an ALICE detector.

Table 2. Main electrical parameters measured on ALICE detectors.

Parameter	Unit	Narrow strips	Wide strips
Leakage current	nA	1.4	0.7
Coupling capacitance C_{AC} (p-side)	pF	171	286
Coupling capacitance C_{AC} (n-side)	pF	153	207
Parasitic capacitance C_p (p-side)	pF	5.7	7.8
Parasitic capacitance C_p (n-side)	pF	7.5	9.3
Ratio C_{AC}/C_p (p-side)		30	36.7
Ratio C_{AC}/C_p (n-side)		20.4	22.3

pA on the n-side, while it is ranging from about 1 nA to 2 nA on the p-side, accordingly with the strip width. Such a difference in the current values between the two sides of the detector is to be attributed only to measurement inaccuracies related to the use of probe-cards. The average fraction of bad capacitors, exhibiting current spikes reaching the upper value on the scale in Fig. 7, is below 1% on both detector sides, according to the quality of the fabrication process. The total fraction of inefficient strips in the tested detectors is lower than 3%, with an average value close to 1%.

Table 2 reports also the average values of the coupling capacitance and of the strip parasitic capacitance, the latter comprising both the interstrip and the back-plane contributions. As can be seen, both these parameters are higher in the case of wide strips; however, the ratio of the two capacitance values is higher than the specification value (20) in both cases. It is worth noting that the coupling capacitance on the p-side is much higher than on the n-side, due to the lower thickness of the thermal oxide on the p-side. Since the intrinsic breakdown voltage of the coupling capacitors is higher than 200V, a value which largely exceeds the one required by the specifications (100V), the oxide thickness on the n-side could be reduced in order to enhance the coupling capacitance. Further details on the experimental results are reported in /9/.

4. ATLAS pixel detectors

4.1 Device description

Pixel sensors were designed by the ATLAS Pixel Collaboration to be efficiently operated in very harsh radiation conditions /10/. These detectors are of the n-on-n type, i.e., n^+ pixels are obtained on the n-side of wafers, whereas a large p^+-n junction is present on the p-side, surrounded by a multiguard termination structure. With respect to the standard p-on-n pixel detectors, these devices require a more complicated, double-side fabrication technology; moreover, the pixels being of n-type, an adequate isolation between them is necessary, which is based on the moderated p-spray technique /11/. In addition to this, as suggested by recent studies on the radiation hardening of silicon, silicon substrates require to be oxygen enriched /12/.

Several batches of ATLAS pixel sensor prototypes have been processed at IRST starting from fall 1998 /13/. With respect to the formerly available microstrip detector process, featuring p-stop blocking implants in between n^+ strips on the detector ohmic side, the fabrication of ATLAS pixel sensor prototypes, requiring p-spray isolation, has imposed a different technological approach. Moreover, the pixel detector design was not fully compatible with IRST layout rules, particularly in the punch-through bias structures placed at one end of the pixels in order to allow for the sensor testing before bump-bonding /10/.

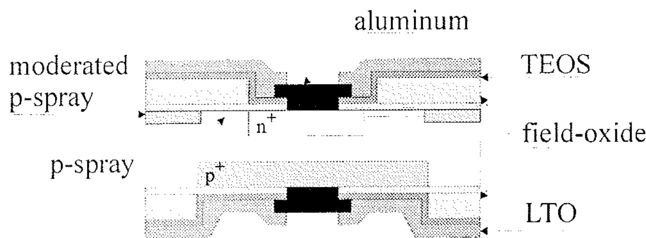

Fig. 8. Schematic cross section of an ATLAS pixel detector structure (not to scale).

Detectors were processed on 100 mm-diameter, FZ, 250-μm-thick, <111>-oriented, n-type silicon wafers, with nominal resistivity of 5 kΩ· cm. At the beginning of the processing sequence, half of the wafers has undergone a preliminary thermal treatment, consisting of a 24 hour oxidation-diffusion process at 1150°C /12/, in order to enrich the oxygen content up to a concentration of about 10^{17} cm^{-3} for radiation hardness purposes. With reference to the schematic cross-section of a single pixel, shown in Fig. 8, the fabrication process can be outlined as follows:

- screen oxide growth (wetO_2, 200 nm); n-side: p-spray implantation (B, 4.5×10^{12} cm^{-2}, 70 keV), moderated p-spray definition and implantation (B, 4.5×10^{12} cm^{-2}, 70 keV);
- TEOS deposition (800 nm); p-side: p^+ diode definition, TEOS dry etching, screen oxide growth (dryO_2, 40 nm), p^+ implantation (B, 5×10^{14} cm^{-2}, 70 keV);
- n-side: n^+ pixel definition, TEOS dry etching, reoxidation (p^+ drive-in), n^+ implantation (P, 5×10^{15} cm^{-2}, 120 keV), reoxidation (n^+ drive-in);
- TEOS deposition (300 nm), segregation annealing (N_2, 6 hours, 750°C), contact definition and opening;
- metal deposition, definition and dry etching; LPCVD-Low Temperature Oxide (LTO) deposition, passivation layer definition and dry etching; contact sintering in forming gas.

4.2 Experimental results

In the following, experimental results will be reported which refer to the second pixel prototypes. The wafer layout for these devices (see photograph in Fig. 9) contains: (i) 3 large sensors (16 cm^2), called tiles, differing in the design and dimensions of the punch-though biasing structures (in the following they will be referred to as SMD, LAD and NOD); (ii) 12 smaller sensors (1 cm^2), called single-chips; (iii) several test structures, including diodes with guard-ring, gated diodes and MOS capacitors.

Preliminary measurements were carried out at IRST to assess the process quality before delivering wafers to the interested groups of the ATLAS Collaboration. Test structures were measured first; all the technological parameters evaluated from the characterization of these devices indicated that the fabrication process is adequate for good quality detectors. Moreover, only minor differences could be observed between oxygenated and standard wafers in terms of both bulk and surface properties.

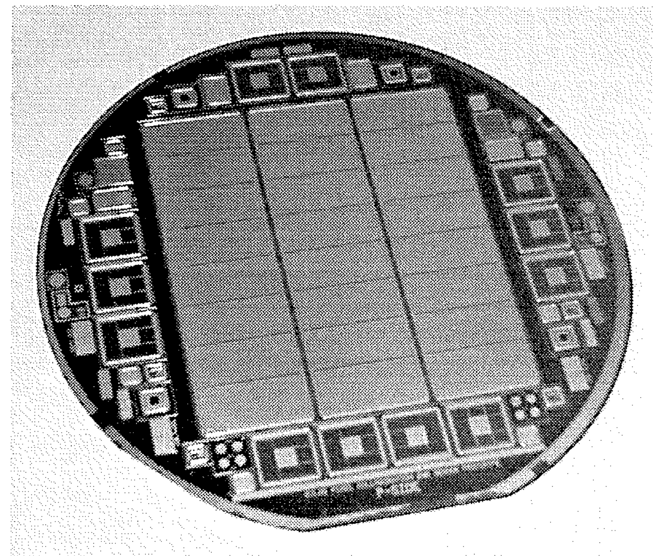

Fig. 9. Photograph of an ATLAS pixel detector wafer (p-side).

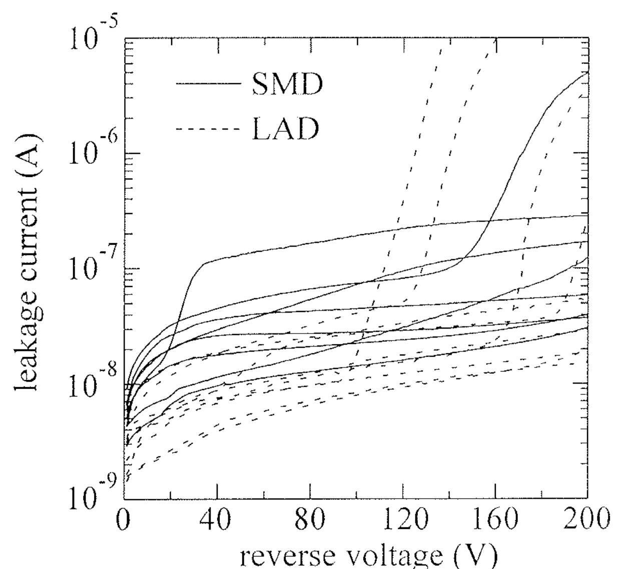

Fig. 10. Typical leakage current curves of SMD and LAD single chips.

The I-V curves of all the single-chips and tiles were then measured using the single-side set-up described in /14/. As an example, Fig. 10 shows some typical leakage current curves for SMD and LAD single-chips: the leakage current values at 150V are normally ranging from 10 to 100 nA. In spite of the non saturating behaviour of the curves, due to a non negligible surface current contribution from the n-side interpixel regions, these leakage current values would comply with the technical specifications of the ATLAS pixel prototype sensors /11/. Fig. 11 shows the breakdown voltage distribution, defined as the voltage at which the measured current exceed 1 μA, for all the single-chips. As can be seen, while the distribution for SMD and LAD detectors is similar, with a low number of early failures

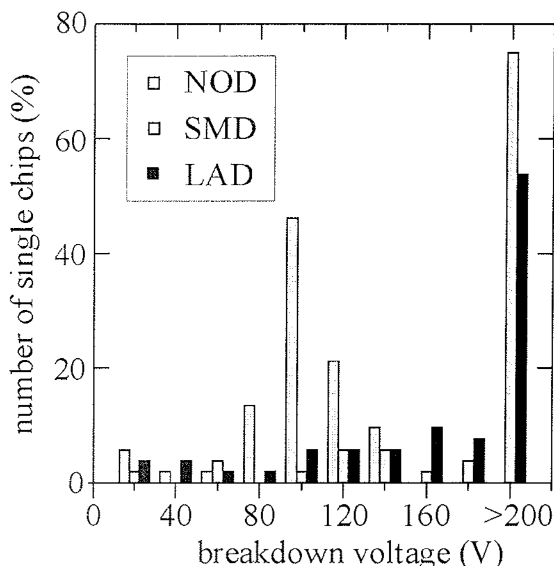

Fig. 11. Distribution of the breakdown voltage of the three types of single-chips.

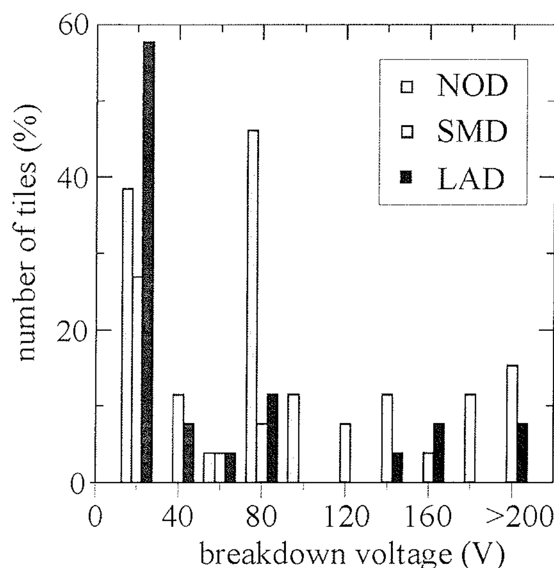

Fig. 12. Distribution of the breakdown voltage of the three types of tiles.

and with most of the chips featuring a breakdown voltage higher than 200V, NOD detectors exhibit a distribution peaked at about 100 V, with no detector reaching 150 V. The weakness of NOD detectors, which was also reported by other manufacturers, although not fully understood, is probably to be attributed to a layout problem.

Fig. 12 shows the breakdown voltage distribution, defined as the voltage at which the measured current exceed 10μA, for all the tiles. As expected from single-chip results, no tile of the NOD type exceeds 100 V of breakdown voltage. On the contrary, the behaviour of SMD and LAD detectors is generally worse than that of the corresponding single-chips, with many detectors suffering early breakdown problems as the full depletion voltage is reached and only a few tiles exhibiting a breakdown voltage higher than 150 V. The reason for this considerable degradation in the characteristics of tiles with respect to the corresponding single-chips is not easy to understand, although it is likely to be attributed to the presence of defects on the n-side of the wafers. On one hand, on a statistical basis, the number of defects encountered on 1-cm^2 single-chips can justify the low yield on 16-cm^2 tiles; on the other hand, these defects could not be observed by means of optical inspection of the wafers and, moreover, the measurement of the total leakage current alone does not allow to identify the type of defects and their position. Light emission microscopy measure-ments are currently being carried out in order to gain deeper insight into the cause of early breakdown events.

5. Conclusions

We have reported on the most recent results from an R&D program on radiation detector technologies at IRST Laboratory. In particular, a fabrication process for double-sided, AC-coupled microstrip detectors has been developed and several batches of good quality detectors with a low defect rate have been manufactured. Within this framework, ALICE detector prototypes have been fabricated and succesfully tested. Moreover, a few spares for the layer 1 and 2 detectors for the Silicon Vertex Detector of the Babar experiment are currently being fabricated.

More recently, IRST has also been committed to the fabrication of ATLAS pixel detector prototypes. Results from the electrical characterization of detectors and related test structures have evidenced that, in spite of the lack of specific experience in the p-spray isolation technique, IRST technology is potentially adequate for the fabrication of these detectors. Nevertheless, the number of process-related defects should be decreased in order to fulfill the detector specifications (in particular in terms of breakdown voltage) with a satisfactory fabrication yield.

Acknowledgements

The fruitful collaboration with Prof. Luciano Bosisio (INFN – Trieste) is warmly acknowledged. We would like to thank also Dr. Mario Zen and the technical staff of IRST Laboratory for fabricating the detectors, Dr. Nicola Zorzi and Dr. Paolo Gregori (IRST – Trento) and Dr. Irina Rachevskaia (INFN – Trieste) for their help in performing measurements and analyzing data. We are also grateful to Dr. Leonardo Rossi (INFN – Genova), Dr. Saverio D'Auria (University of Glasgow, formerly with INFN – Udine) and Dr. Renate Wunstorf (University of Dortmund) for many useful discussions.

References

/1/ Lindström et al., "Radiation hardness of silicon detectors - A challenge from high energy physics", Nuclear Inst. and Meth. in Phys. Res., vol. A426, pp. 1-15, 1999.

/2/ R. H. Richter and G. Lutz, "Silicon radiation detectors - Physics and structures", Informacije MIDEM, vol. 29, nr. 1, pp. 1-9, 1999.

/3/ M. Boscardin et al., "First results on double-sided AC-coupled Si strip detectors", Proc. of MIDEM Conference, pp. 205-210, Rogaska Slatina (Slovenia), 1998.

/4/ G. F. Dalla Betta et al., "Feasibility study for double-sided silicon microstrip detector fabrication at IRST", Nuclear Inst. and Meth. in Phys. Res., vol. A431, pp. 83-91, 1999.

/5/ D. Barbieri et al., "Silicon sensors for the BaBar vertex tracker: design, electrical tests and production quality control", Il Nuovo Cimento A 112, pp. 113-130, 1999.

/6/ G. F. Dalla Betta et al., "A comparative evaluation of integrated capacitors for AC-coupled microstrip detectors", Nucl. Instr. and Meth. A, vol. A411, pp. 369-375, 1998.

/7/ G. F. Dalla Betta et al., "Development of a fabrication technology for double-sided AC-coupled silicon microstrip detectors", to appear in the Nucl. Instr. and Meth. A.

/8/ ALICE Technical Design Report of the Inner Tracking System (ITS), CERN/LHCC 99-12, ALICE TDR4, 18 June 1999.

/9/ M. Boscardin et al., "Development of ALICE microstrip detectors at IRST", presented at Frontier Detectors for Frontier Physics - 8th Pisa Meeting on Advanced Detectors, La Biodola (Italy), May 2000, to appear in the Nucl. Instr. and Meth. A.

/10/ T. Rohe et al., "Sensor design for the ATLAS-Pixel detector", Nucl. Instr. and Meth. in Phys. Res., A421, pp. 224-228, 1998.

/11/ The ATLAS Pixel Sensor Group, "Technical specifications of the ATLAS pixel prototype sensors", 16 February 1999.

/12/ G. Casse et al., "Introduction of high oxygen concentrations into silicon wafers by high temperature diffusion", Nucl. Instr. and Meth. in Phys. Res., A438, pp. 429-432, 1999.

/13/ M. Boscardin et al., "Fabrication of ATLAS pixel detector prototypes at IRST", presented at the International Workshop on Semiconductor Pixel Detectors for Particles and X-rays, Genova (Italy), June 2000, and submitted for publication in the Nucl. Instr. and Meth. A.

/14/ F. Hügging et al., "Design and test of pixel sensors for operation in severe radiation environments", Nucl. Instr. and Meth. in Phys. Res., A439, pp. 529-535, 2000.

G. U. Pignatel
Dipartimento di Ingegneria dei Materiali,
Universita di Trento,
Via Mesiano 77, 38050 Trento, Italy
M. Boscardin, G.-F. Dalla Betta
IRST, Divisione Microsistemi,
Povo, I-38050 Trento, Italy

Prispelo (Arrived): 1.10.2000 *Sprejeto (Accepted): 25.11.2000*

DIAGNOSTICS OF NONLINEARITY OF CURRENT VS. VOLTAGE CHARACTERISTICS - THEORY AND APPLICATIONS

Pavel Mach
Czech Technical University in Prague, Faculty of Electrical Engineering, Department of Electrotechnology, Prague, Czech Republic

INVITED PAPER
MIDEM 2000 CONFERENCE
18.10.00 - 20.10.00, Postojna, Slovenia

Keywords: materials, components, diagnostics of materials, diagnostics of components, diagnostics of nonlinearity of current vs. voltage characteristic, quality evaluation

Abstract: There are two groups of methods used for diagnostics of materials and components: methods, which are focused on investigation of macrophysical properties (such as resistance, dielectric constant etc.) and methods, which reflect microphysical properties (such as nonlinearity or noise). The goal of this paper is to show the use of nonlinearity as a diagnostic tool for evaluation of quality of materials and their changes. Instrumentation, theory and examples of applications of this diagnostics are presented.

Diagnosticiranje nelinearnosti tokovno-napetostne karakteristike - teorija in uporaba

Ključne besede: Materiali, deli sestavni, diagnostika materialov, diagnostika delov sestavnih, diagnostika nelinearnosti karakteristik tok - napetost električna, vrednotenje kakovosti

Izvleček: V splošnem obstajata dve skupini metod, ki ju uporabljamo za diagnosticiranje materialov in komponent: metode, ki temeljijo na preučevanju njihovih makroskopskih lastnosti (kot sta upornost, dielektrična konstanta ipd.) in metode, ki odsevajo mikroskopske lastnosti vzorca (kot sta nelinearnost in šum). Namen tega prispevka je pokazati uporabo nelinearnosti kot diagnostičnega orodja za vrednotenje kvalitete materialov in njihovih sprememb. Predstavljamo opremo, teorijo in primere uporabe tovrstne diagnostične tehnike.

1. introduction

Quality is a parameter, which appertains among basic parameters of technical components and equipment (and not technical only). Therefore a great effort is paid to development of methods, which make investigation and evaluation of quality possible with the simplest, easiest, cheapest and most reliable way.

The measurement of nonlinearity has been developed for investigation of influence of manufacturing technology on properties of thin metal films prepared by vacuum evaporation /1/. Later it has been also used for investigation of quality of production of capacitors, for testing of thick resistive films, quality of joints manufactured of electrically conductive adhesives and their aging and for evaluation of quality of technology for preparation of conductive lines with very low width.

Nonlinearity measurement has also been used for analysis of changes in electrically conductive adhesives after their thermal aging /2/ and for investigation of changes in thick film resistive structures caused by laser trimming. It seems that nonlinearity analysis has continuously growing significance in electronics diagnostics.

2. Principles of Measurement and Measuring Equipment

Two measuring principles are currently used for investigation of nonlinearity of current vs. voltage characteristics. The first principle is shown in Fig. 1. A measured component with the nonlinear I-V characteristics is powered with the sinusoidal current. As a consequence of the nonlinear shape of the I-V characteristics the voltage across the component is periodical, but it is not sinusoidal. Such the signal can be decomposed in a series of harmonics and the value of third harmonics is measured. The equipment for such the measurement is very simple and consists of three parts: a generator of the sinusoidal current, a selective voltmeter for the measurement of the first harmonics voltage and a selective voltmeter for the measurement of the third harmonics voltage. The generator must have minimum distortion of the signal and low noise (the signal to noise ratio must be higher than 150 dB). Its distortion must not change with different impedance of the measured samples. Filters of the selective voltmeters must have high quality to achieve sufficient selectivity. Therefore the equipment based on this principle is usable for one measuring frequency only; the basic frequency is usually 10 kHz the frequency of the third harmonics is 30 kHz.

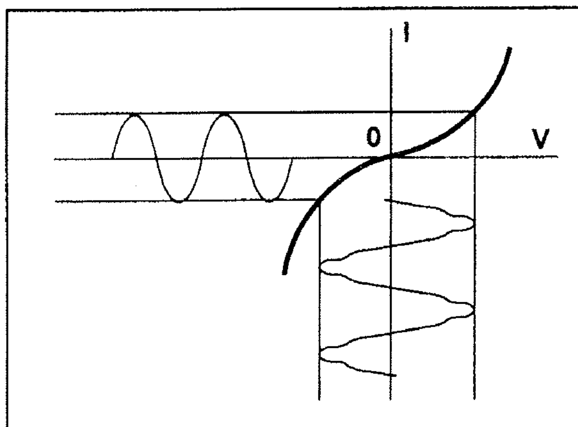

Fig. 1. Principle of measurement of nonlinearity by powering of the sample with a pure sinusoidal current

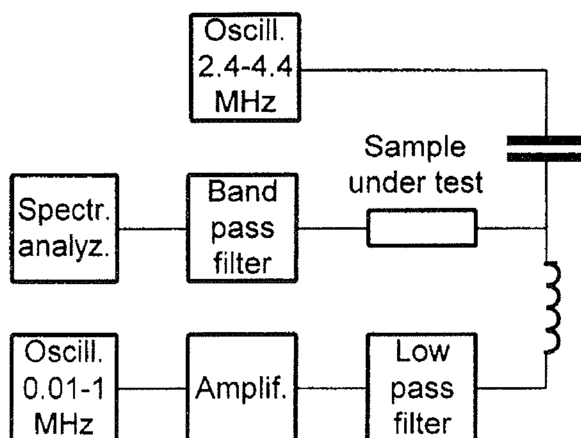

Fig. 2. Schematic diagram of an equipment for measurement of I-V characteristics nonlinearity based on modulation principle

The second principle, which has been used for design of an equipment realized at the Department of Electrotechnology of the CTU in Prague, is based on powering of the sample with two sinusoidal signals (see Fig. 2). Modulation products of third order, which are caused by nonlinearity of the I-V characteristics, are measured with a spectral analyzer. The advantage of this equipment in comparison with the previously mentioned one is ability to measure nonlinearity at the wide frequency range. The equipment has been designed with respect to minimum own noise and nonlinearitry. Therefore capacitors with very low own nonlinearity have been used (it is necessary to avoid to ceramic capacitors, which are mostly manufactured of feroelectric ceramics). As for resistors, it is not possible to use film resistors because of their high nonlinearity and noise. Wire resistors are mostly manufactured of nichrome or manganine alloys. These alloys are feromagnetic and dependence of their impedance on frequency is not linear. Therefore the wire resistors manufactured of platinum wire have been used.

3. Theory of nonlinearity

Nonlinearity of the current vs. voltage characteristics of nominally linear components is often explained by presence of nonlinear mechanisms of conductivity such as tunneling or Shottky emission, which complete the linear mechanism of phonon-electron interaction, which is the dominant one. However, according to the other theory, the main reason of nonlinearity is an increase of temperature of microscopic areas, e.g. of boundaries of grains, when the current flows through the component. Nonlinearity is also explained by magnetic properties of a material s or by thermal diffusion of vacancies.

Nonlinearity is usually joined with inhomogenities, which cause origin of potential barriers spread throughout the material. Therefore its value is substantially higher in multicomponent materials such as thick resistive films than in metals. Very often theory of potential barriers is also used for the description of nonlinearity.

Let us present short description of this theory /4/. The current I_l, which flows through the barrier, can be, in general, described by an equation:

$$I_l = A \cdot \exp\left(-\frac{e\Phi_l}{kT}\right) \quad (1)$$

Where A ... constant of the material, e ... charge of the electron, Φ_l ... height of the potential barrier, k ... Boltzman constant, T ... temperature in K.

When the voltage U will be applied in a positive direction, the value of the current will be:

$$I_l^+ = A \cdot \exp\left(\frac{-e\Phi_l + eU}{kT}\right) \quad (2)$$

When the voltage will be applied in an opposite direction, the value of the current will be:

$$I_l^- = A \cdot \exp\left(\frac{-e\Phi_l - eU}{kT}\right) \quad (3)$$

The total current I_T is calculated as a sum of the currents flowing through all barriers. It is possible, after short mathematical processing, to express I_T by the equation:

$$I_T = 2N_t A \exp\left(-\frac{e\Phi_l}{kT}\right)\left[\frac{eU}{kT} + \frac{e^3U^3}{3!(kT)^3} + \frac{e^5U^5}{5!(kT)^5} + ...\right] \quad (4)$$

As follows from equation (4), potential barriers (number of these barriers is N_t) cause nonlinearity of the odd type. If the number of the barriers will increase, nonlinearity will also increase. If the hight of the potential barriers will increase, the resistance of the sample will increase (see Fig. 3).

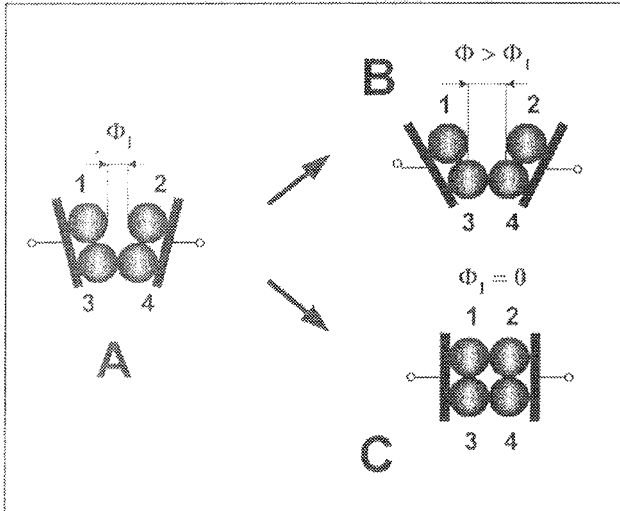

Fig. 3. Possible changes of potential barrier during the time

When the system with the barriers is arranged as shown in Fig. 3 A, there is a potential barrier Φ_l between areas 1 and 2. If we will assume, for simplicity that contacts between areas 1,3 and 2,4 have very high resistance, the total resistance of this system can be expressed as the resistance of two parallel connected resistors R' and R. The resistor R' represents the resistance of the course from the left electrode through the area 1, potential barrier Φ_l and area 2 to the right electrode and the resistor R the resistance of the course from the left electrode through the areas 3 and 4 to the right electrode. After some time the system will have configuration according to Fig. 3B or 3C. If the system will change its configuration according to Fig. 3B, the potential barrier will increase and the total resistance of the system will also increase. If the resistance R' increases to ∞, the total resistance will be equal to R. If the configuration will change as shown in Fig. 3C, the total resistance will decrease and will be equal to R/2.

For description of dependence of the number of the barriers N_t on the temperature T the Arrhenius equation is usually used.

$$N_t = N_0 \exp\left[\frac{K}{\tau}\exp\left(-\frac{E_A}{kT}\right)\right] \quad (5)$$

Here K ... constant of the material, τ ... reaction expectancy, E_A ... energy, which is necessary for reconfiguration (activation energy), N_0 ... number of barriers in balance.

Another theory of nonlinearity is based on an assumption of diffusion of vacancies /3/, which is caused by increase of the sample temperature. The current flowing through the sample causes this increase. For a rectangular thin film resistor with the length **L**, width b, thickness h and resistivity ρ_f, which is powered with the sinusoidal current $I_1\sin(\omega t)$, the temperature of the sample increases by ΔT:

$$\Delta T = T - T_0 = R_T P = \frac{R_T K_1 \rho_f}{h} I_1^2 \sin^2(\omega_1 t) \quad (6)$$
$$\Delta T << T_0$$

Here T ... temperature of the sample when the sample is powered by the sinusoidal current, T_0 ... temperature of the surroundings, R_T ... thermal resistance of the layer, K_1 = L/(b.h).

According to the Matthiessen rule the total resistivity of the layer ρ_f can be written as:

$$\rho_f = \rho_L(T) + \rho_D + \rho_s \quad (7)$$

Here $\rho_L(T)$ ... the part of resistivity caused by dispersion of electrons on phonons, the dependence of this part on the temperature is linear, ρ_D ... the part of the resistivity caused by dispersion of the electrons on vacancies and on other volume imperfectances, ρ_s ... the part of the resistivity caused by dispersion of the electrons on the surface of the thin film.

The change of the temperature will cause the periodical change of vacancies concentration. If it will be assumed that the increase of resistivity will be influenced by the vacancies with the energy of activation E_V only, then dependence of ρ_f on the temperature can be expressed as follows:

$$\rho_f(T) = \rho_{01}(1+\beta\Delta T) + AA_V \exp\left(-\frac{E_V}{k[T_0+\Delta T]}\right) \quad (8)$$

Here ρ_{01} ... part of the total resistivity, which is caused with dispersion of electrons on phonons and with interaction of electrons with the surface of the layer, β ... thermal coefficient of the resistivity of the layer, A ... coefficient of proportionality, A_V ... coefficient of entropy, E_V ... energy of activation of vacancies.

In equation (8) the first part represents a component, with linear dependence of resistivity on the temperature, the exponential part represents a nonlinear component. This part can be expressed as a series of harmonics. When the sample will be powered with the sinusoidal current $I_1\sin(\omega t)$, third harmonics can be expressed as:

$$U_3 = 0.25 R_T K_1^2 \rho_{01}\rho_f\left[\beta + \frac{AA_V E_V}{kT_0^2\rho_{01}}\exp\left(-\frac{E_V}{kT_0}\right)\right] I_1^3 \quad (9)$$

4. Applications of nonlinearity measurements

Diagnostics of nonlinearity of I-V characteristics has been used in many cases. Two of them are presented in this paper.

The use of nonlinearity evaluation for optimization of manufacturing technology of the lines with very low width is shown in Fig. 4. The lines of the width of 50 μm have been prepared by thick film technology of special photosensitive conductive pastes on alumina sub-

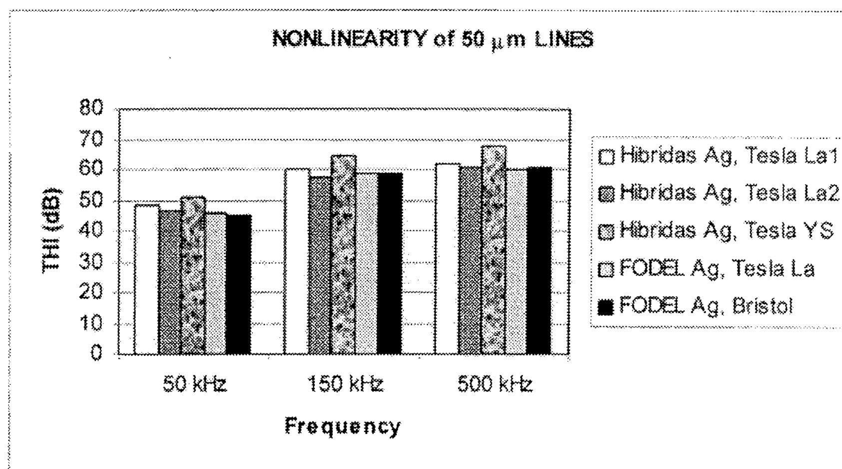

Fig. 4 *Nonlinearity (expressed as THI in dB) of 50 μm lines manufactured of photosensitive thick film pastes Hibridas and Fodel in different factories on alumina substrates*

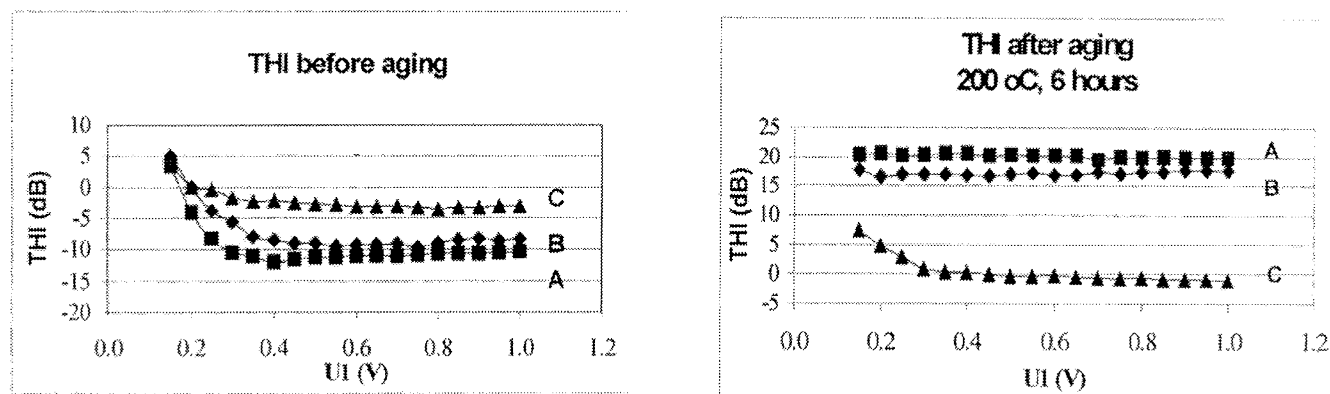

Fig. 5 *Third harmonic index (THI in dB) of joints prepared of adhesives Alpha Metals 171 (A), Alpha Metals 181 (B) and ECA 3 (C) on Cu surface before and after aging at 200 °C*

strates. The quality of the lines has been evaluated according to their resistance and nonlinearity.

Diagnostics of quality of conductive joints manufactured of electrically conductive adhesives has also been carried out by the measurement of nonlinearity of these joints. After manufacturing the joints have been measured, then at the higher temperature, measured again, and the changes of their nonlinearity have been evaluated. According to these changes the changes of a structure of the adhesives have been analyzed. The small part of these measurements is shown in Fig. 5.

5. Conclusions

It has been found that the diagnostics based on the evaluation of nonlinearity of I-V characteristics could be a very useful tool for evaluation of quality of technology and materials.

Main advantage of this type of diagnostics is its simplicity and very high sensitivity on changes in materials. These properties state it to spreading among advanced types of diagnostic methods.

6. Rererences

/1/ CLT 1 Operation manual, Radiometer Copenhagen

/2/ Mach, P.: "Comparison of Adhesive and Soldered Joints", Transaction on the Precision and Electronic Technology, Vol. 3, 1997, pp.119-122

/3/ G. P. Zhigalskij, "Noise of the type 1/f and nonlinear effects in thin metallic films (in Russian)", Uspechi fizičeskich nauk, Vol. 167, No. 5, pp. 624-648, 1997

/4/ Anderson, J. C. and Ryšánek, V., „Prediction of the Stability of Thin-film Resistors," The Radio and Electronic Engineer, Vol. 39, No. 6, June 1970

Pavel Mach
Czech Technical University in Prague,
Faculty of Electrical Engineering,
Department of Electrotechnology
Technická 2, 166 27 Prague 6,
Czech Republic
Phone: ++420 2 2435 2122,
Fax: ++420 2 2435 3949
E-mail. mach@feld.cvut.cz
WWW: http://K313.feld.cvut.cz

Prispelo (Arrived): 1.10.2000 ***Sprejeto (Accepted): 25.11.2000***

UDK621.3:(53+54+621+66), ISSN0352-9045 Informacije MIDEM 30(2000)4, Ljubljana

MATERIALS CHARACTERIZATION BY AUGER ELECTRON SPECTROSCOPY SPUTTER DEPTH PROFILING

Anton Zalar
Institute of Surface Engineering and Optoelectronics, Ljubljana, Slovenia

TUTORIAL INVITED PAPER
MIDEM 2000 CONFERENCE – Workshop on ANALYTICAL METHODS IN MICROELECTRONICS AND ELECTRONIC MATERIALS
18.10.00 – 20.10.00, Postojna, Slovenia

Keywords: IBS, Ion Beam Sputtering, materials characterization, material properties, IBS, Ion Beam Sputtering, AES depth profiling, Auger Electron Spectroscopy depth profiling, semiconductors, microelectronics, MBE growth, Molecular Beam Epitaxy growth, MOCVD, Metal-Organic-Chemical Vapor Depositions, thin films, multilayer structures

Abstract: Depth profiling by ion sputtering in combination with Auger electron spectroscopy (AES) has become a valuable analytical tool in microelectronics and those areas of research and technology where the chemical composition of surfaces, interfaces and thin films is of importance. Its application range from fundamental surface and interface studies to thin-film structures for electronic and microelectronic devices, wear-and corrosion-resistant coatings, surfaces modified by plasma technique or ion implantation, etc. Reactions at surfaces as well as the resulting electrical and mechanical properties can only be understood if the relevant chemical and structural changes in the investigated thin-film structures are known. This requires a quantitative spatially resolved analysis and in-depth distribution of chemical composition with a high depth resolution. However, ion sputtering is not an ideal layer-by-layer erosion but is the result of a complex ion beam-sample interaction process. Various phenomena, the most important of which are due to ion beam induced changes of surface roughness and composition, limit the experimentally achievable resolution. The principles of the method and its fundamental capabilities and limitations will be discussed. The applicability of the AES depth profiling in microelectronics and some other technical fields will be illustrated by depth profiles of the characteristic samples.

Karakterizacija materialov z Augerjevo elektronsko-spektroskopsko (AES) profilno analizo

Ključne besede: IBS naprševanje s curki ionskimi, karakterizacija materialov, lastnosti materialov, IBS naprševanje s curki ionskimi, AES Auger spektroskopija elektronska-profiliranje globinsko, polprevodniki, mikroelektronika, MBE rast molekularna žarkovna epitaksialna, MOCVD nanosi kemični s paro kovina-snov organska, plasti tanke, strukture večplastne

Izvleček: Profilna analiza v kombinaciji ionskega jedkanja s spektroskopijo Augerjevih elektronov je postala zelo uporabno analitsko orodje v mikroelektroniki in na tistih področjih preiskav in tehnologij, kjer je pomembna kemična sestava površin, faznih mej in tankih plasti. Uporablja se za temeljne preiskave površin in faznih mej, kakor tudi za preiskavo tankoplastnih struktur za elektronske in mikroelektronske naprave, za obrabno in korozijsko obstojne prevleke, površine obdelane s plazemsko tehniko ali implantacijo, itd. Reakcije na površinah in z njimi povezane električne in mehanske lastnosti lahko razumemo samo, če so poznane ustrezne kemične in strukturne spremembe v tankoplastnih strukturah. To zahteva kvantitativno prostorsko ločljivo analizo in globinsko porazdelitev kemične sestave z veliko globinsko ločljivost. Pri tem moramo vedeti, da ionsko jedkanje ne predstavlja idealnega primera odstranjevanja plasti za plastjo, ampak je to rezultat kompleksne interakcije ionskega curka s preiskovanim vzorcem. Različni pojavi, od katerih sta najpomembnejša sprememba hrapavosti in sestave, povzročena z ionskim curkom, omejujejo eksperimentalno dobljeno ločljivost. V delu so obravnavani principi metode in njena zmogljivost ter omejitve. Uporabnost AES profilne analize v mikroelektroniki in na nekaterih drugih tehničnih področjih je ilustrirana z globinskimi profili karakterističnih vzorcev.

1. Introduction

Advanced thin-films and composite materials based on progress in thin films and interface science /1/. Properties of materials interfaces on the nanometer scale influence on a great number of materials properties and macroscopic phenomena. The resulting properties as well as reactions at surfaces and interfaces, such as oxidation, corrosion, interdiffusion and segregation can only be understood if the relevant changes of the chemical composition at the interfaces and of regions around them are known. The rapid advancement of semiconductor material growth technologies such as molecular-beam epitaxy (MBE) and metalorganic chemical vapor deposition (MOCVD) has greatly improved the microelectronic devices with atomically abrupt interfaces and ultra-shallow doping profiles. In view of the planar structure of thin films, analysis of the in-depth distribution of chemical composition with high resolution is of primary importance. Numerous nondestructive and destructive methods have been developed for this purpose /2,3/. Among the various techniques, surface analysis methods in combination with ion sputtering are most frequently applied because they are applicable to almost any kind of solid material and allow the attainment of concentration depth profiles over a wide depth range from atomic thin films up to several micrometers. The combination of microsectioning by ion sputtering with surface analysis techniques based on Auger electron spectroscopy (AES) and X-ray photoelectron spectroscopy (XPS), is most frequently applied /4/. The main reason is the small depth of information of these techniques of the order of 1 nm, which is a prerequisite for obtaining depth profiles with a high depth resolution. However, ion sputtering is not an ideal layer-by-layer erosion but is the result of a

complex ion beam-sample interaction process. Various phenomena, the most important of which are due to ion beam induced changes of surface roughness and composition, limit the experimentally achievable depth resolution /5,6/. In this work the principles of the AES depth profiling and its fundamental capabilities and limitations will be discussed and illustrated by depth profiles of the characteristic samples.

2. AES depth profiling: instrumentation and experimental procedure

Any commercial equipment for AES depth profiling comprises an electron energy analyser, an electron source, an ion gun and the sample stage all mounted in a stainless steel chamber in which an ultra-high vacuum (UHV $\leq 10^{-7}$ Pa) can be maintained (Fig. 1). The regime of UHV prevents the contamination of the sample surface during analysis with reactive gases such as CO, H_2O and C_xH_y. Inert gases (e.g. argon, xenon) showing no chemisorption can be tolerated up to pressures that my be several orders of magnitude higher than those of reactive gases /5/.

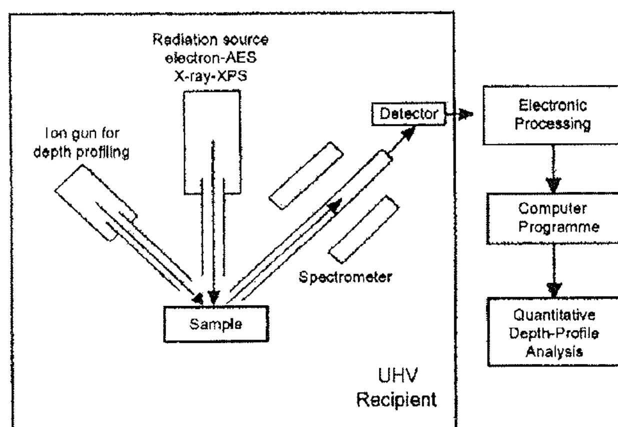

Fig. 1. Schematic showing the arrangement of instrumental parts of a typical AES (XPS) depth-profile analysis instrument (adapted from Ref. /7/).

Instrumentation for AES depth profilng requires a source of energetic ions impinging on the sample surface and an AES analysis of the residual surface after a certain sputtering time. Auger analysis can be done either discontinuously after subsequent sputtering steps or by continuous sputtering and simultaneous electron spectroscopy.

The most frequently used ion guns in AES instruments are simple electrostatic devices where the inert Ar ions are generated by collisional excitation with electrons from a hot filament. The positive ions are accelerated to energies between 0,2 and 5 keV and are focused on the sample surface, creating a sputtering spot of typically 1-5 mm in diameter. The pressure in the ion formation chamber should be about 4×10^{-3} Pa. For precise depth profiling, an ion gun with x/y beam deflection capability should be used. This enables the exact matching of analysed and sputtered areas. Rastering of the well-focused ion beam over an area up to 10 x 10 mm greatly improves the uniformity of the ion density and leads to a flat bottom of the sputtering crater which is necessary for optimum depth profiles. To optimize the sputtering conditions with respect to a specific sample topography, a sample stage with both tilt and rotation capabilities was introduced.

3. Evaluation of depth profiles

In AES depth profiling a continuous sputtering and simultaneous electron spectroscopy is most frequently used together with multiplexing of different element peaks and a display of the respective Auger peak-to-peak heights (APPH) as a function of the sputtering time. Sputter erosion and surface analysis are complex processes and a variety of experimental factors generally impede a straightforward data evaluation /5/.

The raw data of a depth profiling experiment consists of an elemental signal intensity, I , as a function of the sputtering time, t. The aim of the quantification of a depth profile is to obtain the original in-depth distribution of the composition, c(z), from the measured data, I(t). Therefore the following three fundamental procedures are necessary /7/: (a) conversion of the measured sputtering time t into sputtered depth, z=f(t), (b) conversion of the measured elemental intensity I to the elemental concentration, c = f (I), (c) deconvolution of the measured profile by means of a depth-resolution function (DRF).

4. Depth resolution

The aim of any AES depth profiling is to get a depth profile which can be comparable as closely as possible to the original elemental distribution with depth. A measured depth profile generally differs from the true in-depth distribution of composition owing to a large number of distortional effects /5-7/. The factors which contribute to the broadening of the interfaces can be roughly categorized as instrumental factors, effects depending an sample characteristics and the effects of ion beam-sample interactions. The most important causes of profile distortions include original surface roughness and sputtering-induced roughness, atomic mixing, information depth, preferential sputtering and nonuniform ion beam intensity.

A measure of profile broadening is the depth resolution Δz. By convention, the depth resolution corresponds to the distance over which a 16% to 84% (or 84% to 16%) change in signal is measured /5,8/. The generally accepted definition for the depth resolution is $\Delta z = 2\sigma$, where σ is the standard deviation of the corresponding Gaussian resolution function /5/. The depth resolution, Δz, can be directly determined in the depth profile of a sharp A/B interface as shown schematically in Fig. 2.

All contributions Δz_i from different physical phenomena mentioned so far caused the profile broadening. Assuming depth resolution functions of approximately Gaussian shape and mutual independence, these contributions add up in quadrature /5,7/: $\Delta z = [\Sigma (\Delta z_i)^2]^{1/2}$. For the single sandwich layers (A/B/A) and multilayer

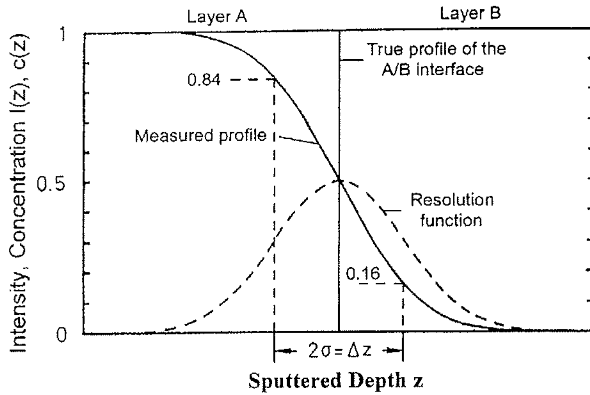

Fig. 2. Broadening of the measured profile and definition of the depth resolution, Δz (84-16%) ≈ 2σ, for a Gaussian resolution function; σ = the standard deviation (adapted from Ref. /5/).

structures (A/B/A/B...), Δz can be extracted from the amplitude of the concentration profiles /5/.

The depth resolution of the multilayered samples with atomically flat interfaces is mainly determined by the influence of the following three fundamental parameters: atomic mixing (M), roughness (R) and information depth (I). Recently, this influence is quantitatively described by the so-called mixing-roughness-information depth model (MRI-model) /9/. Optimized depth profiling with $\Delta z \cong 2$ nm can only be achieved if these three parameters are minimized /11/.

5. AES depth profiles of selected samples

Multilayer structures are of great importance in the fabrication of semiconductor devices and also have become indispensable as reference materials in depth profiling, particularly for the determination of depth resolution Δz as a function of the sputtered depth /10-12/. Quite often, Δz is degraded mainly by the sample surface roughness, and this occurs both on samples with an initial roughness of the surface /13,14/ and on originally smooth samples with roughness induced by ion sputtering during depth profiling /15,16/. It was shown that the decisive parameter influencing the dependence of Δz on surface roughness is the angular distribution of the differently oriented microplanes /17,18/. Sputtering induced surface roughening is generally caused by local differences in the sputtering rate, because the sputtering yield is dependent on the ion incidence angle with respect to the crystallographic orientation of polycrystalline metallic materials /19/. However, even for homogeneous samples with smooth surfaces, the dependence of the sputtering yield on the angle of ion incidence remains a distortional effect.

The effect of an initial roughness on Δz was studied on two different multilayer structures sputter deposited on polished single-crystal (111) silicon substrates /20/. The first sample (No. 1) consisted of an Ni/Cr multilayer with a total of 16 alternating Ni and Cr layers with a single layer thickness of 30 nm. The second sample (No. 2) had on the top of the Ni/Cr multilayer, an additional crystalline Al layer with an average thickness of ~ 40 nm.

Figure 3 shows the AES depth profiles of two different multilayer structures obtained by ion sputtering of stationary samples by using two symetrically inclined ion

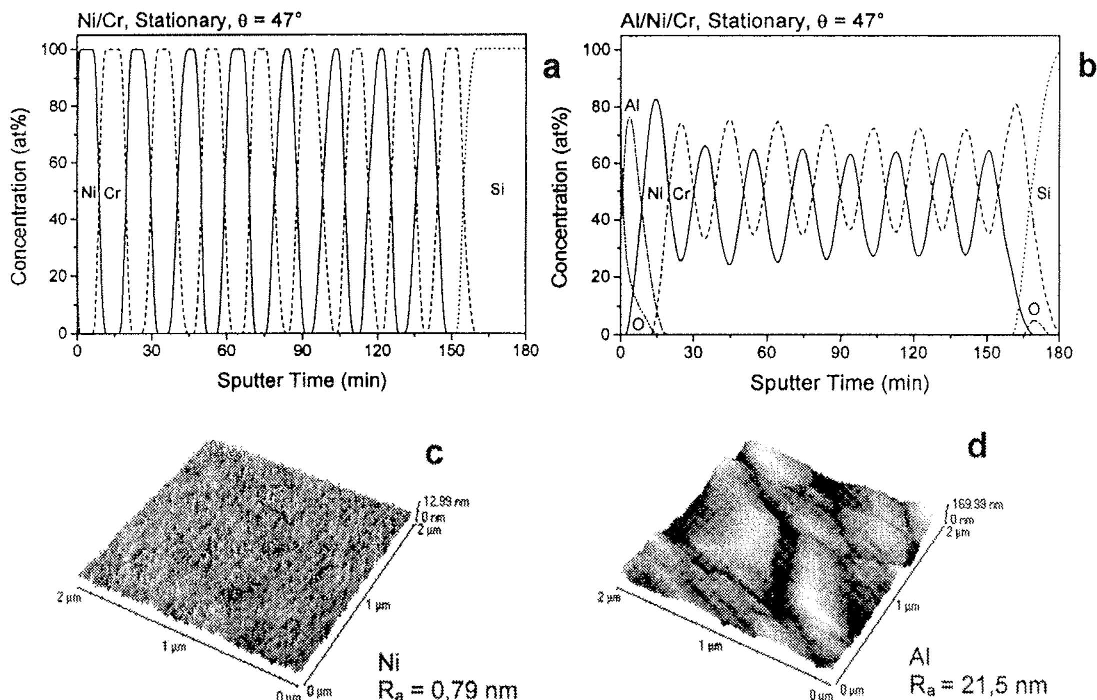

Fig. 3 a,b,c,d. AES depth profiles (a) of the Ni/Cr and (b) Al/Ni/Cr multilayers obtained by ion sputtering of stationary samples with 1 keV Ar^+ ions at an incidence angle of 47°. Atomic force microscopy images showing the surface features of (c) as-deposited Ni and (d) Al surface layers lying on the top of two Ni/Cr multilayer samples /20/.

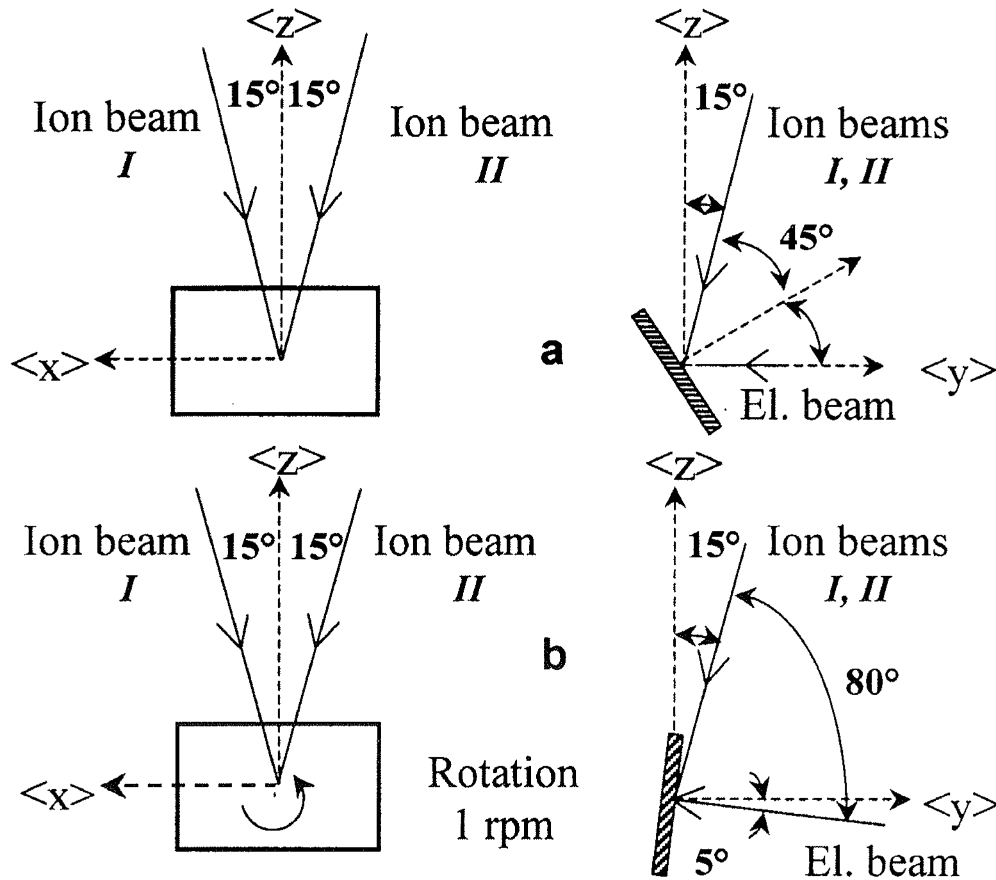

Fig. 4 a, b. Geometry of the experimental arrangement in rectangular x, y, z coordinates in a plane perpendicular (left) and parallel (right) to the electron beam, respectively; (a) stationary sample, $\theta = 47°$ and (b) sample rotation and grazing incidence ion beams, $\theta = 80°$.

guns at an incidence angle of 47° (Fig. 4a); note $\theta = \arccos(\cos 15° \times \cos 45°) \cong 47°$. The AES depth profile of the uncovered Ni/Cr multilayer (Fig. 3a) shows relatively sharp interfaces. In contrast, the depth profile in Fig. 3b obtained on the Ni/Cr sample covered with the crystalline Al layer shows a strong broadening of the interfaces. The surface topography of both as deposited multilayers (No. 1 and No. 2) was examined by atomic force microscopy (AFM). The AFM data reveled that the Ni/Cr multilayer has a smooth surface with a roughness amplitude R_a = 0,79 nm (Fig. 3c) and the Ni/Cr multilayer covered with a crystalline Al layer exhibited a rough surface with R_a = 21,5 nm (Fig. 3d). Obviously, the rough crystalline Al surface layer caused in-depth topographical changes of the Ni/Cr multilayer and strongly deteriorated the depth resolution of the originally sharp internal interfaces.

The degradation of the depth resolution due to angle-dependent effects like surface roughness and crystalline orientation can be reduced by multidirectional ion bombardment which is achieved by sample rotation during depth profiling /21/. For the Al/Ni/Cr sample the optimized depth profile similarly to that shown in Fig. 3a was reached only with rotational depth profiling at a grazing incidence angle of about 80° (Fig. 4b). Multidirectional ion bombardment during rotational AES depth profiling at grazing incidence angle removes the crystalline orientation effect, promotes the smoothing effect and decreases the microroughness of the initially rough Al/Ni/Cr sample surface /20/.

It is often necessary to determine the layer composition or interfacial contamination within metallization structures such as vias and contacts during semiconductor device characterization or failure analysis. Compucentric rotation of the sample during ion sputtering allows the acquisition of depth profiles on specific features which do not reside directly over the stage rotation axis /22/.

Aluminum, a common conductor used in semiconductor devices, is particularly prone to cone formation during sputter etching. Fig. 5a shows as-received circuit and Fig. 5b shows an Al via before AES depth profiling. Figs. 5c,d show the topographies obtained at the Al vias after depth profiling without (Fig. 5c) and with sample rotation (Fig. 5d) during sputter etching. In Fig. 5 are shown the corresponding AES depth profiles obtained without (S) and with (R) sample rotation. The sample rotation prevent the cone formation (Fig. 5c) and the depth profile (R) has a much sharper Al/Si interface, which permits a better estimation of possible interdiffusion or reaction between layers.

As-recieved circuit

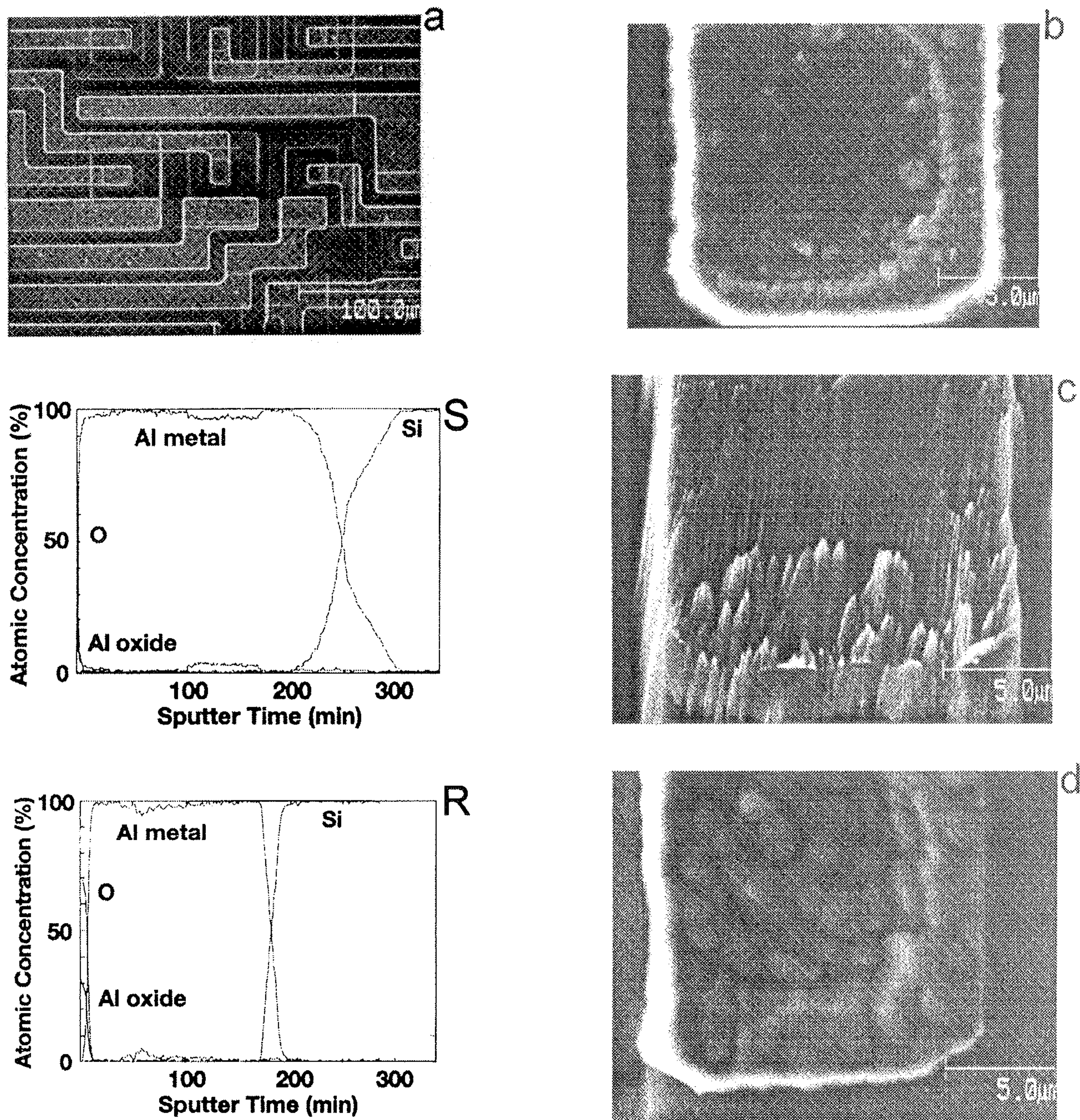

Fig. 5 a, b, c, d. Secondary electron images show: (a) as-received circuit, (b) an Al via before ion etching, (c) an Al via after sputter depth profiling without and (d) with sample rotation. AES sputter depth profiles obtained without (S) and with (R) rotation of the sample are shown too /22/.

The sample rotation during depth profiling was introduced also in other surface analytical techniques such as photoelectron X-ray spectroscopy (XPS) and secondary ion mass spectroscopy (SIMS). The desire to provide hard disk media with higher storage density has caused the development of magnetic media with more complex multilayer structures with different individual layer thicknesses. In Fig. 6 are shown the components of a typical hard disk /23/. XPS depth profiling has been routinely applied to thin film systems up to a few hundred nanometers in thickness. The modern ion guns and the ability to change sputter rates, under computer control, during a depth profiling make it possible to efficiently depth profile thicker films. In Fig. 7 is shown a sputter depth profile through all the layers on the hard disk, approximately 14 μm in thickness /23/. During depth profiling of the thinner layers the ion gun was set at 2 kV and the sputter rate was approximately 6 nm/minute. For the thicker layers, the ion gun was set to 4 kV and adjusted for a sputter rate of 46 nm/minute. This type of flexibility allowed one depth profile to be used to collect detailed information from the thin mag-

netic layers and the thick NiP layer in a reasonable amount of time. Additionally, the spectra from the detailed depth profile made it possible to examine the chemistry at interfaces and within layers /23/.

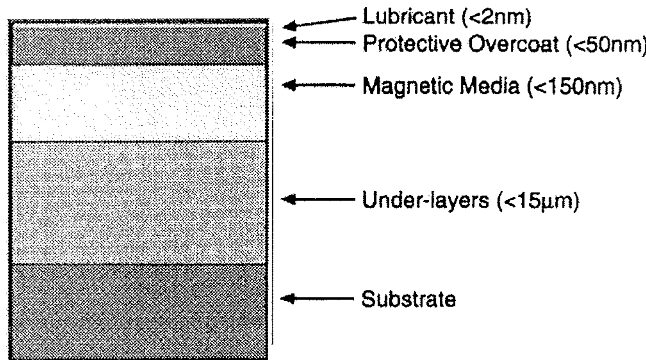

Fig. 6. The scheme of the multilayer structure of a typical hard disk /23/.

The preparation of well-characterized silicide thin films for microelectronics needs a control of interfacial reactions and diffusion processes during heat treatment of metal semiconductor systems. The precise observation of AES depth profiles at interfaces and quantification of the interface width of heat treated samples enables the determination of the main moving species in the early stage of reactions, the calculation of the effective interdiffusivity and the characterization of the new formed reaction products /24,25/.

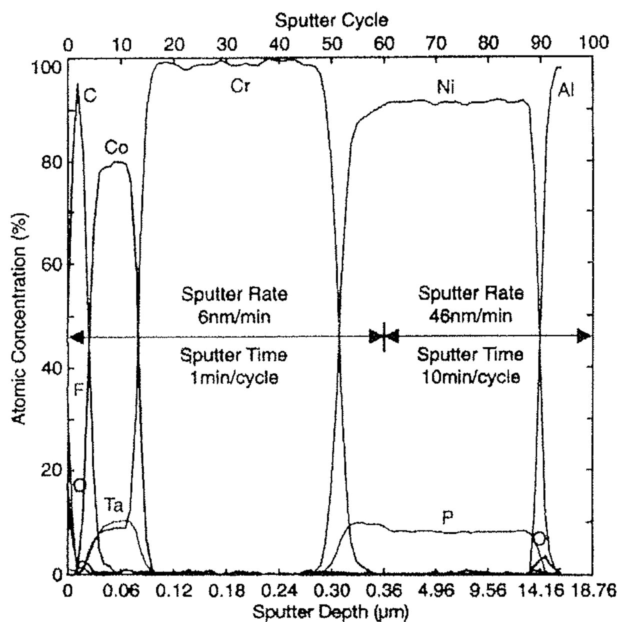

Fig. 7. Sputter depth profile of the thin lubricant film, the thin magnetic layers and the thick underlayers obtained by programming a change in etch rate and sputtering time during the depth profiling /23/.

Figure 8a shows the sandwich structure of Si(33 nm)/Ni(50 nm)/Si(33 nm), with a total thickness of 116 nm which was sputter deposited onto smooth silicon (111) substrate. The reaction of Ni with amorphous silicon thin films was activated in a differential scanning calorimeter (DSC), at heating rate of 40 °C min^{-1}. Already with a heating of the Si/Ni/Si sample from room temperature to 320 °C the reaction between Si and Ni layers is almost accomplished (Fig. 8b), and the reaction product shows a composition close to Ni_3Si_2. However, the selected area diffraction pattern of this cross-sectioned sample showed the presence of two polycrystalline and amorphous phases, namely Ni_2Si and NiSi /24/. The mixture of these two phases is in agreement with an Ni/Si ratio of 3:2, recognized in the AES depth profile in Fig. 8b. The results show the importance of compositional and structural data obtained with different analytical techniques for the precise characterization of reaction products.

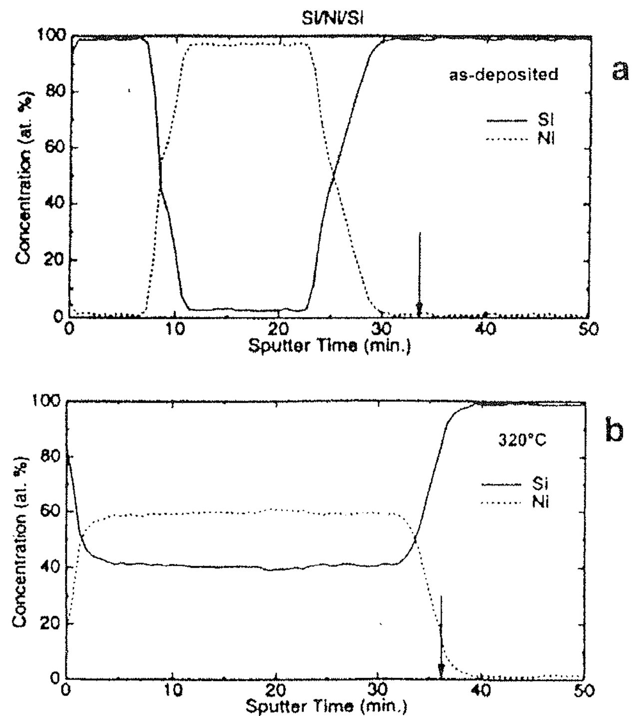

Fig. 8 a, b. AES depth profiles of Si/Ni/Si sandwich layer: (a) as-deposited and (b) after dynamic heating in a DSC instrument at a rate of 40 °C min^{-1} from room temperature to 320 °C.

7. Conclusions

Compositional depth profiling of thin films and multilayer structures by AES in combination with ion sputtering is the most frequently applied method to obtain the in-depth elemental distribution. A precise quantitative depth profiling requires a quantification of both the analysed elemental signal intensities in concentration units, and the sputtering time in a depth coordinate. The large number of physical parameters, depending on

sample characteristics, ion beam-sample interactions, and instrumental factors, lead to a broadening of a measured profile. A measure of profile broadening is the depth resolution Δz. By convention, the depth resolution is $\Delta z = 2\sigma$, which corresponds to the difference of the depth coordinate between 84 and 16 % of the intensity change at an interface. Depth resolution in depth profiling of the multilayer structures with atomically flat interfaces is determined by three parameters: atomic mixing, surface roughness and information depth and their influence is quantitatively described by the MRI-model. Optimized depth profiling with $\Delta z \cong 2$ nm can only be achieved if these three parameters are minimized /11/. Quite often, on technological samples Δz is degraded mainly by the sample surface roughness. The degradation of the depth resolution due to angle-dependent effects like surface roughness and crystalline orientation can be reduced by multidirectional ion bombardment. As illustrated by AES depth profiling of the Ni/Cr and Al/Ni/Cr multilayer samples, and by the Al/Si metallization structure of a semiconductor device, the sputtering of the rotated sample at large ion incidence angle and relative low ion beam energy (≤ 1 keV), promotes the smoothing effect and decreases the microroughness of the initially rough sample surface, thus enabling us to achieve the improved depth resolution. Further, the applicability of the depth profiling is illustrated by the depth profile of the multilayer structure of a typical hard disk and by the characterization of reaction products in the heat treated Si/Ni/Si thin-film structure.

ACKNOWLEDGMENTS

The technical assistance given by Mr. J. Kovač and Mr. B. Praček (Institute of Surface Engineering and Optoelectronics, Ljubljana) is gratefully acknowledged. The author is also pleased to thank to Professor S. Hofmann (Max-Planck-Institut für Metallforschung, Stuttgart) and to the Physical Electronics company (Ismaning) for allowing him to use their experimental results (Figs. 1, 2 and 5-7). The work was supported by the Ministry of Science and Technology of Slovenia (Project J2-7641-1534-00).

8. References

/1/ M. Ohring, The materials science of thin films, Academic Press, London, 1992, ISBN 0-12-524990-X.

/2/ A. W. Czanderna (Ed.), Methods of surface analysis, Elsevier, Amsterdam, 1975, ISBN 0-444-41233-8.

/3/ J. M. Walls (Ed.), Methods of surface analysis, Cambridge univ. press, New York, 1989, ISBN 0 521 30564 0.

/4/ D. Briggs and M. P. Seah (Eds.), Practical Surface Analysis, second edit., Vol. 1. Auger and X-ray Photoelectron Spectroscopy, Wiley, Chichester, 1990, ISBN 0-471-92081-9.

/5/ S. Hofmann, Depth Profiling in AES and XPS, in Ref. 4, 143-199.

/6/ S. Hofmann, "Sputter depth profile analysis of interfaces", Rep Prog. Phys. 61, 1998, 827-888.

/7/ S. Hofmann, "Sputter depth profiling of thin films", High Temperature Materials and Processes, Vol. 17, No. 1-2, 1998, 13-27.

/8/ American society for testing and materials (E 673-90), Surf. Interface Anal., Vol. 17, No. 13, 1991, 951-958.

/9/ S. Hofmann, "Atomic mixing, surface roughness and information depth in high-resolution AES depth profiling of GaAs/AlAs superlatlice structure", Surf. Interface Anal., Vol. 21, 1994, 673-678.

/10/ S. Hofmann, W. Mader, "Determination of the atomic mixing layer in sputter profiling of Ta/Si multilayers by TEM and AES", Surf. Interface Anal., Vol. 15, No. 12, 1990, 794-796.

/11/ A. Rar, S. Hofmann, K. Yoshihara, K. Kayiwara, "Optimization of depth resolution parameters in AES sputter profiling of GaAs/AlAs multilayer structures", Appl. Surf. Sci., Vol. 144-145, 1999, 310-314.

/12/ D. W. Moon, J. Y. Won, K. J. Kim, H. J. Kim, H. J. Kang, M. Petravic, "GaAs delta-doped layers in Si for evaluation of SIMS depth resolution", Surf. Interface Anal., Vol. 29, No. 6, 1999, 362-268.

/13/ A. Zalar, S. Hofmann, "Depth resolution of multilayer Cr/Ni thin films structures deposited on substrates with different roughness", Vacuum, Vol. 37, No 1, 1987, 169-173.

/14/ A. Zalar, S. Hofmann, "Superposition of Auger electron spectroscopy depth profiles obtained on Cr/Ni multilayer samples with different roughnesses", J. Vac. Sci. Technol., A5, 4, 1987, 1209-1212.

/15/ M. Tanemura, S. Fujimoto, F. Okujama, "Auger depth profiling of polycrystalline metal films using Xe^+ and N_2^+ ions", Surf. Interface Anal., Vol. 15, 1990, 537-540.

/16/ K. J. Kim, K. - H. Jung, "Mechanism of facet formation on Ni surfaces by sputtering with oxygen ion beams", Surf. Interface Anal., Vol. 26, No. 3, 1998, 224-232.

/17/ M. P. Seah, C. Lea, Thin Solid Films, Vol. 81, 1981, 257-270.

/18/ T. Wöhner, G. Ecke, H. Rössler, S. Hofmann, "Sputtering-induced surface roughness of polycrystalline Al films and its influence on AES depth profiles", Surf. Interface Anal., Vol. 26, 1998, 1-8.

/19/ W. Hösler, W. Pamler, "Effects of crystalinity on depth resolution in sputter depth profiles", Surf. Interface Anal., Vol. 20, 1993, 609-620.

/20/ A. Zalar, B. Praček, P. Panjan, "Effects of surface structure on depth resolution of AES depth profiles of Ni/Cr multilayers", Surf. Interface Anal., Vol. 29, 2000, in press.

/21/ A. Zalar, "Improved depth resolution by sample rotation during Auger electron spectroscopy depth profiling", Thin Solid Films, Vol. 124, 1985, 223-230.

/22/ K. D. Childs, D. F. Paul, "Compucentric Zalar profile of a 10 μm Al pad using the PHI 680 scanning Auger nanoprobe™", Physical Electrronics application note 9710,1997, 1-3.

/23/ J. Moulder, D. Hook, "The hard disk detective", Physical Electronics application note 9807, 1997, 1-4.

/24/ A. Zalar, S. Hofmann, F. Pimentel, P. Panjan, "Interfacial reactions and silicide formation in Si/Ni/Si and Si/Cr/Si sandwich layers", Surf. Interface Anal., Vol. 21, 1994, 560-565.

/25/ A. Zalar, S. Hofmann, P. Panjan, "Characterization of chemical interdiffusivities at silicon/metal interfaces in initial reaction stages", Vacuum, Vol. 48, No. 7-9, 1997, 625-627.

Anton Zalar
Institute of Surface Engineering and Optoelectronics
Teslova 30, 1000 Ljubljana, Slovenia
anton.zalar@guest.arnes.si

Prispelo (Arrived): 1.10.2000 Sprejeto (Accepted): 25.11.2000

 UDK621.3:(53+54+621+66), ISSN0352-9045

CHARACTERIZATION OF DIELECTRICS ON THE "TIPS OF NEEDLES"

John J. Hren, Victor V. Zhirnov, Zlatko Sitar, & Gregory Wojak
Dept of Materials Science and Engineering
North Carolina State University, Raleigh, USA

TUTORIAL INVITED PAPER
MIDEM 2000 CONFERENCE – Workshop on ANALYTICAL METHODS IN MICROELECTRONICS AND ELECTRONIC MATERIALS
18.10.00 – 20.10.00, Postojna, Slovenia

Keywords: AFM spectroscopy, Atomic Force Microscopy spectroscopy, molecule imaging, atomic resolution, SPM, Scanning Probe Microscopy, AP, Atomic Probes, tips of needles, spectrum of surface, FEM, Field Emission Microscopes, FIM, Field Ion Microscopes

Abstract: Ultra sharp needles are commonly used as electron sources in transmission electron and as probes in several scanning tunneling microscopies to characterize the atomic structure of surfaces and to probe local electronic properties. The physical basis for such measurements has evolved from much earlier research on field electron emission, which continues to this day. Recent attempts to develop miniature field emission based devices (i.e. Vacuum Microelectronics) have led to studies of thin dielectric coatings, which were found to considerably improve both the emissive properties and "ruggedness" of the emitters. In trying to understand the underlying Physics, extensive measurements have been reported on the energy distribution of the field emitted electrons (FEED), as well as the nanostructure of the coatings and their underlying interfaces with the needle shaped substrates (HREM). In turn, these techniques can also be employed more widely as an analytical strategy to determine the correlation between electrical properties and structure of nanometer scale films and particles deposited onto the tips of needle-shaped emitters. Further information on the same specimens can be also obtained by field emission microscopy (FEM), by using such probes in an STM mode, by studying the controlled effects of high electric fields on chemical reactions,or on the structure of ferroelectric or magnetic coatings, etc. Controlled deposits of either nanoparticles or films also offer a unique opportunity to directly probe property changes of a given material during the transition from classical to quantum An important advantage is the ability to achieve truly direct correlation between properties and nanostructure, since no further specimen preparation is required for HREM studies and specimens may be easily transferred from one instrument to another. Examples will be given of the information obtained from thin films & particle deposits of: nanodiamond, aluminum and boron nitride, and aluminum oxide.

Vrednotenje dielektričnih materialov na merilnih konicah

Ključne besede: AFM spektroskopija sile atomske, upodabljanje molekul, ločljivost atomska, SPM mikroskopija s sondo skanirno, AP sonde atomske, konice igel, spektrum površine, FEM mikroskopi emisije polja, FIM Mikroskopi z ioni polja

Izvleček: Ultra ostre konice danes pogosto uporabljamo kot izvore elektronov v transmisijskih elektronskih mikroskopih ali pa kot merilne konice v različnih rasterskih tunelskih mikroskopih z namenom vrednotiti atomsko strukturo površin ali meriti lokalne elektronske lastnosti vzorca. Fizikalne osnove tovrstnih meritev so se razvile iz zgodnjih raziskav poljske emisije elektronov, ki se nadaljuje še danes. Najnovejši poskusi razviti miniaturne elektronske komponente na osnovi poljske emisije (novo področje imenovano vakuumska mikroelektronika) so privedli do raziskav tankih dielektričnih prevlek, za katere se je ugotovilo, da bistveno izboljšajo emisijske lastnosti in robustnost emiterjev. Z namenom razumeti fizikalno ozadje tega pojava, je bilo opravljeno veliko število meritev energijske porazdelitve emitiranih elektronov (FEED), kakor tudi nanostrukture prevlek in površin pod njimi oz. podlag v obliki konic (HREM).Opisane tehnike lahko uporabimo tudi širše kot neko vrsto analitične strategije za ugotavljanje korelacij med električnimi lastnostmi in strukturo filmov in delcev na nanometrskem nivoju nanešenih na emiterje v obliki konic. Dodatno informacijo o vzorcih lahko dobimo z uporabo poljske emisijske mikroskopije (FEM), z uporabo istih konic v STM načinu dela, ko lahko študiramo kontrolirane vplive visokih električnih polj na kemijske reakcije ali celo na strukturo feroelektričnih ali magnetnih prevlek. Kontrolirani nanosi bodisi nanodelcev ali filmov ravno tako ponujajo enkratno priložnost direktne meritve sprememb lastnosti materiala pri prehodu iz klasičnega v kvantno stanje. Zelo pomembna prednost je možnost doseči resnično direktno korelacijo med lastnostmi in nanostrukturo, saj ni potrebna nobena dodatna priprava vzorca za HREM preiskave, vzorci pa se tudi zlahka prenašajo iz enega instrumenta v drugega. V prispevku so podani primeri preiskav in dobljene informacije na nanešenih filmih in delcih in sicer nanodiamanta, aluiminija, borovega nitrida in aluminijevega oksida.

Introduction

Since the mid 1980's, ultra sharp needles have been used as probes for a variety of scanning probe techniques primarily to study a spectrum of surface or near surface features. A seemingly endless variety of such techniques is constantly being invented. Their attractiveness includes: simplicity, high resolution, adaptability to a variety of environments, etc. Only rarely is the probe itself employed as the object of analysis, and then usually to aid in the interpretation of some surface feature. On the other hand, the tips of sharp needles have been the primary object of FEM, FIM, and Atom Probe (AP) studies for many decades. Electron microscopic techniques (SEM, TEM, HREM, ELS, EDS) have been frequently combined with the FIM &/or AP on studies of the tips of needles. In fact, it is very desirable to combine the strengths of the above methods into a powerful analytical strategy that offers unique prospects in studies of thin dielectric films or nanoparticles. The present paper will briefly review some of the features of each relevant technique, describe examples where several modes of analysis have been combined to advantage, give recent results from extensions of this approach, and finally suggest prospects for further extensions, particularly for nm scale dielectric films and particles.

Field Emission, Field Ionization, and the Atom Probe

Field electron emission was the basis for very early attempts to develop a point projection electron microscope or Field Emission Microscope /1/. Attempts to image molecules were made very early and had some success, but the resolution was limited by the transverse spread of the emitted electrons to ~2nm and the high electric fields (~10^9 V/m) affected the molecular deposits. A point projection microscope with higher resolution was soon developed by E. W. Mueller, by simply reversing the bias on the needle, cooling the specimen to cryogenic temperatures, and field ionizing an inert gas, e.g. He or Ne, leaked in as a background gas at pressures of ~10^{-4} Torr. Mueller thus achieved true atomic resolution for the first time (Fig1d) with a Field Ion Microscope (FIM) /2/. But the electric fields required were another order of magnitude higher (~10^{10} V/m), so high that the tip of the needle could be made to field evaporate. The bulk and shear stresses induced by these electric fields were correspondingly high (~1/10 the bulk modulus) and could distort or eliminate features of interest (e.g. point defects, dislocations, boundaries, etc) /3/. However, field evapo-ration could be employed in a pulsed mode (using voltage or laser pulses) to make the needle a controlled source of ions for a time-of-flight (TOF) mass spectrometer that achieved single ion sensitivity and became known as an Atom Probe /4/. If a heavy liquid on the surface of a needle was desorbed by field evaporation, it became the source for a focused ion beam or FIB. By substituting a sensitive two dimensional detector, such as a channel plate, just in front of a phosphor screen, the features of both atomic imaging and TOF spectrometry could be achieved. Such a combined instrument became known as an Imaging Atom Probe /5/.

Surface Studies using Field Electron Emission

Once it became clear that the field emission electron microscope (strictly FEEM but almost always abbreviated FEM) had physically insuperable limita-tions on its resolution (~2nm) and specimen configuration (the tip of a needle of radius $<10^{-6}$ m), it was only infrequently used for its original purpose. But at the same time it became obvious that the FEM was a powerful tool to study the surfaces of conductors and semiconductors /9/. Surface studies, however, required vacuums of ~10^{-11} Torr to permit a sufficient interval to conduct useful experiments and UHV conditions were (and are) not easy to achieve and maintain. But once achieved, such vacuums permitted studies of the properties of truly clean surfaces of most metals and some semiconductors for the first time. The practical consequence was the development of the first experimental tool of the new field of Surface Science and the incentive to develop an entire array of new techniques for surface characterization (e.g. AES, SIMS, etc).

Attempts to clean the (approximately) hemispherical tip of the needle-shaped specimens by heating in UHV conditions, yielded surfaces that were not smooth at the atomic level, but developed flat facets dominated by the closest packed (or lowest energy) planes. The FEM images from such specimens gave a magnified image of the relative probability for electron emission over a range of orientations. The relative size of these facets reflected their relative surface energy, detailed specimen geometry, the applied field during heating, the ultimate temperature and time, background gases & pressures (even at $<10^{-11}$ Torr), etc. By placing a moveable aperture placed near the magnified FEM image and measuring only those electrons that passed through, the Fowler-Nordheim equation could be applied to deduce the work functions of different crystalline orientations and the effects of adsorbates, atomic order, defects, etc. Significantly different values were obtained for different orientations and surface effects, so that the very meaning of the work function became an object of scientific study. Adsorbates, not surprisingly, were found to also react anisotropically; indeed they could alter the measured work function, quite dramatically Atomic and molecular adsorbates could also be viewed directly by the FEM, even as they migrated on specimen surfaces, even at cryogenic temperatures. Thus as many questions as answers emerged. Were these effects due to the experimental conditions or were they fundamental properties? It became obvious that even more data was required from the tips of needles, under closely controlled conditions. But in addition, independent data from the other characterization tools of surface science now became essential.

The Field Emission Energy Distribution (FEED)

Significant new data came first from an obvious extension of the evolving methods of FEM. A more comprehensive theory of the energy distribution of the field emitted electrons was developed and applied to the methods already well known for measuring data for Fowler-Nordheim plots. Adding an electron spectrometer behind a phosphor viewing screen with an aperture and the capability of translating the image (e.g. by deflection) permitted the measurement of both I-V data and the emitted energy distribution of the emitted electrons. With this capability, theory could truly be tested against experimental data. Not only could an understanding of the fundamental physics thus be improved, but the distribution of the electron supply (i.e. the band structure) of the electron source could be measured directly. And the influence of crystallographic orientation, adsorbates, disorder, alloying, defects, etc could now be investigated independently and quantitatively. This experimental approach became known as the Field Emission Energy Distribution (FEED) and has continued to evolve until the present. However, FEED has remained noncommercial; that is, FEED systems have not become very common surface science tools and each remains custom made for the needs of a specific researcher /6/.

Scanning, Transmission and Analytical Electron Microscopy

Researchers conducting Material Science studies of grain boundaries, defects, or precipitates by FEM, FIM and FEED techniques soon recognized that both the Scanning Electron Microscope and Transmission Electron Microscopes (SEM and TEM) were invaluable ancillary tools /7/. This coupling was especially fortuitous for TEM users, since the tips of needles de facto made excellent specimens which required no further preparation. The preparation of representative TEM specimens has always been a fundamental barrier to the correlation between the microstructures and properties. How could you be certain that the microstructural features you observed in a TEM specimen were directly related to the phenomena under investigation, when by the very act of preparing the specimen you were forced to remove most of the material surrounding features of interest? Is the volume of material remaining representative of the bulk specimen properties? By using a needle as the specimen, FEM and/or FIM related analytical methods could be applied first, then viewing the very same specimen in a TEM and/or SEM with no preparation steps between, you can be quite confident of the relationship and relevance of the two sets of data. Of course, all of the ancillary analytical techniques available with TEM or SEM (e.g. EDS, ELS, SE or BSE, etc) can be also brought to bear. A pertinent example comes from some recent studies of oxide films on Al needles . A controlled electric field, inherent to the needle shape, was used to first damage the oxide. The damaged oxide was later exposed to a corrosive environment, which led to the initiation of corrosion at the damaged site. These corrosion products were then analyzed by TEM and ELS. Earlier studies by FIM, IAP, and TEM of the structure and composition of grain boundaries, precipitates, and interfaces, effectively demonstrated the advantages and simplicity of obtaining combined information from specific sites /7/.

Scanned Probe Techniques

Scanning tunneling microscopy, STM evolved quite naturally as variations on the utility of FEM continued to develop. Since the current of emitted electrons was exponentially sensitive to the electric field, which in turn was determined by the applied potential and specimen geometry, why not vary one while keeping the other fixed as a sensing device? Indeed, several kinds of sensors with impressive sensitivity were shown to confirm this as a viable approach. Why not then a device where a sharp needle at constant potential could be used as a probe to slowly scan very near a roughened surface, which should yield large variations in current that could be used to map surface topography? Or as a variation, a constant current is maintained, while the varying potential would reflect topography? These were the kinds of thinking that went into early versions of the development of a Topografiner, as it was called. But this concept did not work as well as hoped because of complications arising from the sensitivity to external vibrations, which then affected the needle to surface spacing. Indeed overcoming this vibrational barrier led to the development of the first STM and a Nobel prize in the mid 1980s. The pleasantest surprise from this achievement was the excellent lateral resolution obtained with the STM, a capablity of resolving the dimensions of a single atom! Indeed this development opened the floodgates to the emergence of many variations on the STM, which are still emerging and referred to as Scanning Probe Microscopes (SPMs).

But common to all SPMs is a probe comprised of the tip of a needle and many are compatible with studies by FEM, FIM, AP and consequently the TEM, SEM, and AEM in combination. It is this formidable combination of techniques, that rely upon or can easily be used to analyze the tips of needles that we direct this paper. We argue that this combination of analytical techniques is unique in special abilities to characterize thin films and nanoparticles, especially dielectrics, which are major objects of modern research in Materials Science. Furthermore, coated needles have the potential for significant direct and indirect applications, e.g. in Vacuum Microelectronics or Nanolithography, or as intense electron sources for microwave communication. Also because of their very scale, the results obtained from their study are applicable to a wide spectrum of novel nanoelectronic devices now under intense development.

Examples of combined studies on the tips of field emitters

Some examples of the analytical approach promoted here are presented to illustrate its power and potential. The objectives of these studies were not to develop analytical tools, but rather to better understand field emission and thereby develop stable, intense electron sources for Vacuum Microelectronic applications. Field emission sources suitable for all such applications are required to operate at vacuum levels much poorer than those required for FEM studies (e.g.at ~10^{-6} Torr rather than 10^{-11} Torr). In addition, such emitters should be easy to fabricate, uniform in their properties, inexpensive, and highly reliable. Considerable progress has been made to achieve these aims in the last decade, most of which has come from understanding why coating needle-shaped emitters of silicon and molybdenum with carbon-based films and fine particles, as well as those of several other wide band gap dielectrics, substantially enhances and stabilizes emission, even under these very modest vacuum conditions. Some examples of the analytical methods employed for these studies and some of the pertinent results are summarized in the following.

Diamond and Amorphous Carbon Coatings on Si and Mo Emitters

The tips of needle-shaped silicon field emitters were coated with nanocrystalline diamond using "biased-enhanced" microwave plasma CVD /8/. Field emission from these emitters was enhanced by several orders of magnitude and the emission stability was significantly improved, as compared to uncoated silicon emitters. Transmission electron microscopy of the interfaces between the diamond deposits and the silicon substrate (Fig. 1) revealed that a thin (5-10 nm) silicon carbide phase formed, even though the maximum temperature during the deposition was limited to 500-600°C.

 Informacije MIDEM 30(2000)4, str. 210-215

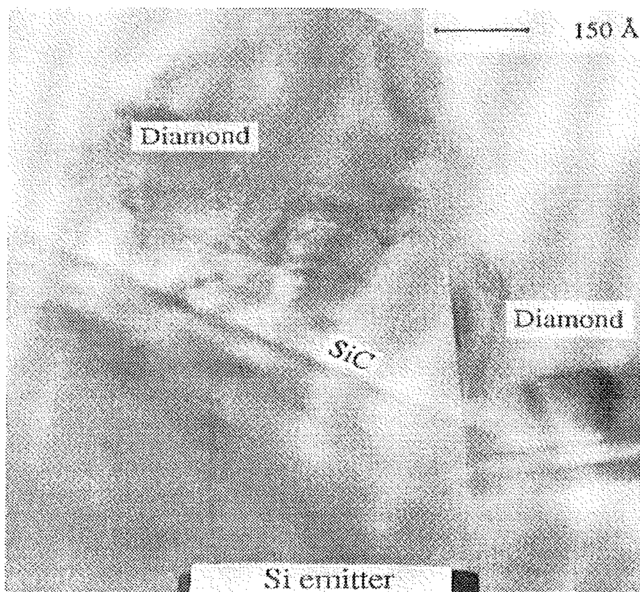

Figure 1 TEM of SiC nucleated at Si-diamond interface.

An attempt was made to achieve similar improvements in emission using what was thought to be "diamond-like" amorphous carbon deposits on silicon needles. The deposits were smooth and were deposited near ambient temperature. However, it became obvious that the emission currents were actually reduced. A TEM study of the coatings using ELS of the coating/silicon interfaces showed the coating to be comprised mainly of sp2 bonded C rather than the sp3 bonding. TEM (Fig 2) and ELS also revealed another unexpected result. There were ~10-20 nm sized crystals of Au present at the film-silicon interface /9/. The presence of these Au nanoparticles appeared to be a result of the method by which the silicon needles were originally grown and then precipitated during their storage and deposition treatments.

Parallel studies on needle-shaped Mo field emitters, examined several methods of depositing coatings. It was discovered that thin, extremely adherent layers of crystalline diamond powder could be deposited onto the tips of needles by dielectrophoresis, an especially simple and inexpensive, ambient coating technique /10/. Surprisingly, emission was further enhanced, even without thermal treatment; however, a low temperature (~400 °C) anneal in a hydrogen ambient, yielded even better emission and improved the emission stability. The thickness and uniformity of the deposits could be quickly checked by the SEM (Fig 3a) and the interface between the diamond deposits and the Mo substrate was observed by TEM to be surprisingly intimate (Fig 3b), but could be further improved by a low temperature anneal, which nucleated a nm scale molybdenum carbide interface layer.

The energy distribution of the field emitted electrons (FEED) from the dielectrophoretic diamond coatings on Mo also gave valuable information about the mechanism of the observed enhancement in emission /11/. FEED measurements were taken before and after

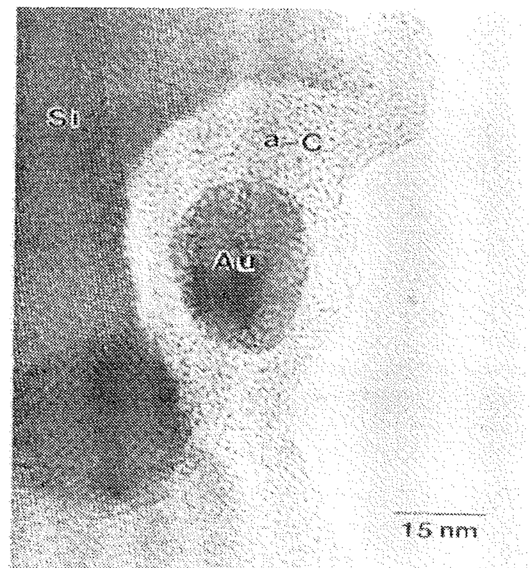

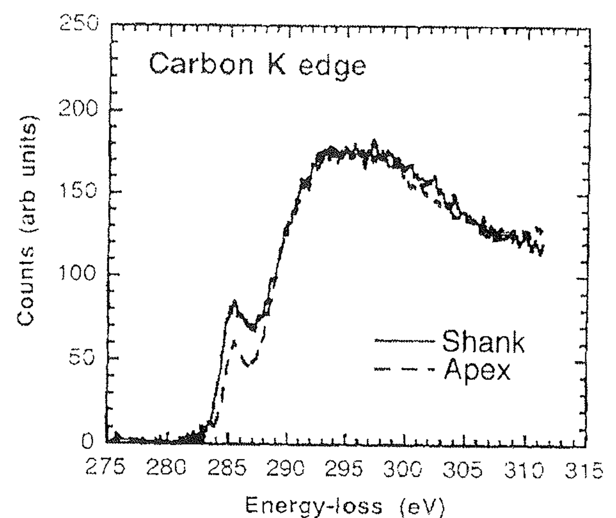

Figure 2. (a) TEM Au precipitates in amorphous C deposit (b) EELS spectra at apex and shank of amorphous C deposit.

deposition and spectra then compared. These measurements revealed that the emitted electrons originated from the diamond/vacuum interface after tunneling from the conduction band minimum of the diamond, but the nature of the Mo/diamond interface also played a significant since role, since it affected the electron supply to the diamond conduction band. A series of FEED studies (Figs 4a and 4b) of BN powders depo-sited by dielectrophoresis onto Mo needles, illustrates its effectiveness in helping to deduce the mechanisms of emission and the basis for the enhancement in emission /6/.

More recently, we have been depositing nanodiamond particles by dielectrophoresis onto Mo emitters, varying the deposition conditions widely. Typical results at very short deposition times are given in Fig. 5. There is a marked preference top deposit at the very tip of the needle, where emission is greatly enhanced.

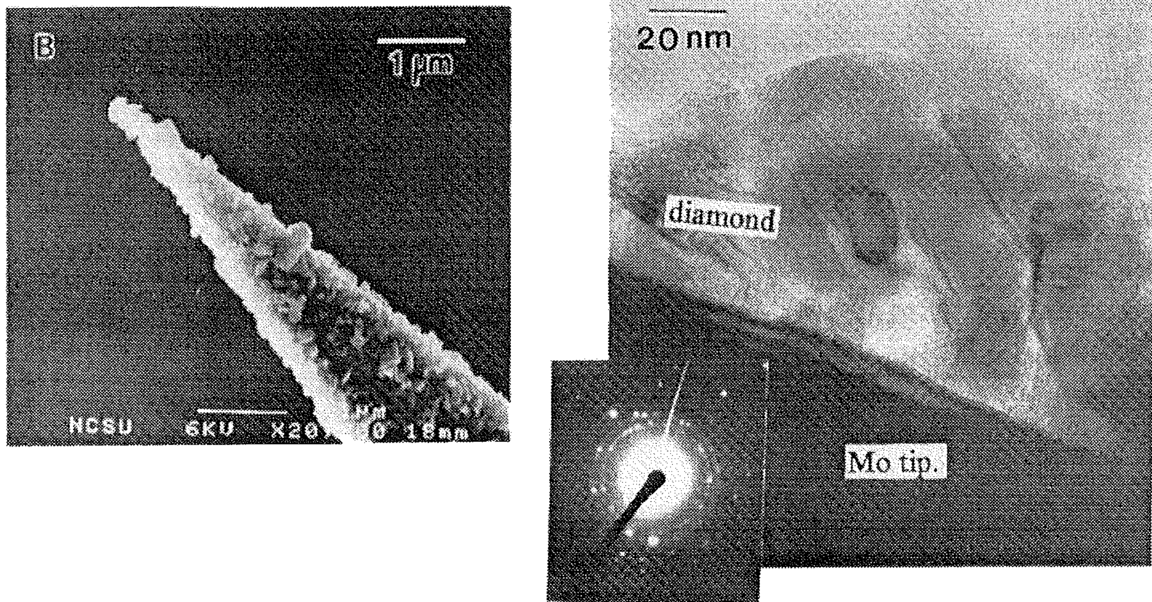

Figure 3. (a) SEM of diamond particles deposited by dielectrophoresis onto Mo needle (b) TEM of the particle-Mo interface of same needle.

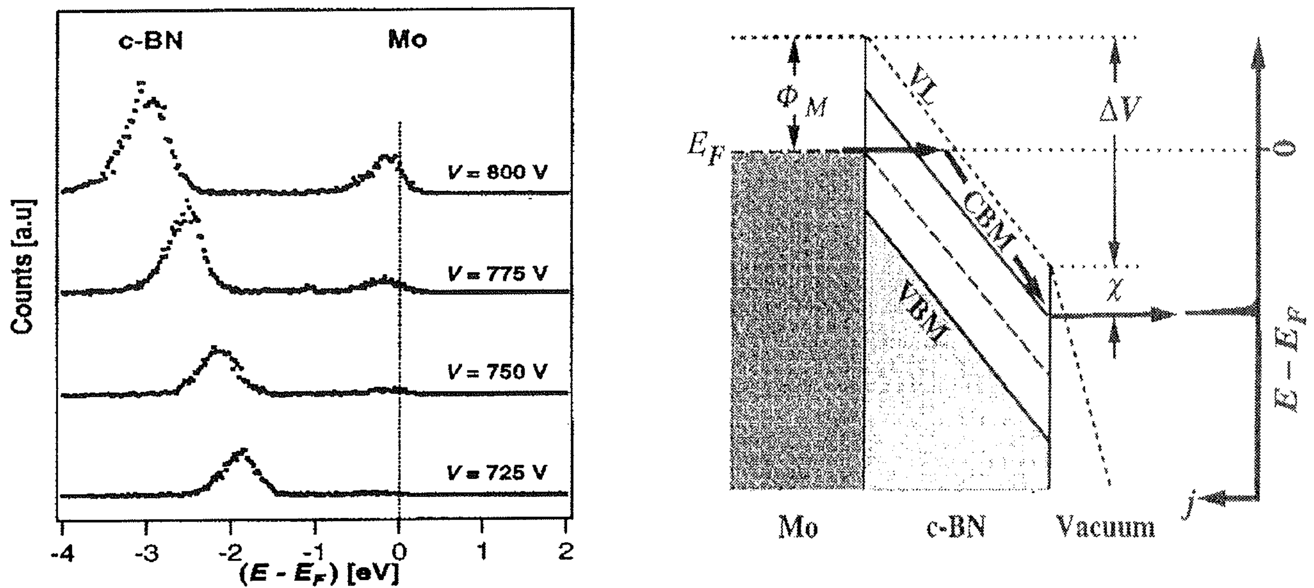

Figure 4. (a) Shift in BN FEED maximum relative to Mo as a function of applied potential, (b) band diagram illustrating emission mechanism.

The potential to study nanoparticles and thin films

No one has reported results from a single material characterized extensively from nanoscale dimension, where "quantum effects" dominate, up to dimensions where the measured properties are identical with those obtained from "bulk" samples. The present methods could achieve this and the experimental data obtained at the "quantum scale" could then be directly compared with first principle theoretical calculation. What other combination of techniques can claim to obtain a comparable result? We suggest that the tip of a needle makes an ideal specimen to achieve such a breakthrough.

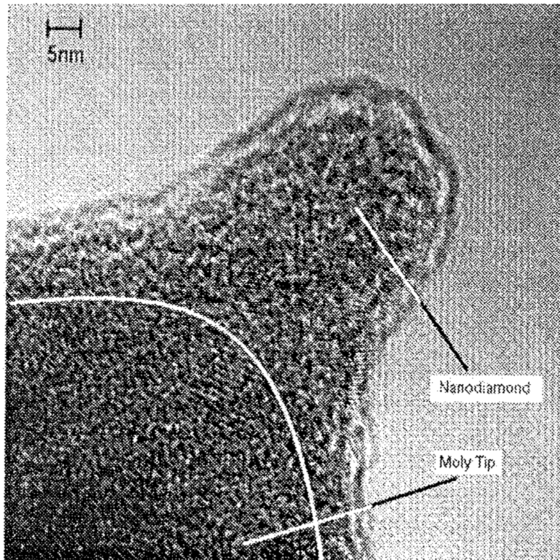

Figure 5 TEM of nanodiamond deposit on Mo needle by dielectrophoresis.

References:

/ 1/ Gomer, R., "Field Emission and Field Ionization", Harvard Univ. Press, (1961)

/ 2/ Mueller, E. W. and T. T. Tsong, Field Ion Microscopy, Elsevier, 1969.

/ 3/ Hren, J. J. and S. Ranganathan, Field-Ion Microscopy, Plenum, 1968.

/ 4/ Tsong,T. T., "Atom Probe Field Ion Microscopy" Cambridge Univ. Press (1990).

/ 5/ Panitz, J. A., J. Vac. Sci. and Technol., 11,206 (1974).

/ 6/ Schlesser, R. et al, Appl Phys Lett 70(12) 1596, 24 Mar 1997.

/ 7/ Murr,L. E., "Electron and Ion Microscopy and Microanalysis, Marcel Dekker (1991)

/ 8/ Liu, J. et al, J Vac Sci Technol B 13(2) 422, Mar/Apr 1995.

/ 9/ Meyers, A. et al, J. Vac Si and Technol B, 2024,May/June 1996.

/10/ Choi, W.B. et al, Appl. Phys. Lett. 68(5) 720, 29 Jan l996.

/11/ Choi et al, J Vac Sci Technol B 16(2) 716, Mar/Apr 1998.

John J. Hren, Victor V. Zhirnov,
Zlatko Sitar, & Gregory Wojak
Dept of Materials Science and Engineering
North Carolina State University
Raleigh, NC 27695-7907,USA
john_hren@ncsu.edu

Prispelo (Arrived): 1.10.2000   Sprejeto (Accepted): 25.11.2000

APPLICATION OF FOCUSED ION BEAM FOR FAILURE ANALYSIS

H. Bender
IMEC, Leuven, Belgium

TUTORIAL INVITED PAPER
MIDEM 2000 CONFERENCE – Workshop on ANALITICAL METHODS IN MICROELECTRONICS AND ELECTRONIC MATERIAL
18.10.00 – 20.10.00, Postojna, Slovenija

Keywords: failure analysis, electronic devices, FIB, Focused Ion Beam, semiconductors, FIB technique, Focused Ion Beam technique, surface imaging

Abstract: The focused ion beam (FIB) technique is an important tool for failure analysis studies on electronic devices. Examples are discussed of the identification by cross-section imaging of failure sites previously localized ex-situ by optical or emission microscopy or in-situ by means of voltage contrast in the FIB system. Ex-situ chemical analysis by Auger electron spectroscopy on FIB prepared cross-sections allows detailed interpretation of the FIB images.

Uporaba curka fokusiranih ionov pri analizi odpovedi

Ključne besede: naprave elektronske, analize odpovedi, FIB curek ionov fokusiran, polprevodniki, FIB tehnika curka ionov fokusiranega, upodabljanje površine

Izvleček: Curek fokusiranih ionov (FIB - Focused Ion Beam) je pomembna tehnika za analizo odpovedi elektronskih komponent. V prispevku obravnavamo primere prepoznavanja mest odpovedi na slikah presekov, katera so bila prvotno identificirana s pomočjo ex-situ tehnik, kot sta optična ali emisijska spektroskopija, oz. in-situ tehnike, kot je napetostni kontrast v FIB sistemu. Ex-situ kemična analiza s spektroskopijo Augerjevih elektronov na presekih vzorcev pripravljenih s FIB tehniko omogoča natančno analizo in tolmačenje FIB slik.

1. Introduction

The focused ion beam system is an indispensable technique for the semiconductor industry. Its major applications are: circuit modification by cutting metal lines and deposition of new metal tracks for optimizing the circuit design /1-3/; cross-section imaging for process development and control /2, 4/; failure analysis /5-7/ of devices by cross-section imaging through suspicious structures and voltage contrast to localize open contacts; preparation for in-situ or ex-situ chemical analysis; preparation of specimens for transmission electron microscopy /8, 9/; mask repair; milling and layer deposition for MEMS structures.

In this paper the technique is briefly introduced and a number of applications of the FIB technique for failure analysis are discussed.

2. The FIB technique

In the FIB system a focused 30-50 keV Ga^+ ion beam is rastered over the sample in a similar way as the electron beam in a scanning electron microscope (SEM). The secondary electrons or ions generated by the interaction of the ion beam with the material are collected synchronously with the rastering of the primary beam and are used to image the surface of the sample.

The contrast in the secondary electron FIB images /10, 11/ is different from the contrast in secondary electron SEM images. As the primary beam is positively charged, isolators will charge positively and will show a low secondary electron yield. Hence, they will be dark on the images. On the other hand, conducting materials will be bright if they are connected to the substrate holder of the system so that the current induced by the primary beam can flow away. If this is not the case, i.e. if the metal tracks are floating, they will also have a dark contrast. This allows the localization of failure sites by voltage contrast /12, 13/ as will be discussed in next section. An important image characteristic is also the channeling contrast in polycrystalline metal layers. In poly crystalline silicon this contrast is however not present due to the immediate amorphization of the top layer (~60 nm deep) of the silicon which suppresses the channeling of the ion beam. The border between conductive and non-conductive materials always shows a bright line, which is a result of the lateral field on the surface between both regions. The different contrast effects are illustrated on figure 1.

Except of the application for imaging, the high energy ion beam can also be used to remove the material locally by milling trenches in the material. This allows after tilting of the sample, the imaging of the cross-sectional structure of the device on the sidewall of these trenches. As the position of the trenches can be localized accurately from the top view image, very site-specific cross-section analysis is possible.

Another important application of the milling with the ion beam is the cutting of metal lines in prototype IC's to study possible design errors. Generally this is done in combination with the inlet of specific gases. This gas assisted etching (GAE) strongly reduces the redeposi-

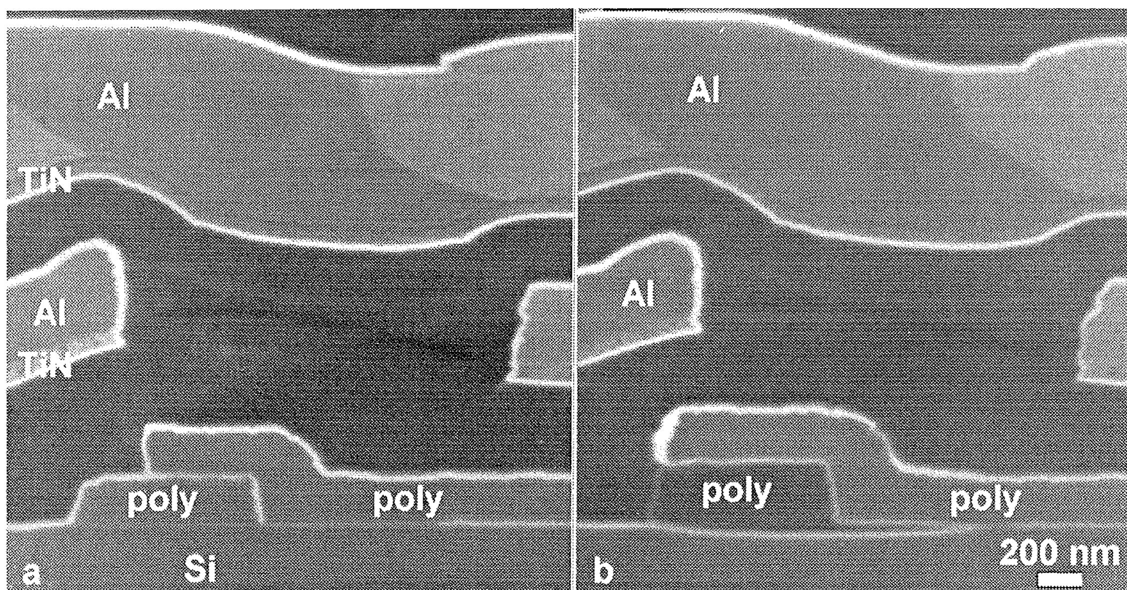

Fig. 1: Cross-section FIB images through a HIMOS memory cell illustrating the different contrast mechanisms on the FIB images: the isolators are dark; the conductors (Al, TiN, Si) are bright; the Al shows channeling contrast; the poly-Si shows no channeling contrast; bright lines mark the border between the dielectrica and the conductors. This bright line also reveals the presence on a thin oxide between the poly lines and the silicon substrate and between the two poly lines. In image (b) a further slice of the device was milled away so that the poly-Si line is now on top of a thick field oxide and is therefore floating with respect to the substrate and now shows a dark contrast.

tion of the removed material, results in an enhanced milling rate, and allows the selective removal of certain types of materials. E.g. Al is etched with I_2 or other halogen gases, passivation layers with XeF_2 and C-based materials with H_2O. Specific gases can also be used to deposit metal lines (Pt or W) or dielectrica (SiO_2). Only where the beam is rastered, the gas molecules are cracked and deposition occurs. The combination of deposition of new metal tracks and the cutting of metal lines allows the local rewiring of the metal interconnects in the devices.

The selective etching of dielectrica with the XeF_2 is also used for the local depassivation of devices for e-beam testing. Organic passivation layers (e.g. polyimide) can be removed very selectively with the H_2O milling (Fig.2).

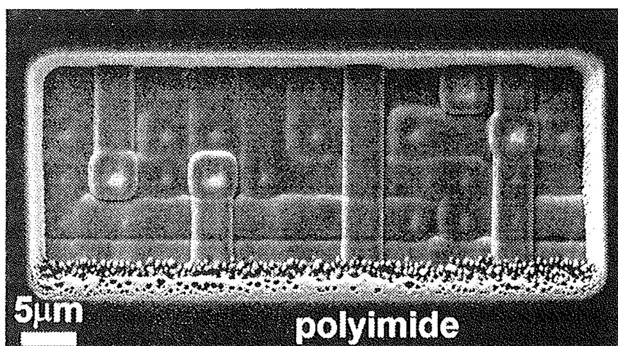

Fig. 2: Selective removal of a window through a 7 μm thick polyimide passivation layer by application of gas assisted milling with the H_2O gas. Due to the high selectivity the milling stops at the nitride passivation layer on the device.

3. Applications for failure analysis

The focused ion beam technique can be used to characterize the nature of failure sites in device structures. The localization of the defect sites can be done ex-situ by e.g. the liquid crystal method, optical microscopy or emission microscopy, or in-situ by means of voltage contrast.

3.1 Failures localized by optical microscopy

Figure 3 shows FIB cross-section images through poly-resistor structures. Fig. 3a illustrates a device before the electrical testing, showing the Al metal tracks, the W plugs and the polycrystalline silicon line. After electrical testing a dark spot could be seen by optical microscopy

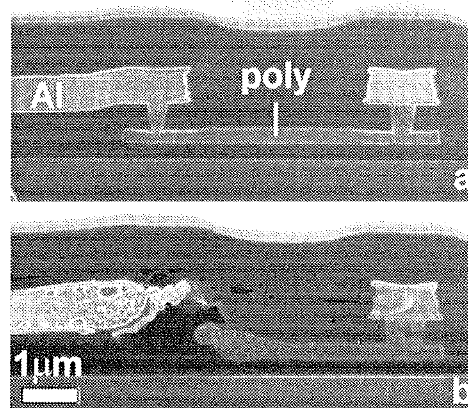

Fig. 3: FIB cross-section images through an untested poly-resistor (a) and after electrical testing (b).

through the passivation layer. Fig. 3b shows that the device structure is severely damaged by the testing: the Al and poly line have a sponge-like structure, a large void is formed at the position of the W plug which has totally disappeared, and also in the metal line on the right hand side a void is formed. The damage clearly indicates that a strong overheating occurred due to a too high current flowing through the device.

3.2 Failures localized by emission microscopy

Failure sites can be localized in devices by emission microscopy /14/. While electrically biasing the devices the local heating at failures will result in the emission of IR light. FIB cross-sectioning can subsequently be done at these positions to study the nature of the failure.

Fig. 4 shows an example where the defect could be seen already in the top view FIB image so that the exact localization of the defect in the FIB was very easy. The cross-section image (Fig. 4b) reveals a crater-like structure. The lower metal track is broken and shows a short with the upper metal line. Resist residues or a particle might have been on the origin of this defect.

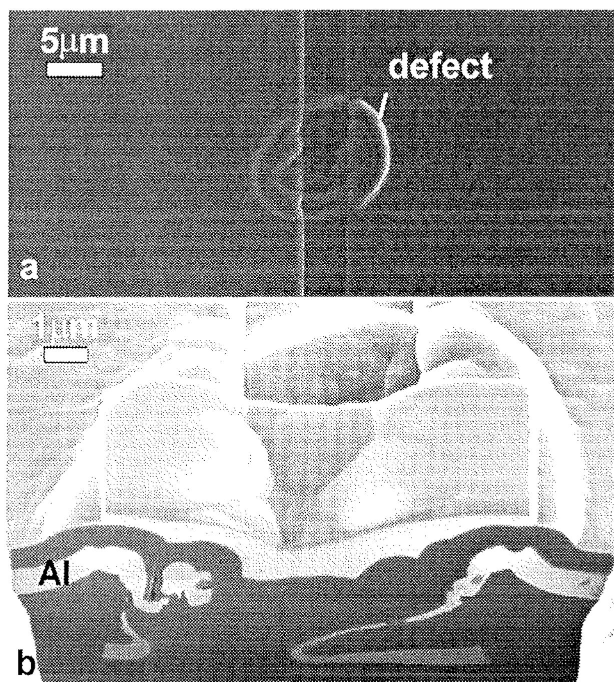

Fig. 4: Top view (a) and cross-section (b) FIB images of a large defect localized by emission microscopy.

The exact localization of the defect in the FIB is generally not so trivial as in the previous case because mostly no unusual topography is present on the surface. Also, the light spot seen with the emission microscope is larger than the actual defect so that some uncertainty exists on the defect position. Therefore the FIB investigation will often need a procedure consisting of the gradual milling of the crater through the failure site and the intermediate imaging on the crater sidewall. Figure 5 illustrates a conductive residue between two Al lines which is revealed in this way.

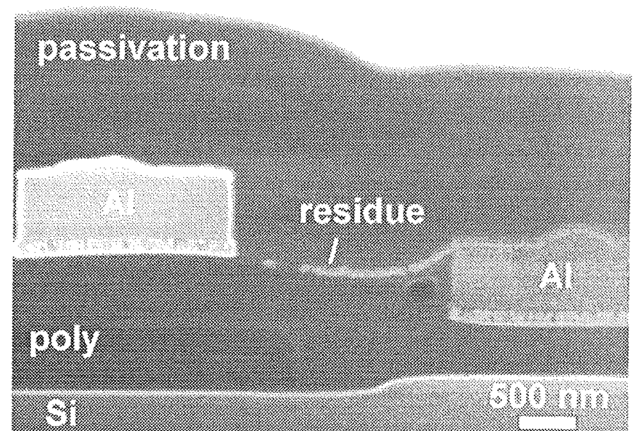

Fig. 5: FIB cross-section showing a conductive path between two Al lines at a failure position which is revealed by emission microscopy. (Because the poly line is floating, it shows a dark contrast).

Light emission in the emission microscope can also be due to failure mechanisms which cannot be revealed by cross-section FIB imaging. E.g. gate oxide pinholes cannot be seen on the FIB images because of its limited image resolution. To fully characterize such defects, investigation by transmission electron microscopy is necessary. For the site-specific preparation of the thin TEM specimens, the FIB specimen preparation technique is indispensable /8,9/.

3.3 Failures localized by voltage contrast

Electrical testing can be used to localize open contacts or vias. In unpassivated devices, i.e. test structures or devices which are depassivated, voltage contrast /12, 13/ can directly reveal the position of open contacts.

Figure 6 illustrates the technique for a large contact chain. The different probe pads above the chain are connected to different nodes in the chain and allow the electrical testing of parts of the chain. On the initial image (Fig. 6a) part of the probe pads and of the Al lines are dark, indicating that they are connected to open contact plugs in the chain and are hence floating with respect to the silicon substrate. The higher magnification image (Fig. 6b) shows also the presence of dark Al interconnections in the chain. The cross-section image (Fig. 6c) confirms that for these dark Al interconnects both contact plugs are open due to a very irregular etching of the contact holes. Because of the bad etching also the W filling of the contact holes is very poor. The Al interconnect on the left of the cross-section image has only one open contact and was therefore still bright on the top view image. Therefore the voltage contrast technique on such contact chains is not very sensitive to reveal opens because this requires that both contacts are simultaneously open, i.e it will work only well on rather bad chains.

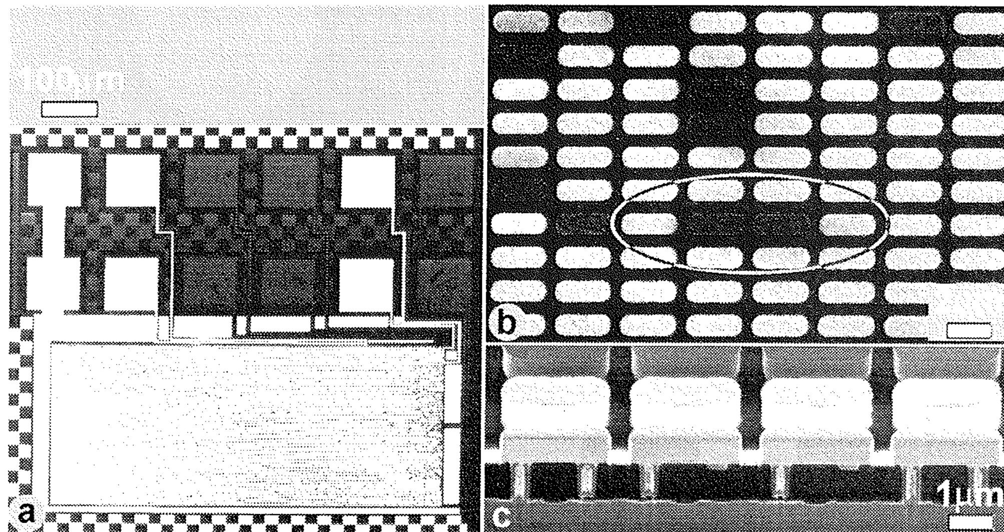

Fig. 6: Voltage contrast experiment on a contact chain test structure: (a) the initial top view image of the chain, (b) detail of the chain at higher magnification and (c) FIB cross-section image through the contacts encircled in (b).

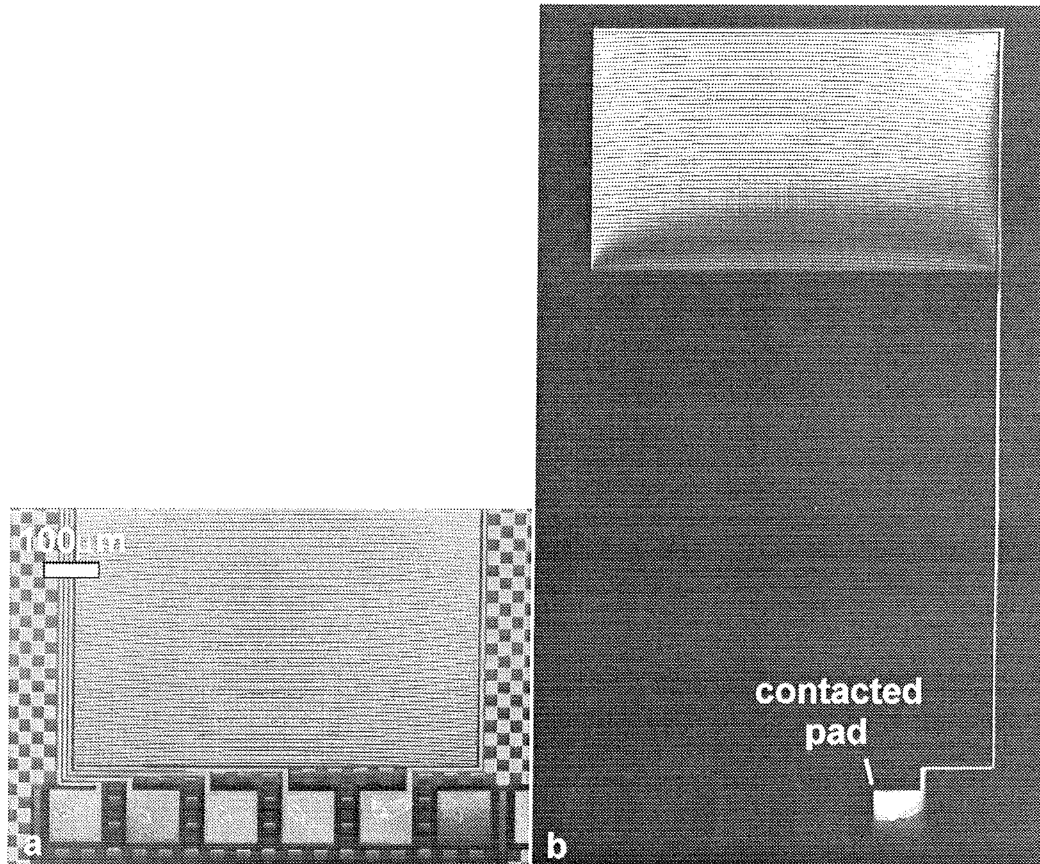

Fig. 7: Initial top view FIB image of part of a via chain (a), and (b) the full chain after contacting the marked pad to the substrate so that the open via position can be revealed.

This limitation of the voltage contrast sensitivity does not hold for via chains. Such chains are fully isolated from the silicon substrate. Figure 7 shows the initial FIB image of part of such a chain. All Al shows initially a brighter contrast than the dielectrics. This is actually only a transient effect. Due to the charge build-up also the Al will become dark after a few image scans. Subsequently a probe pad which is connected to the start (or end) of the chain is contacted to the substrate. This is done by milling a small hole through the pad into the substrate. Generally the redeposited material will already result in a sufficient contact between the pad and

the substrate. To ensure better contact the hole can also be filled with some Pt deposition. Due to this connection the pad becomes bright and also the Al line and the chain until the open contact will now show a bright contrast (Fig. 7b). Cross-section imaging can then be done at the position of the open contact (Fig. 8). The bright line at the bottom of the open via indicates the presence of an isolating material between the W filling and the lower metal. Most probably this is due to a too undeep etching of the via.

The use of a low charge dose during the localization of the failure site is essential. A too high charge can result in a discharge during the FIB imaging of the charge build-up on the floating metal so that the original failure cause is destroyed (Figure 9). This risk is particularly high for single vias connected to large Al areas. In such cases the discharge often occurs during the milling of the crater for the cross-section imaging for which a rather high beam current must be used. Therefore the connection to the substrate through neighboring metal tracks or by ex-situ deposition of a conductive gold layer should be considered before milling the crater.

Depending on the nature of the bad contact, a too high current during the localization can result in leakage through the failure site so that the voltage contrast is lost. Therefore moderately bad contacts are generally difficult to reveal.

It should also be remarked that once a cross-section is made the voltage contrast is generally lost (see e.g. Fig. 6c). This is due to the redeposition of the sputtered material between the small Al lines so that a conductive path to the substrate is formed.

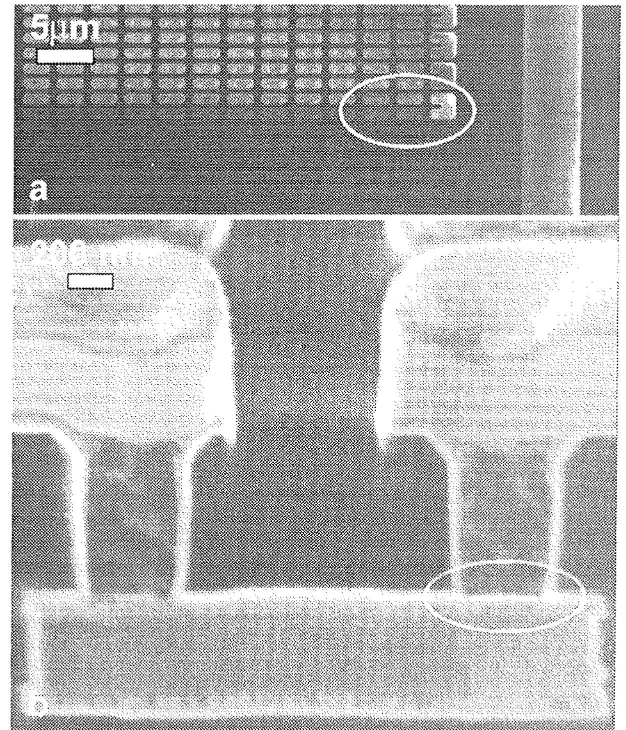

Fig. 8: Higher magnification (a) of the position of the open contact in the via chain shown in fig. 7, and (b) cross-section image through the open via revealing the presence of an isolating material at the bottom of the via.

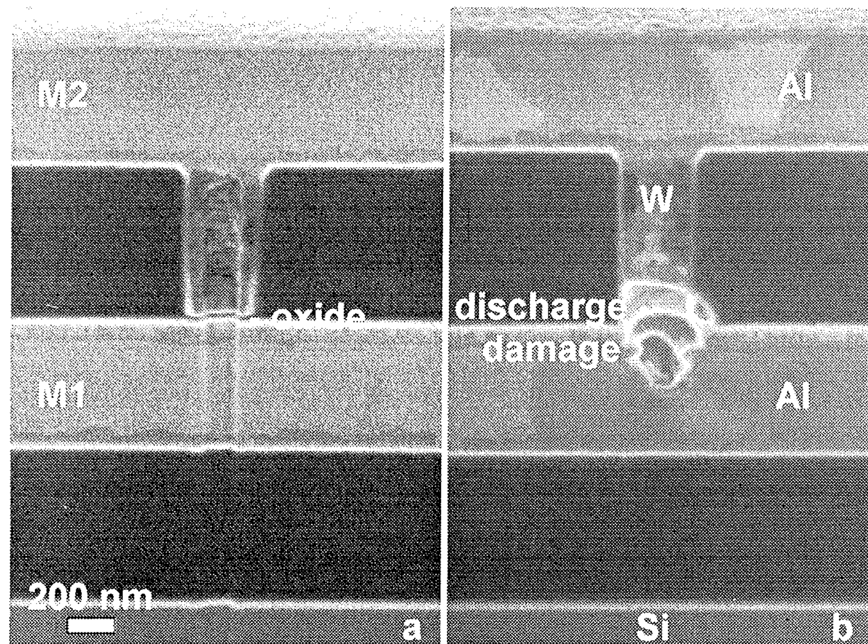

Fig. 9: FIB cross-section image through M1-M2 Kelvin structures in which the vias are open due to too undeep etching: (a) the upper metal was contacted to the substrate prior to the preparation of the cross-section, the cause of the open is clearly seen; (b) the upper metal was not contacted resulting in a discharge of the charge build-up on the large M2 plate during the milling of the cross-section so that the real cause of the open is destroyed.

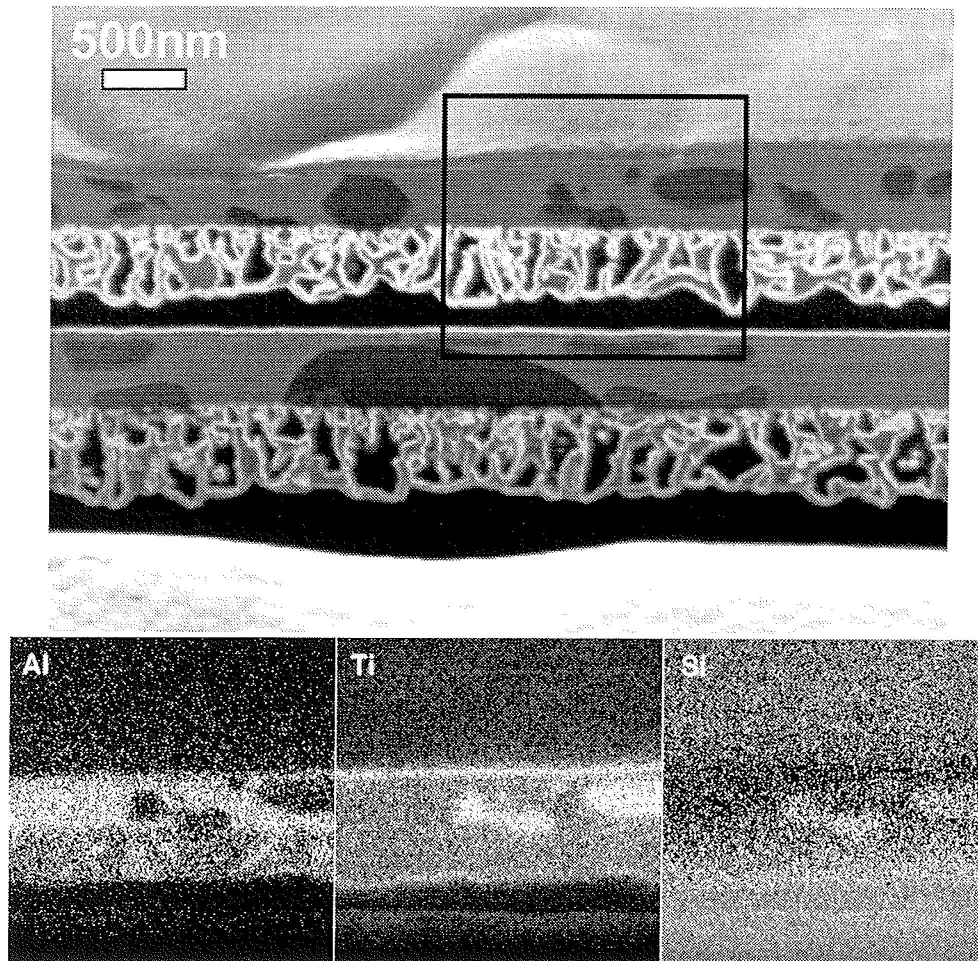

Fig. 10 FIB cross-section image (a) through a two metal metalllisation structure which was heated to 575°C and (b) Al, Ti and Si Auger mappings of the area marked in (a).

3.4 Chemical analysis by Auger spectroscopy

Chemical analysis at the failure sites is often required to fully understand the nature of the defect. This is possible in-situ if a secondary ion mass spectrometer (SIMS) is available or by energy dispersive X-ray spectroscopy (EDX) in dual-beam FIB systems (i.e. combining a FIB and a SEM column). Ex-situ analysis is possible by e.g. Auger electron spectroscopy.

Fig. 10 shows Auger mappings of Al, Ti and Si on a FIB cross-section through an Al interconnect structure which was heated to 575°C for 30 min /15/. The formation of Al-Ti-Si inclusions in the Al and the diffusion of the Al in the dielectric layer can be seen.

4. Conclusions

The focused ion beam technique has a wide range of applications for failure analysis studies of electronic devices. Except of the discussed topics other possible applications are, e.g., local depassivation for e-beam testing, deposition of probe pads for electrical testing, or investigation of electromigration test structures /16/.

5. References

/1/ L.R. Harriot, A. Wagner and F. Fritz, "Integrated Circuit Repair Using Focused Ion Beam Milling", J. Vac. Sci. Technol. B 4, (1986), 181-184.

/2/ F.A. Stevie, T.C. Shane, P.M. Kahora, R. Hull, D. Bahnck, V.C. Kannan and E. David, "Applications of Focused Ion Beams in Microelectronics Production, Design and Development", Surf. Interface Anal. 23, (1995), 61-68.

/3/ K.N. Hooghan, K.S. Wills, P.A. Rodriguez and S. O'Connell, "Integrated Circuit Device Repair using FIB system: Tips, Tricks, and Strategies", in: Proc. 25th International Symposium for Testing and Failure Analysis (ISTFA 99), ASM International, Materials Park, Ohio, (1999), 247-254.

/4/ H. Bender, "Focused Ion Beam and Transmission Electron Microscopy for Process Development", in: Analytical and Diagnostic Techniques for Semiconductor Materials, Devices, and Processes, eds B.O. Kolbesen, C. Claeys, P. Stallhofer, F. Tardif, J. Benton, et al, Electrochemical Society, Pennington, (1999), 232-247.

/5/ D.C. Shaver and B.W. Ward, "Integrated Circuit Diagnosis Using Focused Ion Beams", J. Vac. Sci. Technol. B 4, (1986), 185-188.

/6/ R.G. Lee and J.C. Morgan, "Integration of a Focused Ion Beam System in a Failure Analysis Environment", in: Proc. 17th International Symposium for Testing and Failure Analysis (ISTFA 91), ASM International, Materials Park, Ohio, (1991) 85-95.

/7/ D. Verkleij, "The Use of the Focused Ion Beam in Failure Analysis", Microelectron. Reliab. 38, (1998), 869-876.

/8/ E.C.G. Kirk, D.A. Williams and H. Ahmed, "Cross-sectional transmission electron microscopy of precisely selected regions from semiconductor devices", Inst. Phys. Conf. Ser. 100, (1989), 501-506.

/9/ H. Bender, "Focused Ion Beam Preparation for Transmission Electron Microscopy Studies of ULSI Devices", Inst. Phys. Conf. Ser. 164, (1999), 593-602.

/10/ T.K. Olson, R.G. Lee and J.C. Morgan, "Contrast Mechanisms in Focused Ion Beam Imaging", in: Proc. 18th International Symposium for Testing and Failure Analysis (ISTFA 92), ASM International, Materials Park, Ohio, (1992), 373-382.

/11/ D.L. Barr and W.L. Brown, "Contrast formation in focused ion beam images of polycrystalline aluminum", J. Vac. Sci. Technol. B 13, (1995), 2580-2583.

/12/ A.N. Campbell, J.M. Soden, J. Rife and R.G. Lee, "Electrical Biasing and Voltage Contrast Imaging in a Focused Ion Beam System", in: Proc. 21st International Symposium for Testing and Failure Analysis (ISTFA 95), ASM International, Materials Park, Ohio, (1995), 33-41.

/13/ X. Yang and X. Song, "The Application of FIB Voltage-Contrast Technique Combining with TEM on Subtle Defect Analysis: Via Delamination after TC", in: Proc. 23rd International Symposium for Testing and Failure Analysis (ISTFA 97), ASM International, Materials Park, Ohio, (1997), 115-119.

/14/ M. Rasras, I. De Wolf, H. Bender, G. Groeseneken, H.E. Maes, S. Vanhaeverbeke and P. De Pauw, "Analysis of Iddq Failures by Spectral Photon Emission Microscopy", Microelectron. Reliab. 38, (1998), 877-882.

/15/ S. Sedky, A. Witvrouw, H. Bender and K. Baert, "Experimental Determination of the Maximum Post Processing Temperature of MEMS on Top of Standard CMOS Wafers", IEEE Trans Electron Devices (2000), in press.

/16/ A. Witvrouw, H. Bender, Ph. Roussel and K. Maex, "Modelling and microstructural characterisation of incubation, time dependent drift and saturation during electromigration in Al-Si-Cu stripes", Microelectron. Reliab. 39, (1999), 1603-1616.

ACKNOWLEDGMENTS

C. Drijbooms is acknowledged for the FIB analyses and J. Van Houdt, S. Decoutere, M. Rasras, I. De Wolf, B. De Jaeger, I. Heyvaert and S. Sedky for the collaboration on the different research topics discussed in this paper.

H. Bender
IMEC
Kapeldreef 75,
B-3001 Leuven, Belgium,
hugo.bender@imec.be

Prispelo (Arrived): 1.10.2000 *Sprejeto (Accepted): 25.11.2000*

UDK621.3:(53+53+621+66), ISSN0352-9045 Informacije MIDEM 30(2000)4, Ljubljana

ATOMIC FORCE MICROSCOPY

I. Muševič
Faculty of mathematics and physics, University of Ljubljana, Ljubljana, Slovenia
and
J. Stefan Institute, Ljubljana, Slovenia

TUTORIAL INVITED PAPER
MIDEM 2000 CONERENCE – Workshop on ANALYTICAL METHODS IN MICROELECTRONICS AND ELECTRONIC MATERIALS
18.10.00 – 20.10.00, Postojna, Slovenia

Keywords: STM, Scanning Tunneling Microscopy, atomic force, AFM, Atomic Force Microscopy, force spectroscopy, AFM spectroscopy, surface topography, SPM, Scanning Probe Microscopy, EFM, Electric Force Microscopes, MFM, Magnetic Force Microscopes, SNOM, Scanning Near-field Optical Microscopes, PWB, Printed Wiring Boards

Abstract: Since the invention of the Scanning Tunneling Microscope (STM), a number of related surface probing techniques have been developed, capable of resolving single atoms or molecules at a free surface. In particular, the Atomic Force Microscopy (AFM) is well recognized as a promising tool for observing nanometer-scale structures of non-conductive surfaces, soft matter objects like single organic molecules, polymers, biological tissues, etc. Basic principles of operation of various Surface Probe Microscopy techniques application in various fields are discussed. Application of AFM Force Spectroscopy on polymer-coated surfaces is described.

Mikroskopija na atomsko silo

Ključne besede: STM mikroskopija skanirna tunelna, sila atomska, AFM mikroskopija sile atomske, spektroskopija sile, AFM spektroskopija, topografija površine, SPM mikroskopija s sondo skanirno, EFM mikroskopi s silo električno, MFM mikroskopi s silo magnetno, SNOM mikroskopi skanirni optični s poljem bližnjim, PWB plošče ožičenja tiskane

Izvleček: V letih po odkritju vrstičnega tunelskega mikroskopa (Scanning Tunneling Microscope, STM) je bilo razvitih veliko podobnih tehnik mikroskopiranja površine, katerih ločljivost je velikostnega reda dimenzij posameznega atoma ali molekule. Med njimi posebno mesto zavzema mikroskop na atomsko silo (Atomic Force Microscope, AFM), ki je zaradi enostavnosti delovanja in visoke ločljivosti postal nepogrešljivo orodje pri analizi topografije neprevodnih površin, mehke snovi, polimerov in bioloških snovi. V članku bom opisal osnove delovanja STM in AFM, njuno uporabo na različnih raziskovalnih področjih in še posebej predstavil spektroskopijo sile na polimernih površinah.

1. Introduction

The Atomic Force Microscope (AFM), as first described by Binnig et al. /1/ in 1986, is by now a well established tool for the studies of surface topography and surface forces in a variety of condensed matter systems, such as solid crystals, polymers, biological systems, molecular crystals, etc. The principle of operation of an AFM /2/ is based upon the measurement of the attractive or repulsive forces between the nanometer-sharpened tip and the substrate. This allows for the observation of either (i) **the surface topography**, or (ii) **the distance-dependence of the forces** between the tip and the surface. In combination with different materials for the surface-sensing tip (metal, isolator, ferromagnet, etc.) one can test and observe a wide variety of interfacial forces acting between the tip and the substrate and can therefore extract a qualitatively different information on the surface structure. These two basic modes of operation of an AFM can be used in very different environments, as we can perform the AFM experiments at ambient conditions, in vacuum and even in the presence of liquids. This makes an AFM a powerful experimental tool for very different fields of surface science.

2. Principles of operation of surface probe microscopes

The principle of operation of a Surface Probe Microscope (SPM) is simple: a small (i.e. submicron) probe is scanned across the surface and is held in close proximity to the surface by a feedback-loop electronics, as shown in Fig. 1. The close proximity between the probe and the surface is sensed by a specific interaction between the probe and the surface. Regarding to the type of this interaction, the class of SPM devices can be divided as follows:

(i) **Scanning Tunneling Microscope** (STM). In this instrument, an electron tunneling current is measured between a very sharp metallic tip with a radius of curvature of less than 10 nm and a metallic surface. When the separation between the metallic tip and a conductive surface is less than 1 nm, a quantum electron tunneling current appears across the gap. As the tunneling current increases exponentially with decreasing separation, one can position the tip very accurately. As a consequence of the exponential dependence of the tunneling current, the electrons are tunneling

to the surface via the orbital of the atom, that is closest to the surface. This results in extremely high lateral resolution of an STM, which can routinely image single atoms or molecules. The disadvantage of an STM is the inability to image non-conductive surfaces.

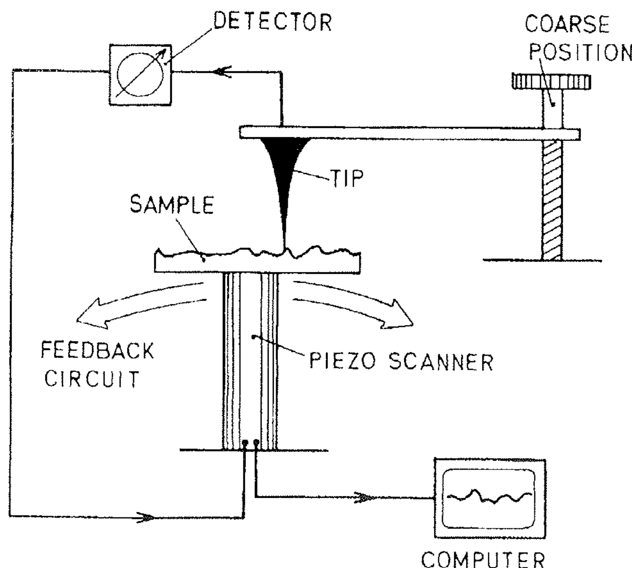

Fig.1. In an SPM, a small probe is scanned across the surface and is held in the close proximity to the surface. The distance between the probe and the surface is sensed and this information is sent to the feedback electronics. A piezoelectric scanner is used to position the sample, and the electronics adjusts in real time the vertical position of the sample, as the probe is scanned across the surface. The positioning signal is recorded as a function of the lateral position of the sample and this is a record of the sample topography in a single scanning line.

(ii) **Atomic Force Microscope** (AFM). In this instrument, the forces between a sharp tip and a surface are monitored as a function of the separation between a tip and a surface /3/. The AFM can therefore be used to image both conductive and non-conductive surfaces. At large separations, the force is zero. By approaching, we always reach a regime of some attractive (i.e. van der Waals) or repulsive (i.e. electrostatic) forces on the tip. The tip is mounted on a flexible micro-cantilever (see Fig. 2), and the bending of the cantilever is monitored by means of a deflection of a focused laser light (see Fig. 3). The force on the tip is calculated from the deflection of the cantilever, once we know the elastic constant of the cantilever. By further approaching the surface, a repulsive regime is reached, where the tip is in "hard contact" with the surface and Pauli exclusion principle gives rise to strong repulsion. The AFM can operate in two regimes: contact and non-contact. In the contact regime, the tip is in hard contact with the surface. The resolution of the AFM is in this case very high, although somewhat lower than in STM and one can routinely image flat surfaces with an atomic resolution (see Fig.4.). The non-contact regime is more suitable for soft surfaces. Here, the forces on the surface are smaller, but also the resolution is lower.

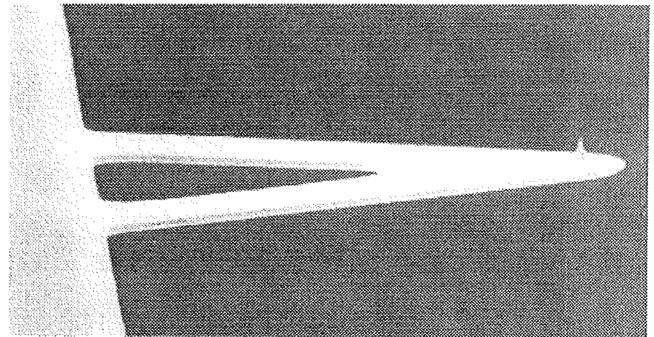

Fig. 2. AFM tip is mounted to a flexible cantilever (courtesy Park Scientific Instruments). The curvature radius of the tip is 10-20 nm

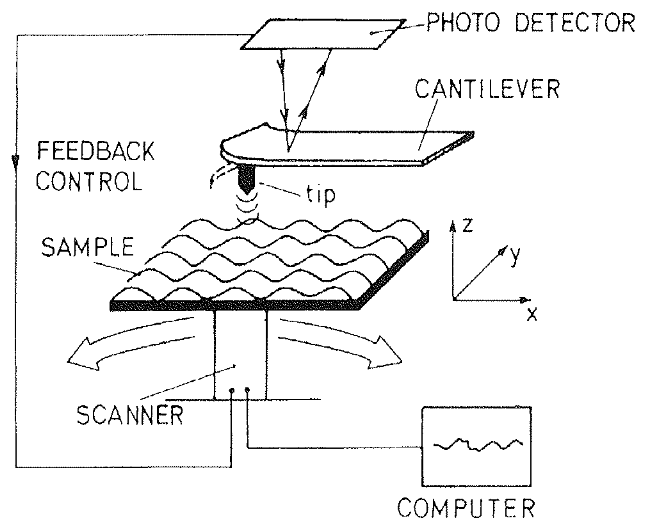

Fig. 3. The bending of the AFM cantilever is monitored via the deflection of a focused laser beam. A four-quadrant photodiode can monitor the deflection of the cantilever with an atomic resolution.

(iii) **Electric and Magnetic Force Microscope** (EFM and MFM). In this version of the AFM, the tip is made or coated either by conductive (i.e. highly doped Si) or ferromagnetic (Fe, Co) material. In the EFM, the voltage is applied to the conductive tip and one can measure the electrostatic forces due to charges on the surface. This particular technique is very suitable in the studies of fer-

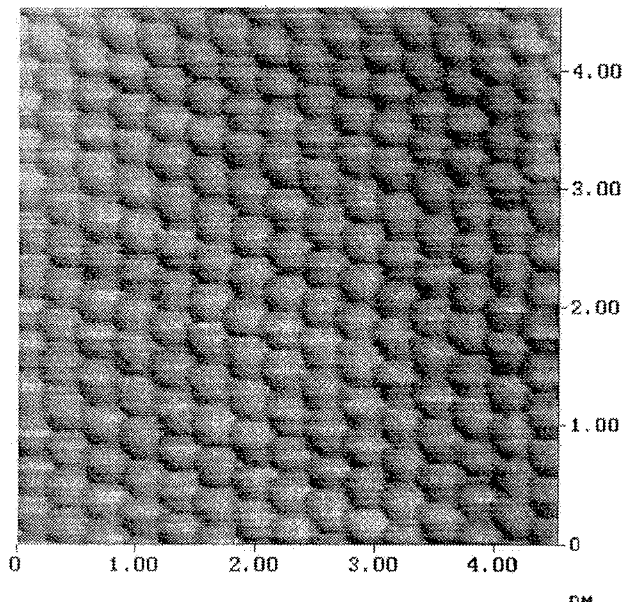

Fig. 4. Atomic resolution of an AFM on a freshly cleaved surface of $NbSe_2$. Dimensions of the image are 4.5nm x 4.5nm. One can clearly see Se atoms. The image has not been filtered or modified graphically.

roelectric and piezoelectric materials and one can image ferroelectric and piezoelectric properties of these surfaces with submicron resolution. The technique can also be used in testing electrical connections in microelectronic circuits. In the MFM, magnetic forces are measured between the ferromagnetic tip and the magnetic surface. The technique allows for submicron detection of ferromagnetic domains. We should also mention the Magnetic Resonance Force Microscope (MRFM) /4/ which was developed with the aim to spatially resolve chemical constitution of the surface. Here, the magnetic force is mediated by nuclear magnetization of specific nuclei, which is induced by NMR technique.

(iv) **Scanning Near-Field Optical Microscope** (SNOM) /5/. Here, a very sharp tip of an optical fiber is scanned at a close proximity to the surface. Optical signal from a transparent sample is collected by some mechanism, as for example near total internal reflection at a surface of the sample. One can therefore monitor variations of the dielectric constant of the surface with submicron resolution.

Whereas the mechanism of surface detection is different for the above mentioned microscopes, all of them reconstruct the image of the surface from data collected during regular scanning of the probe above the surfaces under imaging. Usually, the probe transverses the sample in a "zigzag" fashion, and the data are collected at regular time intervals. The scan rate (i.e. the inverse time for a single scan) can vary from 1 s to 1/100 of a second in commercial microscopes. In some cases, real-time imaging can be performed with a rate of several frames per second. The number of points, collected during a single scan is typically 512, so that an image can be taken typically in a time of one to several minutes.

3. Force spectroscopy in colloidal systems

Whereas imaging of surfaces is of prime importance for the monitoring of surface quality and topography, an Atomic Force Microscope is a powerful tool for measuring forces between surfaces in the presence of liquids. As an example, I shall here describe the application of AFM force spectroscopy to the forces in colloidal systems and to the study of mechanism of deposition of nano and microparticles from colloidal solution to the polymer surface. The technological problem is the production of conductive layers on printed wiring board (PWB) laminates, which are used during the through-hole metallization process in printed wiring board (PWB) laminates. The primary conductive coatings are usually chemically deposited and result in substantial production of hazardous waste. Water-based deposition of conductive coatings formed by densely packed mesoscopic particles of carbon black or graphite onto printed wiring board (PWB) laminates is a promising candidate for environment-friendly technology of PWB mass production /6,7/. There are two competing physical mechanism that have to be controlled in the process of deposition: (i) On one hand, the water dispersion of mesoscopic conductive particles has to be stable. For this purpose, surfactants are used, which adsorb onto the surfaces of particles. Due to dissociation, these surfactants become charged in aqueous solution and the resulting electrostatic repulsive forces between equally charged surfaces leads to stabilization of dispersion against van der Waals attraction. (ii) On the other hand, the electrostatic properties of particles in dispersion have to be near the point where the particles can approach the polymer surface to a certain minimum distance, so that coagulation and adsorption onto a surface can occur. This point is

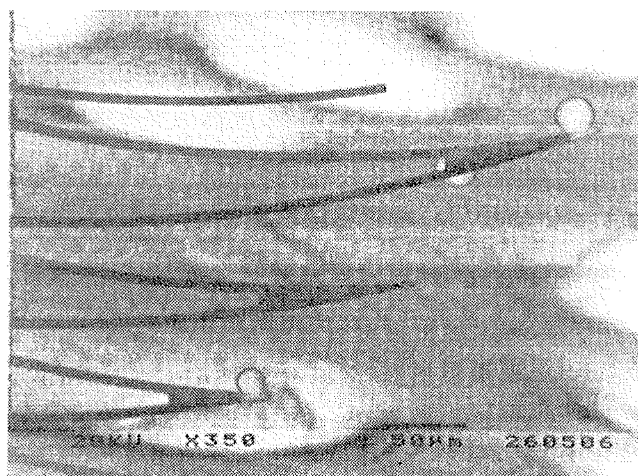

Fig. 5. For the study of colloidal forces, glass microspheres are attached on the AFM cantilever. The surface of the glass spheres can be coated or chemically modified.

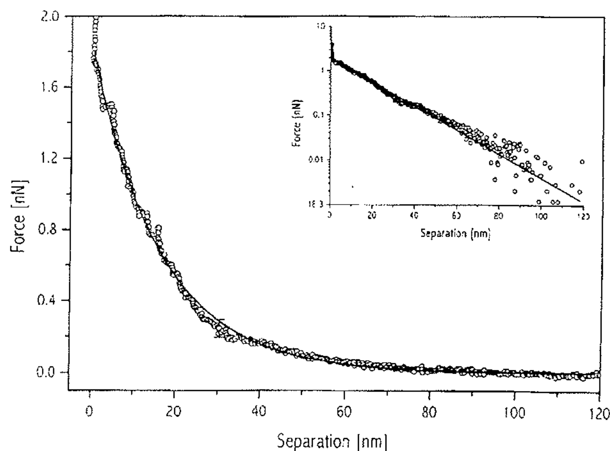

Fig.6. Electrostatic double-layer repulsive force as a function of separation between the surfaces of a glass microsphere and mica in pure water. The inset shows the same data in log-lin scale with a linear fit yielding Debye screening length of 16.4(1±0.02)nm and the force amplitude 1.8(1±0.01)nN.

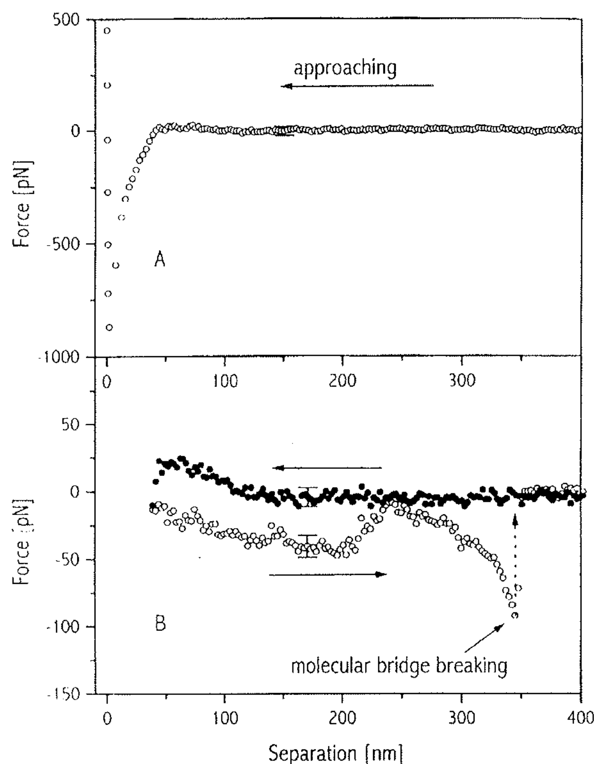

Fig.7. The forces between gelatin-coated 15 μm glass sphere mica surface in pure water. (A) When full approach of the two surfaces is performed, one can observe electrostatic attractive double-layer force. (B) In the "fly fishing mode", approach of the two surfaces is stopped at a separation of 50-100 nm. When retracting, one can observe irregular, saw-tooth-like molecular bridging force between the two surfaces, mediated by the gelatin molecules.

controlled by the appropriate addition of a salt (i.e. charged ions), which screens the electric field of the surfaces and allows particles to approach to shorter distances during their Brownian motion.

In the studies of forces in colloidal systems, the forces to the AFM tip are far too small to be measured very accurately. For this purpose, a microsphere made of glass or some other material is attached onto the cantilever (see Fig. 5) and the forces on this microscopic object are measured as a function of separation between the sphere and the surface. Fig. 6. shows the force between a 15 μm soda-lime glass sphere, attached to a AFM tip and a freshly cleaved mica surface in the presence of pure water. The force is electrostatic repulsive and decays exponentially with increasing separation. The surfaces of glass and mica are both negatively charged in pure water and the corresponding electrostatic force is repulsive. In the next step, a thin layer of gelatin was adsorbed onto the glass sphere. The interaction forces between a freshly cleaved mica surface and gelatin-coated sphere in pure water are shown in Fig. 7. Here, the so-called "fly fishing mode" approach of the sphere was applied, where the approaching was stopped at a given separation to the surface and the AFM probe was then retracted. Although the two surfaces obviously did not come into a hard contact, there is some small attractive force between the two surfaces, when the sphere is moved away. This force is interpreted as a molecular bridging force, mediated by the gelatin macromolecules. The gelatin layer on the glass surface is "hairy" and expands with randomly coiled loops and tails deep into water. When this "hairy" interface is brought into a certain minimum distance from the bare mica surface, gelatin molecules are adhered to the mica surface and create molecular bridges between a sphere and a surface. These bridges are observed upon retracting the sphere from the surface, as they are irreversibly broken by the external pulling force and the heat is dissipated at the interface. In spite of relative weakness of this molecular bridging force, the range of the force is as large as several hundreds of nanometers, and a binding energy for a micrometer sphere is several thousands of k_BT.

This simple example clearly shows the power of force spectroscopy in colloidal systems. In my opinion, many interesting applications of force spectroscopy will be developed in near future. In particular, molecular-specific interaction and molecular recognition on the basis of force spectroscopy will play a very important role in biosensors and molecular-specific devices /8/.

4. Conclusions

It is not easy to give any conclusions in the field, which is so rapidly developing, as the SPM community over the past ten years. However, it is more or less clear, that several important fields are emerging, that would play substantial role in tomorrow high technology: (i) SPM methods in micro and nanoelectronics will play the role of a basic tool for testing and controlling the technological parameters. (ii) piconewton and sub-piconewton force-oriented devices and sensors will play an important role in molecular recognition, detection and imaging. (iii) SPM oriented devices and methods will play an important role in nanotechnology. Molecular structures

will be tailored, produced and analyzed with sub-nanometer precision. (iv) SPM based nanodevices for high density information storage will be developed. For more specific information, the reader is advised to visit:
http://www.di.com/;
http://www.nanonics.co.il/fs _products.html;
http://www.pacificscanning.com/;
http://www.molec.com/.

5. ACKNOWLEDGMENT

The author would like to thank M. Kočevar, M. Bele and S. Pejovnik for their substantial contribution to the program of the AFM Force Spectroscopy at the "J. Stefan" Institute over the past several years.

References:

/1/ G.Binnig, C.F.Quate, C.Gerber, Phys.Rev.Lett. 56, 930(1986).

/2/ T.Thundat, R.J.Warmack, G.Y.Chen, and D.P.Allison, Appl.Phys.Lett. 64, 2894(1994).

/3/ M.Radmacher, J.P.Cleveland, P.K.Hansma, Scanning 17, 117(1995)

/4/ J.A.Sidles, J.L.Garbini, K.J.Bruland, D.Rugar, O.Zueger, S.Hoen, C.S.Yannoni, Rev.Mod.Phys 67, 249(1995).

/5/ R.Wiesendanger, Ed., Scanning Probe Microscopy, Springer, 1998.

/6/ J.O. Besenhard, O. Claußen, H.P. Gausmann, H. Meyer, GER Patent No. 41 41 416, 1991;
J. O. Besenhard, H. Meyer, H. P. Gausman and H. Mahlkow, GER Patent No. 41 41 744, 1991, and US Patent 5 705 219, 1998.

/7/ M.Bele, S. Pejovnik, J. O. Besenhard, V. Ribitsch, Colloid. Surf. A143, (1998);
M.Bele, S. Pejovnik, J. Mater. Sci. Lett. 18,1941(1999).

/8/ J.Fritz, M.K.Baller, H.P.Lang, H.Rothuizen, P.Vettiger, E.Meyer, H.-J.Guentherodt, Ch.Gerber, J.K. Gimzewski, Science 288, 316(2000).

I.Muševič
Faculty of mathematics and physics,
University of Ljubljana,
Jadranska 19,
Ljubljana, Slovenia
and
J.Stefan Institute,
Jamova 39,
Ljubljana, Slovenia
igor.musevic@ijs.si

Prispelo (Arrived): 1.10.2000	*Sprejeto (Accepted): 25.11.2000*

UDK621.3:(53+54+621+66), ISSN0352-9045

THE APPLICATION OF ELECTRON MICROSCOPY METHODS IN THE STUDY OF INVERSION BOUNDARIES IN ZnO-BASED VARISTORS

Nina Daneu, Aleksander Rečnik and Slavko Bernik
Jožef Stefan Institute, Ljubljana, Slovenia

TUTORIAL INVITED PAPER
MIDEM 2000 CONFERENCE – Workshop on ANALYTICAL METHODS IN MICROELECTRONICS AND ELECTRONIC MATERIALS
18.10.00- 20.10.00, Postojna, Slovenia

Keywords: ZnO varistors, Zinc Oxide varistors, ZnO ceramics, Zinc Oxide ceramics, IBs, Inversion Boundaries, electron microscopy methods, electronic microscopy, crystallography, SEM, Scanning Electron Microscopy, CTEM, Conventional Transmission Electron Microscopy, CBED, Convergent Beam Electron Diffraction, HRTEM, High-Resolution Transmission Electron Microscopy, HAADF-STEM, High-Angle Annular Dark Field Scanning Transmission Electron Microscopy, Z-contrast imaging, EDS, Energy Dispersive Spectroscopy

Abstract: Inversion boundaries in ZnO-based varistor ceramics were studied by various electron microscopy techniques. Scanning electron microscopy observations disclose a flat internal boundary in every ZnO grain. Etched cross-sections reveal the inversion of crystal domains over the fault plane. Microdiffraction experiments using a conventional transmission electron microscope proved that the faults are inversion boundaries, lying in basal planes of the hexagonal ZnO structure. The local structure was assessed by high-resolution transmission electron microscopy and chemistry of the fault was interrogated by energy dispersive spectroscopy. Regardless the type of the dopant (Sb, Sn, Ti, In, Fe, Ga, etc.) inversion boundaries possess a local cubic structure comprising a mixed close-packed cationic layer of octahedral coordination.

Uporaba metod elektronske mikroskopije za študij inverznih mej v varistorski keramiki na osnovi ZnO

Ključne besede: ZnO varistorji cink oksidni, ZnO keramika cink oksidna, IBs meje inverzne, metode spektroskopije elektronske, mikroskopija elektronska, kristalografija, SEM mikroskopija elektronska skanirna, CTEM mikroskopija elektronska konvencionalna, CBED difrakcija curka elektronskega konvergentnega, HRTEM mikroskopija elektronska z ločljivostjo visoko, HAADF-STEM mikroskopija elektronska skanirna s poljem temnim obročastim kota velikega, Z-kontrast upodabljanje, EDS spektroskopija z energijo razpršeno

Povzetek: Inverzne meje v varistorski keramiki na osnovi ZnO smo preiskovali z različnimi metodami elektronske mikroskopije. Opazovanje mikrostrukture na vrstičnem elektronskem mikroskopu pokaže ravno mejo v vsakem zrnu ZnO. Na inverzijo kristalnih domen preko ravnine defekta kaže že jedkana površina mikrostrukture. Z mikrodifrakcijskimi eksperimenti na konvencionalnem transmisijskem elektronskem mikroskopu smo dokazali, da so te napake inverzne meje in da ležijo v bazalnih ravninah heksagonalnega ZnO. Lokalno strukturo napak smo preiskali z visokoločljivostno transmisijsko elektronsko mikroskopijo, njihovo kemijsko sestavo pa smo analizirali z energijsko disperzijsko spektroskopijo. Ne glede na vrsto dopanta (Sb, Sn, Ti, In, Fe, Ga,) imajo inverzne meje lokalno kubično strukturo, ki se sestoji iz oktaederske plasti kationov.

1 Introduction

Inversion boundaries (IBs) play an important role in microstructure development /1/, as well as they are believed to affect the electrical properties /2/ of ZnO-based varistor ceramics. Inversion boundaries develop in ZnO grains only when ZnO is doped with specific metal oxides such as SnO_2 /1/, Sb_2O_3 /3-5/, TiO_2 /6/, In_2O_3 /7/, Fe_2O_3 /8/, Ga_2O_3 /9/, among others. The addition of SnO_2 to ZnO significantly influences the grain growth via the inversion boundary induced grain growth mechanism /1/. ZnO grains with IBs start to grow anisotropically along the direction of the fault plane until they collide. With the increasing amount of SnO_2 more ZnO grains initially contain IBs and the final grain size gets smaller. The most extensively studied system that exhibits IBs is certainly Sb_2O_3 doped ZnO because Sb_2O_3 is an essential dopant of varistor ceramics when fine-grained microstructure is required. It is believed that Sb_2O_3 influences the grain growth through the formation of secondary spinel grains and IBs in the ZnO grains. Final microstructures, obtained with the addition of small amounts of Sb_2O_3 are fine-grained and the final grain size gets even smaller with increasing addition of Sb_2O_3 /10/. Therefore, Sb_2O_3 is reported as an inhibitor of ZnO grain growth /11/. On the contrary, the addition of TiO_2 to ZnO ceramics results in a large final grain size and is typically added when coarse-grained microstructure is required. TiO_2 is believed to be a grain growth promoter /12/. Because of their influence to the final microstructure Sb_2O_3 is used in high-voltage, while TiO_2 is added for low-voltage varistor applications.

To understand the influence of these planar faults to ZnO grain growth we have to understand their nucleation mechanism and therefore the knowledge about their exact structural and chemical characterisation is required. In order to determine the local structure and chemistry of planar fault one should employ appropriate methods which enable its direct observation. To assess the information from sub-nanometer regions of the specimen we have to produce probes of that order of magnitude. Here electron microscopy provides a unique capability to retrieve a local structural informa-

tion that can not be recovered by statistical information obtained with X-ray crystallography. Apart from structural information, electrons and their energy dissipation products are bearing a valuable chemical information of the local structure owing to a wide variety of electronic transitions. In this paper the identification of inversion boundaries is given beginning with scanning electron microscope observations down to the detailed structural and chemical characterisation of these faults with the methods of analytical and phase contrast transmission electron microscopy.

2 Crystallography of inversion boundaries

ZnO crystallises in hexagonal wurtzite structure, in which the close-packed zinc and oxygen layers are exchanging in a ...αAβB... manner, where α and β are zinc, while A and B are oxygen atoms. Unit cell parameters are a=0,3253 nm and c=0,5213 nm /13/. Another parameter, typical for this structure is u, which is the atomic shift between oxygen and zinc atomic layers and amounts to 0.382 in hexagonal ZnO. Because of this, the structure does not poses a centre of symmetry in the direction of the c-axis, which is hence called the polar axis of the structure. According to the direction of the polar c-axis two basic types of planar faults can be distinguished in hexagonal ZnO: (a) stacking faults ...αA–βB | γC–βB..., where the direction of the polar axis over the fault is preserved and (b) inversion boundaries, where the direction of the polar axis is reversed across the fault plane. IBs can be of two configurations, head-to-head if the polar axes point toward the boundary or tail-to-tail if they point away from the boundary.

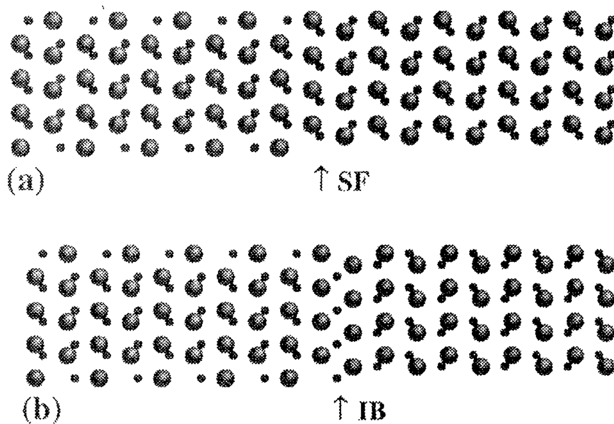

Fig. 1: Atomic structures of (a) stacking fault and (b) head-to-head inversion boundary.

Our recent studies of the crystallography of IBs in Sb_2O_3 doped ZnO indicate that the stacking across the fault plane is α_I A–β_IB–α_I A–β_IB |β_{oct}| Cγ_{II}–Bβ_{II}–Cγ_{II}–Bβ_{II} ... while the translation produced by such head-to-head IB is (1–2u)·[0001] + 1/3·[10$\bar{1}$0]. The IB plane itself comprises a close-packed layer of cations located at the octahedral interstices of this interface structure /14/.

The schematic drawings of basal plane stacking fault and head-to-head inversion boundary are illustrated in Figure 1.

3 Methods of investigation

Unlike the X-rays, lenses for electrons are readily made, allowing to produce electronprobes down to 0.2 nm in diameter. There are several reasons why electrons are more convenient as a probe for the studies of local structures in solids. They are strongly scattered by solids, allowing scattering and imaging experiments to be performed with a high information level. In general, structural information is obtained from elastically scattered electrons, whereas the information about the chemistry of the specimen is recovered from inelastically scattered electrons and electron decay products. In past few decades numerous methods exploiting different properties of electrons were developed, allowing the local structures of crystal defects to be studied.

The information about the structural and compositional properties of planar faults can be obtained employing a high-resolution transmission electron microscopy (HRTEM) combined with the energy dispersive X-ray spectroscopy (EDS) in the vicinity of the interface. Quantification of HRTEM and EDS data results in a detailed information about the orientation of the host crystal blocks, atomic-column positions along the interface in the selected projections, rough atomic-column displacements, chemical composition of the fault plane, and in some favourable cases also the oxidation state of the investigated atoms. It is important to note that non-periodic structural features, like point defects, happen to be beyond the capabilities of this approach.

3.1 Scanning electron microscopy (SEM)

Scanning electron microscopy is the most widely used tool for general microstructural characterisation of the samples. Depending on the detected electron signals, either topographic or chemical information can be obtained. Typically, for the grain size and morphology observations, the samples are etched thermally or chemically. Chemical etching with dilute hydrochloric acid results in dissolving of the intergranular material and therefore ZnO grains are easily observed. Additionally we observe that ZnO grains are etched differently depending on crystallographic orientation of the exposed surface. This phenomenon is characteristic also for other compounds having sphalerite or wurtzite structure /15/. Consequently planar faults, such as IBs become clearly visible after chemical etching. Another interesting feature produced by etching are the characteristic triangular etch pits on the surfaces of the ZnO grains. These etch-pits are always oriented in one direction in a single crystal domain. In ZnO grains contain planar faults the etch-figures always point towards the fault plane, and over the fault their orientation is reversed (Figure 2). These observations provide an indication, that the crystal orientation is reversed over the boundary, however the exact crystallographic plane of the fault can be assessed by a detailed investigations using transmission electron microscopy.

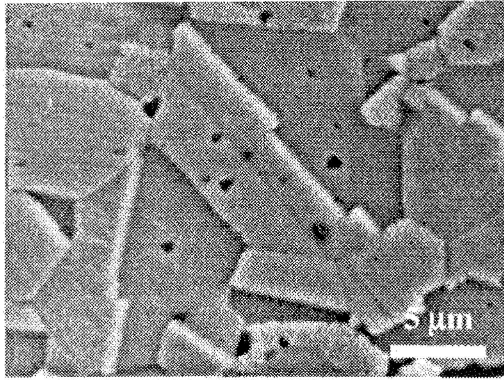

Fig. 2: SEM image of ZnO ceramics, doped with 0.1 mol% Sb_2O_3 and sintered at 1200°C for 16 hours. IBs intersecting ZnO grains are clearly visible. Triangular etch-pits in ZnO grains always point in the same direction within one crystal domain. In the grains with planar faults etch-pits always point towards the boundary, while over the fault their orientation is reversed, indicating the reversal of the polar c-axis.

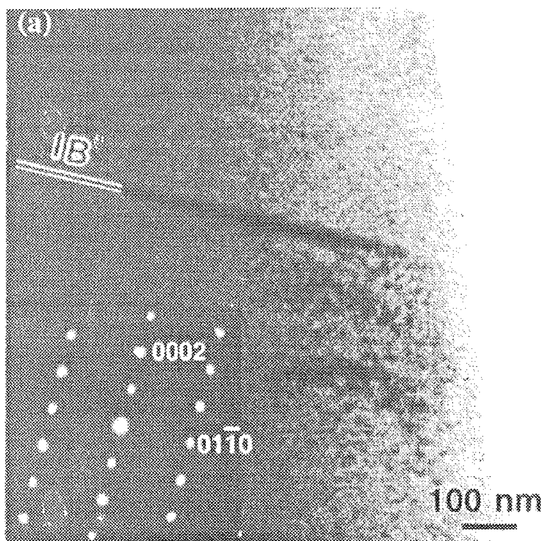

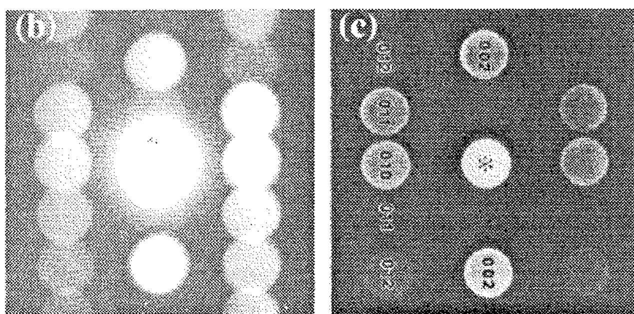

Fig. 3: (a) TEM image of a ZnO grain in the [11$\bar{2}$0] orientation, shows that the fault lies in the basal planes of the ZnO structure. Above are the (b) experimental and (c) simulated CBED patterns for the upper ZnO crystal domain while in the lower domain the pattern is mirrored (not shown here) indicating a head-to-head configuration of the inversion boundary.

3.2 Conventional transmission electron microscopy (CTEM)

Conventional transmission electron microscopy is the next step for identification and characterisation of the observed planar faults. TEM image in Figure 3 shows a planar fault intersecting the ZnO grain in the middle. According to the diffraction pattern, the fault lies in the basal planes of ZnO crystal. To determine the absolute orientation of the c-axis on both sides of the boundary we used a direct method, proposed by Mader and Rečnik /16/. Owing to non-centrosymmetric crystal structure, the scattering factors for **g** and **-g** reflections are different. The difference can be observed in a convergent beam electron diffraction (CBED) pattern, obtained with as small condenser aperture, that the diffraction disks do not overlap. Microdiffraction patterns on both sides of the boundary suggest a reversal of the polar c-axes. The absolute orientation of the crystal domains can be determined by matching the experimental microdiffraction patterns to calculated CBED patterns /17/ for a thin crystal regime.

3.3 High-resolution transmission electron microscopy (HRTEM)

In high-resolution transmission electron microscopy there are some instrumental and crystallographic limitations that have to be taken into account when choosing the appropriate zone axis for observation. The main obstacle is the resolution limit of the microscope and only in a few low-index crystallographic projections the fault can be aligned parallel to the electron beam. To study the basal plane IBs in ZnO this reduces the possibilities to [11$\bar{2}$0] and [10$\bar{1}$0] projections with a required resolution of 0.2817 nm in first and 0.1627 nm in the second instance. To obtain a 3D information about the local structure of the fault, and moreover to acquire the information on the atomic arrangement in the IB plane, lattice images in both projections were recorded under different defocusing conditions. Lattice images of IBs in Sb_2O_3 doped samples in the [11$\bar{2}$0] and [10$\bar{1}$0] projections have revealed the presence of heavy atoms in the boundary plane obeying an ...ABBABB... linear repeating sequence /14/. The translational state and coordination of the boundary plane could also be deduced from experimental HRTEM images. A lateral expansion of the IB observed in the lattice images allowed to differentiate this fault from stacking faults which are also abundant in ZnO /14/.

Our studies of IBs produced by doping ZnO with SnO_2 and In_2O_3 resulted in similar translation state across the fault plane and identical crystallography as determined for Sb_2O_3 doped samples. The only obvious difference was the linear repeating sequence in the boundary plane when viewed along the [10$\bar{1}$0] projection, which indicates that the distribution of dopant ions in the boundary plane is different for Sb_2O_3, SnO_2 and In_2O_3. While the linear repeating sequence for Sb-rich IB was ...ABBABB... /14/ this was in the case of Sn-rich IB ...AABBAABB... /16/ and ...AAA... /17/ for In-rich IB. Figure 4 shows typical lattice images of IBs viewed along the [10$\bar{1}$0] projection in SnO_2 and Sb_2O_3 doped ZnO. HRTEM results for different IBs show that the atomic arrangement of the IB octahedral plane and the

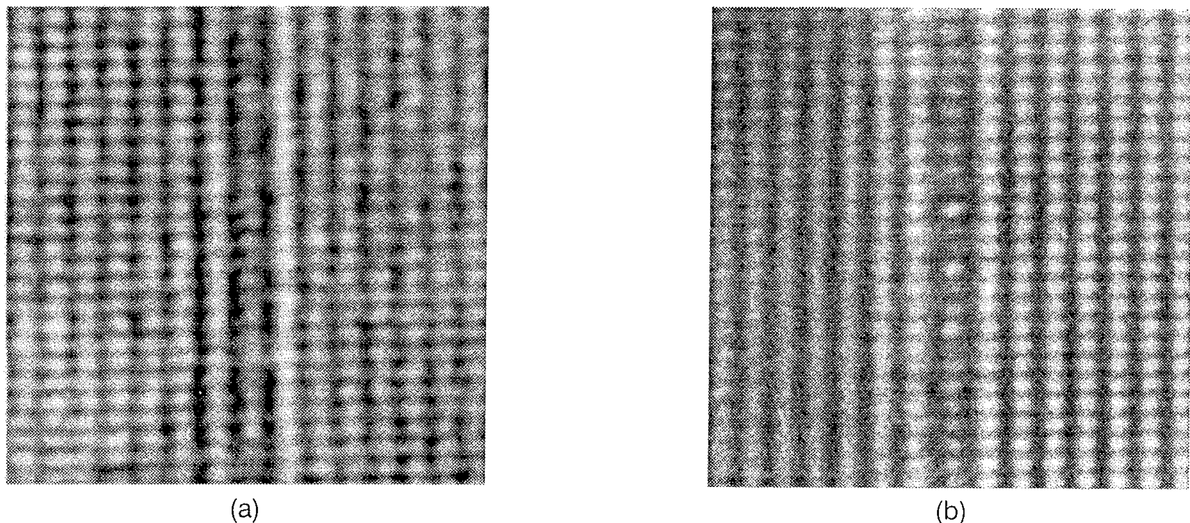

Fig. 4: HRTEM images of IBs in (a) SnO_2 doped ZnO and (b) Sb_2O_3 doped ZnO in $[10\bar{1}0]$ projection; note the periodicity of ...AABBAABB... and ...ABBABB... respectively.

amount of the dopant atoms mainly depend on the oxidation state of the dopant element. Therefore, to establish the content of the dopant in the fault plane one must obtain analytical information from IB.

3.4 Z-contrast scanning transmission electron microscopy (HAADF-STEM)

The correlation between the atomic structure and chemistry of solids became available by the atomic resolution high-angle annular dark field scanning transmission electron microscopy (HAADF-STEM), known as Z-contrast. The Z-contrast imaging can be performed using a field emission gun electron micro-scope equipped with a high-angle annular detector. HAADF-STEM in principle provides incoherent images that can be directly inverted to the object. While this is generally applicable for perfect crystal structures, image simulations are necessary for a quantitative elemental analysis /18/. To obtain the information on the local atomic arrangement in the IB octahedral plane we employed Z-contrast imaging of IBs in the $[10\bar{1}0]$ zone axis. In the case of Sb-rich IBs we observed similar linear periodicity as from HRTEM images /19/. The intense white dots in the boundary plane produced by pure Sb columns are in the Z-contrast images separated by two dots of lower intensity, implying a boundary composition of $SbZn_2$.

3.5 Chemical analysis with energy dispersive spectroscopy (EDS)

HRTEM and Z-contrast imaging of IBs, formed with different dopants showed, that (a) inversion boundaries are single layers within the inverted ZnO crystal domains and (b) the phase contrast of different IBs is different. These observations indicate that IBs, formed with different dopants have different chemical composition and local structure. To quantitatively determine the chemical composition of different types of IBs one should employ energy dispersive spectroscopy (EDS), however, because of the very low dopant content (less than one monolayer) in the IB plane an appropriate method of exact dopant content in the boundary must be used. A single EDS analysis shows qualitatively that inversion boundaries formed with different dopants, contain only the IB forming element. To quantitatively determine the dopant level on IBs we used a method where dopant content in a boundary is estimated from a series of EDS analyses using different beam diameters. A series of EDS analyses on the IB plane with different beam diameters is performed, where the centre of the beam must be kept exactly the same in all measurements. From the dependency of the measured intensity ratio between the Zn–K_α line and a characteristic dopant line vs. the beam diameter, the integral amount of the dopant in the boundary layer can be calculated, assuming a straight boundary plane within a cylindrical volume of analysis /14/. Using this method we determined about 1/3 of a monolayer of Sb, 1/2 of a monolayer of Sn, and one full monolayer of In on inversion boundaries in ZnO doped with Sb_2O_3, SnO_2 and In_2O_3, respectively.

4 Summary

We have shown that a combination of various imaging and analytical techniques using scanning and transmission electron microscopy provides a powerful tool to study inversion boundaries in ZnO. The first evidence for the presence of inversion boundaries was given in SEM by observation of triangular etch-pits on both sides of planar faults intersecting the ZnO grains. The microdiffraction method performed in a CTEM on both sides of the boundary confirmed this presumption. To study the local structure and chemistry of IBs we used atomic resolution microscopy techniques. The structural information was obtained by studying the fault of interest in different zone axes by phase contrast HRTEM. The interpretation of experimental images is possible by the comparison with simulated ones. On the other hand the images obtained with HAADF-STEM method are incoherent and can be directly inverted to the object, which makes this technique a very promis-

ing tool for the studies where we need to correlate structure and chemistry of the fault. The combination of imaging methods combined with Z-contrast and EDS analysis of IBs showed, that different dopants form IBs with different local structure and chemistry.

References

/1/ N. Daneu, A. Rečnik, S. Bernik and D. Kolar, J. Am. Ceram. Soc., 83 (2000) 3165-71.

/2/ B. A. Haskell, S. J. Souri and M. A. Helfand, J. Am. Ceram. Soc., 82 (1999) 2106-10.

/3/ M. Trontelj and V. Kraševec, Science of Ceramics, 14 (1988) 915-920.

/4/ J. Bruley, U. Bremer and V. Kraševec, J. Am. Ceram. Soc., 75 (1992) 3127-28.

/5/ M. A. McCoy, R. W. Grimes and W. E. Lee, J. Mater. Res., 11 (1996) 2009-19.

/6/ D. Makovec and M. Trontelj, J. Am. Ceram. Soc., 77 (1994) 1202-8.

/7/ A. Loewe, M. Trontelj and W. Mader, Proceedings of the 1st Slovene-German Seminar on Joint Projects in Materials Science and Technology, Portorož, Slovenia, (1994) 35-40.

/8/ F. Wolf, A. Loewe and W. Mader, Abstracts of the 3rd Slovene-German Seminar on Joint Projects in Materials Science and Technology, Bled, Slovenia, (1998) 10-11.

/9/ J. Barf and W. Mader, Abstracts of the 3rd Slovene-German Seminar on Joint Projects in Materials Science and Technology, Bled, Slovenia, (1998) 86-87.

/10/ J. Kim, T. Kimura and T. Yamaguchi, J. Mater. Sci., 24 (1989) 2581-86.

/11/ T. Senda and R. C. Bradt, J. Am. Ceram. Soc., 74 (1991) 1296-1302.

/12/ D. Makovec, D. Kolar, and M. Trontelj, Mater. Res. Bull., 28 (1993) 803-11.

/13/ H. Schultz and K. H. Thiemann, Sol. State Commun., 32 (1979) 783-785.

/14/ A. Rečnik, N. Daneu, T. Walther and W. Mader, J. Mater. Res., to be published.

/15/ E. P. Warekois, M. C. Lavine, A. N. Mariano and H. C. Gatos, J. Appl. Phys., 33 (1961) 690-96.

/16/ W. Mader and A. Rečnik, Phys. Stat. Sol. (a), 166 (1998) 381-95.

/17/ P. A. Stadelmann, Ultramicroscopy, 21 (1987) 131-45.

/18/ T. Yamazaki, K. Watanabe, A. Rečnik, M. Čeh, M. Kawasaki and M. Shiojiri, J. Electron Microscopy, 49 (2000) in press.

/19/ A. Rečnik, W. Mader and M. Kawasaki, Proceedings of the 4th Multinational Congress on Electron Microscopy, Veszprém, Hungary, (1999) 113-118.

Nina Daneu
Aleksander Rečnik
Slavko Bernik
Jožef Stefan Institute
Jamova 39, 1000 Ljubljana, Slovenia
nina.daneu@ijs.si,
aleksander.recnik@ijs.si,
slavko.bernik@ijs.si

Prispelo (Arrived): 1.10.2000 *Sprejeto (Accepted): 25.11.2000*

KONFERENCA MIDEM 2000 - POROČILO
MIDEM 2000 CONFERENCE REPORT

36th INTERNATIONAL CONFERENCE ON MICROELECTRONICS, DEVICES AND MATERIALS WITH THE WORKSHOP ON ANALYTICAL METHODS IN MICROELECTRONICS AND ELECTRONIC MATERIALS

The 36th International Conference on Microelectronics, Devices and Materials MIDEM 2000 was organised by MIDEM - The Society for Microelectronic, Electronic Components and Materials. The conference took place from 18 to 20 October 2000 at the Hotel Jama in Postojna. Conference sponsors were the Ministry of Science and Technology, Republic of Slovenia, Iskra Emeco, Kranj, Jožef Stefan Institute, Ljubljana, the Faculty of Electrical Engineering, University of Ljubljana, IMAPS, Slovenian Section and IEEE, Slovenian Section. The conference continued the tradition of the annual international conferences organised by the MIDEM Society. These conferences have always attracted a large number of Slovene and foreign experts working in these fields. The Conference was opened by short welcoming addresses from the conference chairman Dr. Marko Hrovat, Jožef Stefan Institute and Prof. Dr. Anton Jeglič, State Secretary for Science of the Ministry of Science and Technology of Slovenia.

The topics covered by the conference were quite diverse. 51 papers were presented in six sessions over three days: Integrated Circuits; Sensors; Thick Films; Optoelectronics; Ceramics, Metals and Composites; and Device Physics and Modelling. Sessions on Integrated Circuits and Thick Films were ntroduced by a distinguished invited speakers giving an overview presentation on related fields. The following invited papers were presented:

- G. Pignatel, University of Trento, Italy
  "Recent Developments in Silicon Radiation Detectors at IRST"

- P. Mach, Czech Technical University in Prague
  "Diagnostics of Nonlinearity of Current vs. Voltage Characteristics - Theory and Application"

Since 1998, workshops dedicated to each year's selected special topic have been added to the programme of the MIDEM Conferences. In the framework of the workshop, four to six invited speakers present the chosen topics from different points of view, thus offering the audience a variety of valuable information. Time for thorough discussions is provided between the invited presentations, and the Conference attendees are encouraged to present their research results in the Conference session dealing with the same topic. During MIDEM'2000, the Workshop on Analytical Methods in Microelectronics and Electronic Materials was organized by Ceramics Dept., Jožef Stefan Institute. Selected topics associated with advanced analytical methods like AFM, SEM, TEM, EDX, AES, ESCA, XPS etc. were presented, covering the basic physical principles, as well as actual and possible applications of these methods in microelectronics and in the analysis of electronic materials. In the framework of the workshop six invited speaker presented the chosen topic from different aspects, thus offering the audience valuable information. Time for extended discussion was provided between invited presentations. The following invited papers were presented:

- I. Muševič, Jožef Stefan Institute, Ljubljana
  "Atomic Force Microscopy"

- A. Zalar, ITPO, Ljubljana, Slovenia
  "Materials Characterization by Auger Electron Spectroscopy Sputter Depth Profiling"

- S. Bernik et.al., IJS, Ljubljana
  "The Application of Electron Microscopy Methods in the Study of Inversion Boundaries in ZnO Varistors"

- H. Bender, IMEC, Belgium
  "Application of Focused Ion Beam for Failure Analysis"

- J Hren, North Carolina State University, USA
  "Characterisation of Dielectrics on the "Tip of Needles"

- H. P. Karnthaler, University of Vienna, Austria
  "High TEM Analysis of Atomic Structures of Metals, Alloys and Ceramic Materials"

Some statistical data:

- Number of participants: total 64, 12 from abroad
- Number of papers published in the Proceedings: total 51, 11 from abroad
- Participant countries: Slovenia, Italy, Austria, Germany, Czech Republic, Belgium, USA and Croatia
- The Conference Proceedings were published prior to the Conference and contain 336 pages.

Ljubljana, Nov. 2000 *Marko Hrovat*

KONFERENCA MIDEM 2000
SEZNAM UDELEŽENCEV

MIDEM 2000
LIST OF PARTICIPANTS

	NAME	COMPANY - INSTITUTION	ADDRESS	P.CODE	CITY	
1	ALJANČIČ UROŠ	FAKULTETA ZA ELEKTROTEHNIKO	TRŽAŠKA 25	1000	LJUBLJANA	SLO
2	AMON SLAVKO	FAKULTETA ZA ELEKTROTEHNIKO	TRŽAŠKA 25	1000	LJUBLJANA	SLO
3	ARČON IZTOK	POLITEHNIKA NOVA GORICA	VIPAVSKA 13	5001	NOVA GORICA	SLO
4	AUSSERLECHNER UDO	INFINEON TECHNOLOGIES	SIEMENSTRASSE 2	9500	VILLACH	A
5	BELAVIČ DARKO	HIPOT-HYB	TRUBARJEVA 7	8310	ŠENTJERNEJ	SLO
6	BENČAN ANDREJA	INSTITUT JOZEF STEFAN	JAMOVA 39	1000	LJUBLJANA	SLO
7	BENDER HUGO	IMEC	KAPELDREEF 79		LEUVEN	B
8	BERNIK SLAVKO	INSTITUT JOZEF STEFAN	JAMOVA 39	1000	LJUBLJANA	SLO
9	BRECL KRISTIJAN	FAKULTETA ZA ELEKTROTEHNIKO	TRŽAŠKA 25	1000	LJUBLJANA	SLO
10	ČAKARE LAILA	INSTITUT JOZEF STEFAN	JAMOVA 39	1000	LJUBLJANA	SLO
11	DRAŽIČ GORAN	INSTITUT JOZEF STEFAN	JAMOVA 39	1000	LJUBLJANA	SLO
12	GRADIŠNIK VERA	SVEUČILIŠTE U RIJECI, FAKULTET ZA TURISTIČI I HOTELSKI MENADŽMENT	IKA, PRIMURSKA 42	51410	OPATIJA	CRO
13	HOMOLKA HEINZ	TU-WIEN	GIUSSHAUSSTRASSE 27-29	1040	WIEN	A
14	HREN JOHN	NORTH CAROLINA STATE UNIVERSITY	RALEIGH, NC27695	7907	RALEIGH	USA
15	HROVAT MARKO	INSTITUT JOZEF STEFAN	JAMOVA 39	1000	LJUBLJANA	SLO
16	JANKOVEC MARKO	FAKULTETA ZA ELEKTROTEHNIKO	TRŽAŠKA 25	1000	LJUBLJANA	SLO
17	JAVORIČ SAŠA	INSTITUT JOZEF STEFAN	JAMOVA 39	1000	LJUBLJANA	SLO
18	JEGLIČ ANTON	MINISTRY OF SIT OF THE RS	TRG OF 13	1000	LJUBLJANA	SLO
19	KARNTHALER PETER	UNIVERSITY OF WIENNA	BOLTZMANNG. 5	1090	WIENNA	A
20	KEK DARJA	INSTITUT JOZEF STEFAN	JAMOVA 39	1000	LJUBLJANA	SLO
21	KLANJŠEK-GUNDE MARTA	NATIONAL INSTITUTE OF CHEMISTRY	HAJDRIHOVA 19	1000	LJUBLJANA	SLO
22	KOKALJ MATEJA	MIDEM	DUNAJSKA 10	1000	LJUBLJANA	SLO
23	KOLLE CHRISTIAN	INFINEON TECHNOLOGIES	SIEMENSTRASSE 2	9500	VILLACH	A
24	KOMAC MILOŠ	MZT	TRG OF 13	1000	LJUBLJANA	SLO
25	KOMELJ MATEJ	INSTITUT JOZEF STEFAN	JAMOVA 39	1000	LJUBLJANA	SLO
26	KOROŠAK DEAN	FAKULTETA ZA GRADBENIŠTVO	SMETANOVA 17	1000	LJUBLJANA	SLO
27	KOSEC MARIJA	INSTITUT JOZEF STEFAN	JAMOVA 39	1000	LJUBLJANA	SLO
28	KRČ JANEZ	FAKULTETA ZA ELEKTROTEHNIKO	TRŽAŠKA 25	1000	LJUBLJANA	SLO
29	LEVSTEK ANDREJ	FAKULTETA ZA ELEKTROTEHNIKO	TRŽAŠKA 25	1000	LJUBLJANA	SLO
30	LIMPEL META	MIDEM	STEGNE 11	1521	LJUBLJANA	SLO
31	MACH PAVEL	CHECK. TECH. UNIVERSITY	TECHNICKA 2	16627	PRAGUE	CZE
32	MAČEK MARIJAN	FAKULTETA ZA ELEKTROTEHNIKO	TRŽAŠKA 25	1000	LJUBLJANA	SLO
33	MAČEK SREČKO	INSTITUT JOZEF STEFAN	JAMOVA 39	1000	LJUBLJANA	SLO
34	MALIČ BARBARA	INSTITUT JOZEF STEFAN	JAMOVA 39	1000	LJUBLJANA	SLO
35	MOZETIČ MIRAN	ITPO	TESLOVA 30	1000	LJUBLJANA	SLO
36	MOŽEK MATEJ	FAKULTETA ZA ELEKTROTEHNIKO	TRŽAŠKA 25	1000	LJUBLJANA	SLO
37	MURKO DARJA	INSTITUT JOZEF STEFAN	JAMOVA 39	1000	LJUBLJANA	SLO
38	MUŠEVIČ IGOR	FAKULTETA ZA MATEMATIKO IN FIZIKO	JADRANSKA 19	1000	LJUBLJANA	SLO
39	PAIRITCSH HERBERT	INFINEON TECHNOLOGIES	SIEMENSTRASSE 2	9500	VILLACH	A
40	PANJAN PETER	INSTITUT JOZEF STEFAN	JAMOVA 39	1000	LJUBLJANA	SLO
41	PELICON PRIMOŽ	INSTITUT JOZEF STEFAN	JAMOVA 39	1000	LJUBLJANA	SLO
42	PEVEC ALBIN	FAKULTETA ZA ELEKTROTEHNIKO	TRŽAŠKA 25	1000	LJUBLJANA	SLO
43	PIGNATEL GIORGIO	UNIVERSITY OF TRENTO	MESIANO 77	38050	TRENTO	I
44	PLETERŠEK ANTON	FAKULTETA ZA ELEKTROTEHNIKO	TRŽAŠKA 25	1000	LJUBLJANA	SLO
45	POMPE IGOR	TC SEMTO	STEGNE 25	1000	LJUBLJANA	SLO
46	RAIČ DUŠAN	FAKULTETA ZA ELEKTROTEHNIKO.	TRŽAŠKA 25	1000	LJUBLJANA	SLO
47	REICHMANN KLAUS	TU-GRAZ	STREMAYRG. 16/3	8010	GRAZ	A
48	RESNIK DRAGO	FAKULTETA ZA ELEKTROTEHNIKO	TRŽAŠKA 25	1000	LJUBLJANA	SLO
49	ROČAK DUBRAVKA	INSTITUT JOZEF STEFAN	JAMOVA 39	1000	LJUBLJANA	SLO
50	SAMARDŽIJA ZORAN	INSTITUT JOZEF STEFAN	JAMOVA 39	1000	LJUBLJANA	SLO
51	SANTO-ZARNIK MARINA	HIPOT-HYB	TRUBARJEVA 7	8310	ŠENTJERNEJ	SLO
52	SMETANA WALTER	INST. OF INDUSTRIAL ELECTRONICS & MATERIAL SCIENCE	GUßHAUSSTRASSE 27-29	1040	WIEN	A
53	STARAŠINIČ SLAVKO	FAKULTETA ZA ELEKTROTEHNIKO	TRŽAŠKA 25	1000	LJUBLJANA	SLO
54	STRLE DRAGO	FAKULTETA ZA ELEKTROTEHNIKO	TRŽAŠKA 25	1000	LJUBLJANA	SLO
55	ŠORLI IZTOK	MIDEM	DUNAJSKA 10	1000	LJUBLJANA	SLO
56	ŠTERN ANTON	FAKULTETA ZA GRADBENIŠTVO	TRŽAŠKA 25	1000	LJUBLJANA	SLO
57	TASEVSKI MILAN	SIPO-MZT	KOTNIKOVA 6	1000	LJUBLJANA	SLO
58	TRONTELJ JANEZ	FAKULTETA ZA ELEKTROTEHNIKO	TRŽAŠKA 25	1000	LJUBLJANA	SLO
59	TRONTELJ JANEZ Jr.	FAKULTETA ZA ELEKTROTEHNIKO	TRŽAŠKA 25	1000	LJUBLJANA	SLO
60	TROST ANDREJ	FAKULTETA ZA ELEKTROTEHNIKO	TRŽAŠKA 25	1000	LJUBLJANA	SLO
61	VRTAČNIK DANILO	FAKULTETA ZA ELEKTROTEHNIKO	TRŽAŠKA 25	1000	LJUBLJANA	SLO
62	VUKADINOVIČ MIŠO	FAKULTETA ZA ELEKTROTEHNIKO	TRŽAŠKA 25	1000	LJUBLJANA	SLO
63	ZALAR ANTON	ITPO	TESLOVA 30	1000	LJUBLJANA	SLO
64	ZORKO SAMO	ISKRA EMECO	SAVSKA LOKA 4	4000	KRANJ	SLO

ZOISOVA PRIZNANJA - ZOIS PRIZES

Docent dr. Marko Topič

ZOISOVO PRIZNANJE za pomembne znanstvene dosežke na področju tankoplastnih polprevodniških struktur

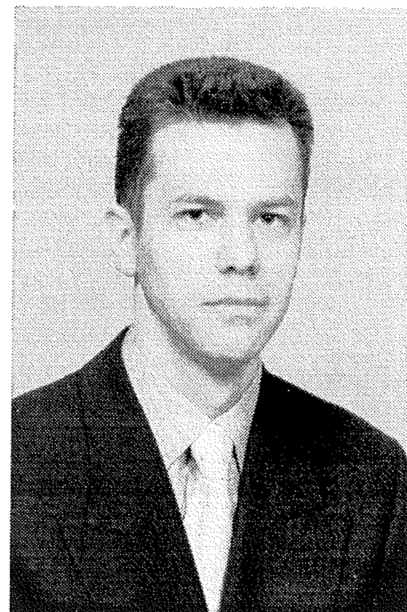

Med štirimi dobitniki Zoisovih priznanj za leto 2000 za pomembne znanstvene dosežke na področju temeljnih in aplikativnih znanosti je tudi docent dr. Marko Topič, univ. dipl. inž. el., ki je priznanje prejel za objave več študij in rezultatov svojega raziskovalnega dela na področju tankoplastnih polprevodnikov.

Docent Topič raziskuje tankoplastne polprevodnike, ki imajo kot novejši polprevodniški materiali pomembno mesto v številnih aplikacijah na področju tankoplastnih tehnologij, a so hkrati zaradi izjemne zapletenosti zgradbe še vedno v fazi intenzivnih raziskav. Rezultati raziskav so pomemben prispevek k razumevanju notranjih lastnosti amorfnega silicija in večplastnih amorfnosilicijevih heterostruktur, mikrokristalnih silicijevih heterostruktur in struktur iz polikristalnih heteroatomnih polprevodniških materialov, kot so npr. CdS, $CuInSe_2$ in $Cu(In,Ga)Se_2$.

Dr. Topič pri raziskavah združuje eksperimentalno delo z računalniškimi simulacijami s simulatorjem ASPIN, ki je bil razvit na Fakulteti za elektrotehniko in ga je dr. Topič posodobil in izpopolnil do te mere, da predstavlja nepogrešljiv pripomoček pri načrtovanju in optimizaciji amorfnosilicijevih in drugih tankoplastnih polprevodniških struktur, ki so sestavljene iz amorfnih, mikrokristalnih in drugih plasti. Pri vpogledu v fizikalna dogajanja znotraj struktur, vključno z dogajanji na mejah med različnimi materiali, ima kvalitetna računalniška simulacija nadvse pomembno vlogo.

Rezultate raziskovalnega dela s področja tankoplastnih polprevodniških tehnologij je mogoče uporabiti tudi v mikroelektroniki, kjer se pogosto pojavljajo povsem sorodni problemi (npr. obravnava defektnih stanj, heterospojev ipd.).

Aktualnost raziskav potrjuje dejstvo, da proizvodnja sončnih celic strmo narašča. Razpoložljiva moč v letu 2000 proizvedenih celic naj bi dosegla že 100 MW. V proizvodnji zavzemajo vedno večji delež tehnologije tankoplastnih sončnih celic. Izboljšanje izkoristka tankoplastnih sončnih celic ($Cu(In,Ga)Se_2$, a-Si:H, ...) v zadnjih letih je dalo raziskavam nov zagon. Narašča tudi uporaba tankoplastnih polprevodniških tehnologij v elektroniki.

Dr. Topič nadaljuje tudi raziskave senzorja barv v sodelovanju s Forschungszentrum Jülich, v Jülichu, Nemčija. Zaradi odmevnosti svojih dosedanjih objav je marca letos prejel raziskovalno štipendijo Fondacije Alexander von Humboldt, ki jo je v času od maja do novembra 2000 izkoristil za raziskave tankoplastnih polprevodnikov z veliko energijsko režo in možnostjo njihove uporabe kot UV detektorjev.

Izvirnost in kvaliteto njegovih dosežkov potrjujejo tudi odlične ocene tujih recenzentov za članke, poslane v objavo v mednarodne znanstvene revije. V obdobju 1994-2000 je objavil kot prvi avtor oz. soavtor preko 40 referatov v zbornikih specializiranih mednarodnih konferenc in 20 člankov v serijskih mednarodnih znanstvenih publikacijah. Skoraj vsi članki (19) so v revijah, ki so uvrščene v SCI. Med njimi jih je kar 15 v najuglednejših revijah za to znanstveno področje, v katerih nastopa Marko Topič 12-krat kot prvi oz. vodilni avtor.

Rezultati in dosežki, ki so bili na mednarodnih konferencah deležni velike pozornosti, so pripomogli k intenzivnejšemu sodelovanju in navezovanju novih sodelovanj z uglednimi institucijami po svetu.

S svojimi odmevnimi raziskavami je pomembno prispeval k razumevanju lastnosti amorfnega silicija, večplastnih amorfnih in mikrokristaliničnih silicijevih heterostruktur in struktur iz heteroatomnih materialov.

V imenu članov MIDEM in v svojem imenu iskrene čestitke.

Predsednica Društva MIDEM
Marija Kosec

PS:Ne tako davno nazaj smo dr. Topiču čestitali za Zlati znak Jožefa Stefana, sedaj za Zoisovo priznanje. Kaj bo naslednje?

Dr. Goran Dražič

ZOISOVO PRIZNANJE
za pomembne znanstvene dosežke na področju elektronske mikroskopije

Dr. Goran Dražič se že vrsto let ukvarja z metodami elektronske mikroskopije in mikroanalize, v zadnjih letih še prav intenzivno z analitsko elektronsko mikroskopijo, področjem, ki je postalo nepogrešljivo pri študiju sodobnih anorganskih materialov.

Delo dr. Gorana Dražiča obsega uporabo in razvoj metod analitske elektronske mikroskopije pri študiju različnih sodobnih keramičnih in kovinskih materialov. Na področju kvantitativne energijske spektroskopije rentgenskih žarkov se je dr. Dražič doma in v tujini uveljavil kot strokovnjak za analizo nanometrskih področij. S prilagoditvijo analitskih metod je določil stopnjo kemijske homogenosti na nanometrskih področjih v keramičnih materialih na osnovi svinčevega cirkonata-titanata. Poznavanje kemijske homogenosti v teh materialih lahko bistveno pripomore k boljšemu razumevanju procesov, ki nastopajo ob sintezi in s tem k izboljšanju lastnosti in uporabnosti materialov. Predlagal je tudi način za določanje kemijske sestave trdne topnosti v primerih, ko pride do izločanja nanometrskih precipitatov v matrici trdne raztopine in način za določanje kemijske sestave nanometrskih amorfnih filmov na mejah med zrni z uporabo analitskih elektronskih mikroskopov nižje ločljivosti.

Za večino objav nagrajenca, ki nedvomno vsebujejo izvirne dosežke, ki pomembno prispevajo k področju, s katerim se ukvarja, je značilno, da so rezultat skupnega dela z različnimi strokovnjaki s področja sinteze materialov, pri čemer je dr. Dražič pokrival mikrostrukturno karakterizacijo. Pri mnogih novih materialih so se pojavljali številni analitski problemi, ki niso bili rešljivi z rutinsko uporabo metod analitske mikroskopije, pač pa z izvirnim pristopom k vsakemu problemu posebej.

Dr. Dražič je tako v zadnjih letih plodno sodeloval z znanstveniki iz različnih slovenskih institucij (Kemijski institut, Fakulteta za kemijo in kemijsko tehnologijo, Naravoslovno tehnična fakulteta, Strojna fakulteta, itd.) in s strokovnjaki iz Nemčije, Švice, Francije, Španije in Amerike (univerze oziroma instituti v Jülichu, Lulei, Laussani, Toulousu, Madridu, Dresdnu, Gaithersburgu, itd.).

Rezultati njegovega dela, vpetega v številne domače in mednarodne znanstveno-raziskovalne projekte, so bili od leta 1993 objavljeni v 27 izvirnih znanstvenih člankih od katerih je 11 člankov objavljenih v revijah z nadpovprečnim IF in 28 objavljenih predavanjih na znanstvenih konferencah, od tega 5 vabljenih predavanjih. Kandidatova dela, objavljena v zadnjih sedmih letih, so bila citirana v bazi ISI (podatki iz novembra 1999) 69 krat, od tega posamezna dela tudi do 15 krat.

V imenu članov MIDEM in v svojem imenu iskrene čestitke.

Predsednica Društva MIDEM
Marija Kosec

VESTI - NEWS

News from European Semiconductor, October - November 2000

Glasgow opto spin-off

COMPOUND SEMICONDUCTOR Technologies (CST) has been opened as a £7.5m optoelectronics foundry for devices built on III-V materials. Based in the West of Scotland Science Park, Glasgow, the company has been formed to pioneer and commercialise new opto technology.

Local government and educational agencies are hoping to position Scotland at the forefront of the optoelectronics revolution through the start-up. The venture has been set up by Scottish Enterprise, Glasgow University, Strathclyde University, Scottish Enterprise Glasgow and the Strathclyde European Partnership, to act as a "hub" linking academia with the optoelectronics industry. Researchers from both Glasgow and Strathclyde University will work together within the facility.

Unveiling a plaque at the official opening of the facility, Sir lain Vallance, British Telecom's chairman, said: "In the coming decade optoelectronics will supersede electronics as the engine which will drive e-commerce, the internet and the global telecommunications industry. The new and imposing research and foundry facility which we have seen here today will go a long way towards making this possible."

CST's chief executive, Neil Martin, reports: "With major 'incubation' contracts for two photonics start-up companies - and others in negotiation - we should be well ahead of target by the end of the year. As part of our commitment to playing a leading role in this global market, plans are now nearing completion to establish a presence on the East and West Coasts of the US."

Quick switch

ISRAELI COMPANY -Trellis Photonics has achieved submicrosecond photonic switching speeds, claimed as the fastest optical speed to date. Other techniques typically deliver switching in the millisecond range. The Trellis device uses "electroholography" - wavelength specific holograms written into potassium lithium tantalate niobate (KLTN) crystals, turned on by applied electric fields.

"The inherent speed of electroholography makes our Intelligent Lambda Switch the fastest photonic switch in the world," says Tim Cahall, Trellis Photonics' CEO.

"The solid state nature of electroholography maximises switching speed," says Prof. Agranat, Trellis' director and founder. "While a sub-microsecond switching time is impressive, when compared to other technologies, we expect to achieve faster switching times soon."

The Intelligent Lambda Switch is due to be available in Q2 next year.

Circular LCDs

SONY PLANS to build a 300 mm semiconductor plant in Kumamoto, Japan, to expand manufacturing capacity of small-size high-temperature poly-silicon LCDs and CCD image sensors. These devices are currently produced at a facility in Kokubu, Japan. Construction for the new plant will begin in November with production due to start in October next year.

The small-size high-temperature poly-silicon LCDs produced by Sony use a special process called HT p-Si TFT (thin-film transistor). Unlike "normal" LCDs (a-Si TFT) produced on square glass plates, these are produced on circular quartz wafers. Sony has realised UXGA resolution on its 1.8" LCDs.

The new plant (cleanroom 20,000 m^2) will be the first Sony 300 mm plant and will also house new manufacturing technologies such as localised cleanroom technology, a mini-production line and "zero-emission" recycling of cleansing fluids.

Initial capital expenditure is estimated at ¥ 10 bn in the current financial year. Cumulative investment is forecast at ¥100 bn by the end of 2005.

The plant will employ approximately 300 people at start-up, 140 of whom will be new recruits. Mass production of LCDs is planned to begin in 2002 at 3000 wafers per month, and CCDs in 2003 at 2000 wafers per month. Within the 2005 time frame, production will be increased to 12,000 wafers per month, which will double the current monthly production of LCDs and CCDs.

Atmel expands in Europe

The fate of the mothballed Siemens fab on North Tyneside is finally secured, as Atmel agrees to move in and start ramping microcontrollers and flash memory by next April. With the help of a regional support grant of £ 27.8 m, Stephen Byers, the trade and industry secretary said he was confident Atmel's arrival would give fresh impetus to the area.

The deal will create 1300 jobs in the area and bring Atmel's total manufacturing capacity to 60% in Europe. Atmel now has five manufacturing facilities, and 14 design centres in Europe.

The facility is equipped, except for the lithography tools. George Perlegos, Atmel's CEO said early production would be on relaxed geometry 0.35 μm and 0.25 μm CMOS devices. "We are buying all our lithography tools from ASML (not scanners) and we expect to migrate down to 0.18 μm by 2002."

Donald Colvin, Atmel's CFO defended the company's knock down price of less than £100 m for the plant. "This is no slash and burn operation, we're here for the duration. We are going to invest $ 800 m in this fab to bring it up to full capacity," he said.

Organic LED

AN ACTIVE matrix-driven organic LED is claimed as the first to obtain high resolution by its developers, Japan's Semiconductor Energy Laboratory (SEL) and Germany's Covion Organic Semiconductors.

An experimental VGA organic electroluminescent (EL) display panel has its primary organic EL emission in white. The peripheral circuits are driven by integrated polysilicon thin film transistors (TFTs), and the contrast ratio of the panel is >100.

SEL's role in the co-operation has been development of the OLED device and the polysilicon TFT driver. Covion contributed the white OLED with thermally stable spiro materials used in the device.

Smooth grey scales were obtained by controlling the OLED light emitting time using voltage applied time control. The driving method derives from SEL's established core active matrix driver manufacturing technology.

Covion claims to be the first company to offer small molecule and polymer OLED materials on a commercial scale for the flat panel display and optoelectronics markets.

Bluetooth to penetrate up to 17 segments

DESPITE MARKET delays, Bluetooth-enabled device shipments could reach 1.4bn nodes in 2005, according to Allied Business Intelligence (ABI). The figure for 2001 is just 56 m. Semiconductor revenues resulting from Bluetooth could be $ 5.3 bn in 2005.

"Bluetooth's scope of adoption is not limited to the cellular phone industry and we will begin to see Bluetooth transceivers embedded in everything from PC equipment to industrial devices," says ABI director of Residential & Networking Technologies, Navin Sabharwal, author of the ABI report "Bluetooth: More Than A Cable Replacement".

Sabharwal is forecasting penetration of Bluetooth into 17 different market segments, including mobile handsets, notebooks, desktops and PDAs.

By 2005 cellular mobile handsets will account for less than 47% of all Bluetooth nodes shipped in that year, compared with 65% in 2002. A shift to PC-centric, consumer electronics applications will be aided by silicon producers targeting Bluetooth, creating an intensely competitive market. This will drive steep declines in Bluetooth silicon prices and allow for a sub-$5 Bluetooth module beyond 2003.

"We are unlikely to see a significant volume of Bluetooth-enabled devices until mid-2001, and the market will only begin to accelerate in 2002," says Sabharwal. "Lack of inexpensive silicon, interoperability problems and limited applications could serve to dampen the market in the early phase, but as these issues are addressed, Bluetooth adoption by equipment vendors and actual use by consumers should be robust."

A few weeks before ABI's report, Micrologic Research made somewhat different predictions. Bluetooth semiconductor revenues for 2005 were put at $4.3bn. And sub-$5 modules are not expected by Micrologic for the forseeable future (a $16 figure was suggested as more likely). Micrologic sees cellphone service providers subsidising Bluetooth to encourage subscribers to use data services increasing purchased airtime. This market research expected Bluetooth to appear in a handful of products by the end of this year, but said that it will be mid-to-late 2001 before more than a token number of products are available, and late 2002 before the market begins to gain significant momentum.

Joint assembly and test

OKI ELECTRIC Industry and ST Assembly Test Services have jointly developed an RF chip package and production test solution for Oki's CMOS Bluetooth devices.

Oki has a Bluetooth RF transceiver IC, designed jointly by Oki Electric Industry and Oki Techno Centre, Singapore (OTCS). This device was tested using the RF MicroWave-6000 option on a Teradyne platform.

"It is usual for RF chips to be designed using BiCMOS or SiGe processes due to the high speed performance requirements," says Dr Hiroshi Nakamura, general manager of RFIC Development & Design at OTCS. "Our challenge was to create a chip which is cost competitive, without compromising the speed specification. With our first silicon Bluetooth prototype, we have managed to incorporate vital intermediate frequency (IF) and RF circuits on a low cost, integration-friendly, bulk CMOS process."

Packaging and test company STATS was brought on board the project by Oki to develop both the packaging design and test program. STATS is an adopter member of the Bluetooth Special Interest Group (SIG).

Two become one

ASM LITHOGRAPHY and Silicon Valley Group (SVG) are to combine their efforts in a merger to become the world's No.1 provider of lithography tools. ASML is to acquire all of SVG's divisions, which includes track systems and thermal processing. The combined company will operate under the name ASML. The track equipment of SVG allows a complete photolithography cell to be supplied by ASML, in keeping with the industry trend to provide complete process solutions.

But what of SVG's thermal processing business? Doug Dunn, ASML's CEO, said: "Thermal was an unexpected bonus in the deal, and we have no intention of deconsolidating that part of the business." Dunn added that the career prospects for employees of both companies would be "far richer" following the merger.

ASML employs around 3700 staff, and SVG around 3600. According to Dunn these figures will be maintained. The final convergence of the two companies will take place once a backlog of 193 nm exposure tool orders has been addressed. Then ASML will be able to draw upon SVG's 157 nm catadioptric intellectual property.

New fab for Germany

MICROSYSTEMS PRODUCER Standard MEMS and Philips Semiconductors have formed a joint venture to build a 200 mm MOS wafer manufacturing facility for micro-electro-mechanical systems (MEMS) and integrated discrete semiconductors in Itzehoe, Germany. Other minority interests in the joint venture will be held by the Fraunhofer Institute for Silicon Technology (ISiT) and MGB Schleswig-Holstein (a regional venture capital company).

The fab will be dedicated to the production of MEMS and CMOS products using 0.35 μm and 0.25 μm CMOS processes.

The fab will have a capacity of 300,000 200 mm wafers per year. Silicon output will be shared between Standard MEMS and Philips Semiconductors, while Fraunhofer ISiT and MGB of Schleswig-Holstein will be strategic, financial partners in the venture.

Building of the new fab will commence in December this year, with the first silicon being produced in the second half of 2002. The new fab will create up to 200 new jobs. The site in Itzehoe, north of Hamburg, Germany, has been chosen due to the proximity to Fraunhofer ISiT's existing 150 mm wafer fab site. This ensures local availability of a technical infrastructure.

Nicholas Ortyl, Standard MEMS' president and CEO, said: "Philips Semiconductors has a very close alignment to our own business objectives in CMOS technology. We look forward to becoming an important design and production resource to Philips Semiconductors."

Pushing down the k to 2.4 in production

TRIKON TECHNOLOGIES has successfully etched 100 nm diameter, 7:1 aspect ratio features through its own Low-k Flowfill dielectric material (k~2.7). The processing was performed on Trikon's Omega 201 MORI high density plasma etch system. The achievement was part of a collaborative effort with International SEMATECH, using a CARL bilayer resist scheme originally developed by Infineon Technologies and European chemicals company Clariant. An in-situ resist/polymer strip has also been developed which has no adverse affect on k values down to ~2.4.

This follows up on previous etch achievements on the Omega 207 MORI in producing 30 nm diameter contact holes and 25 nm trenches, with aspect ratios up to 30:1, through conventional oxide.

The Omega 201 MORI system has three processing modes: a high-density 'helicon' mode, a medium-density, 'magnetically enhanced reactive ion etch' (RIE) mode and a 'downstream' mode.

The company has also pushed its Low k Flowfill CVD dielectric for gap-fill aluminum to a k value of 2.4. The material is aimed at production of 0.1 μm device designs.

"As with all of our Low k Flowfill materials, the carbon content of the film is much lower than other, similar products, making process integration more straight forward," says CVD product marketing manager Andy Noakes. "Our k=3.3 low k Flowfill solution is already being used in full-scale production while our k=2.8 version is in qualification, delivering 36% performance gains compared with undoped HDP."

Trikon says its Flowfill process has also shown itself to be highly reliable and that it is running in production at greater than 85% uptime; 90% in many cases.

Organic LEDs

IN RECENT months, there has been much activity in developing the technology needed to produce displays based on light emitting organic materials.

Wide-scale commercial use of such materials seems closer with the release of Motorola's new Timeport P8767 digital phone. This is to use organic electroluminescence (OEL) technology from Japanese company Tohoku Pioneer in its display.

Tohoku Pioneer claims to be the only company mass-producing OEL displays. The new phone is the first mobile to use Tohuku's multi-color graphic display product. The first commercial use of its technology was in 1999 in car stereo headphones produced by Japanese electronics company Pioneer.

The new phone is the first product of an alliance between Motorola and Tohuku, announced in January. The Timeport P8767 is shipping now with availability in the US.

Tohuku's OEL material uses a carbon-based compound organised into thin layers which posses the ability to emit light when electric current is passed through them. The OEL technology has been in development for several years at Tohuku and a multi-color version was produced in 1999.

German CVD tool company AIXTRON and Universal Display Corporation (UDC) of Princeton NJ have entered into an exclusive agreement to develop and fabricate OLED (organic light emitting device) production equipment. The tools will use OVPD (organic vapor phase deposition). UDC holds the rights for a number of patents for OLEDs including the OVPD process. Under the agreement, AIXTRON receives a worldwide, exclusive license for the OVPD related patents. Development will be carried out jointly. AIXTRON will also have exclusive sales rights on the final tool. Plans to install a demonstration pre-production system next year at the UDC facility are underway.

Meanwhile, US company MicroDisplay says it has succeeded in surmounting the primary technical difficulties in adapting wafer scale assembly manufacturing processes to the production of microdisplays. The company has started shipping volume quantities of SVGA resolution liquid crystal on silicon (LCOS) displays to its primary customer Daeyang E&C of Seoul, Korea. This is claimed as the first known instance of LCOS displays being shipped in volume from a wafer scale assembly plant.

Shipment began in August and will be followed by monthly deliveries increasing in volume through to the end of this year. With additional anticipated investment and third party alliances, production volume will be increased to tens of thousands of displays by Q1 of 2001. The terms of the agreement currently include a purchase agreement for more than 150,000 units of MicroDisplay's MD800G6 SVGA MicroMonitor.

IMAPS NEWS - VESTI

Taking place January 16-18, 2001, in San Diego, CA, APEX will be the ONLY show where you will be able to compare electronics assembly equipment from all the major manufacturers. They'll be joined by nearly 400 other exhibitors representing every facet of the electronics assembly supply chain - from bare boards through test.

If you attend trade shows to see new electronics assembly equipment, if you expect to talk to product experts and see demonstrations, if you wish to compare the offerings of the major manufacturers, you will only be able to do it at APEX. The complete conference brochure, including exhibitor information, is now available at http://www.apex2001.org.

For more information on:

VISITING over 170,000 sq. ft. of exhibit booths, featuring the newest technologies the industry has to offer - Click here for the exhibitors list: http://exhibitors.ipc.org

FREE KEYNOTE SESSIONS every day, featuring undersea explorer Dr. Bob Ballard, the 2000 NEMI Roadmap, and and a special interactive panel on E-commerce and "B to B" issues. Go to http://www.apex2001.org/html/apex2001events.htm #keys

NETWORKING AND RELAXING at the industry's best and biggest party, featuring the fun disco sounds of KC and the Sunshine Band, along with floors of casino gambling and virtual reality games. Attendance is FREE to our exhibitors' customers, a $70 value. Click here to learn more:
http://www.apex2001.org/html/apex2001events.htm #gala

LEARNING from internationally recognized experts at one or more of 60 world-class full or half day professional development courses on topics relating to optimizing assembly processes, integrating today's advanced IC packaging technologies or making better business decisions about your supply chain, For course descriptions, click here
http://www.apex2001.org/html/apex2001profdev.htm

CATCHING UP on the newest technologies at the industry's best conference focused on electronics assembly. This year's program features a special symposium on lead-free assembly processes and reliability, plus 30 more sessions. For complete descriptions and schedule, go to:
http://www.apex2001.org/html/apexconferences.htm

Register now - it's easy! Click here
http://www.apex2001.org/html/registerapex.htm
for complete details (or call 847-790-5360 or toll-free US/Canada 877-472-4724). See you in January!

Visit IMAPS web site at http://www.imaps.org for the latest information on these and other upcoming IMAPS events

Submit an Abstract for this event NOW! Plan on attending March 26-27, 2001 Announcement

Advanced Technology Workshop on Ceramic Technologies for Microwave:
Handsets
Bluetooth
Broadband
LMDS

Adam's Mark Hotel
Denver, CO, USA
March 26-27, 2001

sponsored by IMAPS and Ceramic Interconnect Initiative (CII)

Papers are invited for proposed Sessions on:

Portable Wireless Applications and Bluetooth
Base Stations
Broadband and MM Wave
Integrated Passives
Design, Modeling and Simulation
Test and Measurement
Power

Submit an Abstract:

200 word abstract electronically by November 10, 2000 using the online submittal form at www.imaps.org/abstracts.htm; Questions: abstracts@imaps.org or 703-758-5164 ask for Jackki

General Chairs:
W. Kinzy Jones, Ph.D.
jones@eng.fiu.edu

Technical Chairs:
Peter Barnwell, Ph.D.
peter@4hcd.com

Samuel J. Horowitz, Ph.D.
samuel.j.horowitz@usa.dupont.com

For a media kit on this event contact, Mike Martell, Martell Communications
mmc@loa.com

Visit IMAPS web site at http://www.imaps.org for the latest information on these and other upcoming IMAPS events

International Symposium on Advanced Packaging Materials:

Processing, Properties, and Interfaces

Chateau Elan, Braselton, GA - March 11-14, 2001

Sponsored by:

IMAPS, IEEE/CPMT, and Packaging Research Center, Georgia Tech

Participating Societies:
American Society of Metals, The American Ceramic Society,

Society of Plastics Engineers, and Materials Reseach Society

Papers are sought in the following areas:

Adhesives
Bumping Materials & Processing
Consumer Electronic Material Issues
(Celluar Phones)
Integral Passive Materials
Interfacial Adhesion
Manufacturing Process Control
Mechanics of Materials
Microwave Materials
On-Chip Interconnect Materials
Optoelectronics
Substrates, HEI, and Dielectrics
Thermal Management Materials
Underfills & Encapsulant Materials

Send your 200 word abstract electronically by September 1, 2000 using the online submittal form at www.imaps.org/abstracts.htm
Questions/Suggestions - abstracts@imaps.org
or Jackki - 703-758-5164

General Chair, James E. Morris, Ph.D., jmorris@binghamton.edu

General Chair Elect, Philip Garrou, Ph.D., pegarrou@dow.com

Technical Chair, Andreas Schubert, Ph.D., schubert@izm.fhg.de

Technical Chair, Jianmin Qu, Ph.D., jianmin.qu@me.gatech.edu

An exhibition will also be held - contact Ann Bell - abell@imaps.org or 703-758-5166 for pricing and availability.

Visit IMAPS web site at http://www.imaps.org for the latest information on these and other upcoming IMAPS events

Announcing - Call for Papers

2001 International Conference on Electronics Packaging (ICEP) and 15th Microelectronics Show this was the IEMT/IMC Symposium

April 18-20, 2001

Tokyo Ryutsu Center, Tokyo, Japan

General Chair - Noboru Ichinose, Waseda University

Vice General Chair - Shinichi Nishi, Konica

Contact for Registration, Technical Program, and Exhibition Secretariat 2001 ICEP JIEP, 3-12-2 Nishiogikita Suginamu-ku, Tokyo 167-0042, JAPAN
Telephone - 81-3-5310-2010
Fax - 81-3-5310-2011
E - imaps-j@jiep.or.jp
Web: http://www.jiep.or.jp/index.html

sponsored by - IMAPS Japan, JIEP, IEEE/CPMT Japan Chapter

Visit IMAPS web site at http://www.imaps.org for the latest information on these and other upcoming IMAPS events

Announcement and Call for Papers
The Fourth International Symposium on High Density Packaging and Component Failure Analysis in Electronics Manufacturing (HDP'OO)
December 14 - 16, 2000

Co-sponsored and jointly organized by

DaimlerChrysler SIM Technology Co., Ltd, Shanghai, China.
&
Chalmers University of Technology, Division of Electronics Production, Department of Production Engineering, Goteborg, Sweden

Electronics manufacturing and assembly technology are playing a key technology for the progress of Chinese electronics industry. Today many multi-national companies are establishing new facilities in China for expanding their global business and interest. However, many domestic Chinese electronics companies are still using old-fashioned electronics assembly technologies. The recently established joint-venture companies use more advanced electronics assembly technologies such as surface mount, chip-on-board etc. There is a great gap in technology level between these two types of companies. Therefore, there is a need to find a forum for the domestic Chinese Electronics industry to find out the latest technologies in the developed world. The foreign advanced countries also need to have a forum to establish contacts with the Chinese scientists, engineers and decision makers.

The purpose of this Symposium is to satisfy such a need and to establish a regular forum for information exchange between Chinese industrial community and foreign specialists.

The Symposium will be organised in the following way: The first one day will be held in Chinese. The speakers will be mainly Chinese Speaking foreign experts and Chinese domestic experts from DaimlerChrysler SIM Technology and others from famous Chinese companies, universities and research institutions. The second day will be held in English with speakers and invited speakers from other countries and also from the English speaking experts. Special sessions on novel emerging technologies and failure analysis will be arranged to suit the needs in discussing high-tech research and in technology transfer to Chinese electronics industry. You are welcome to submit a paper to the Symposium and join all the three days. But as the Symposium will be held in Chinese in the first day, thus, it is recommended that foreign participants start to join the Symposium with the dinner on December 14 of the Symposium day together with the Chinese delegates and join the rest symposium of English speaking parts. The last day will be aimed for visits to local manufacturing companies in Shanghai. Please note that this Symposium will be taken place just a few days after the Electronics Packaging Technology Conference (EPTC) this year in Singapore (December 5-7, 2000). So you may plan the trip together.

Scope for the Symposium:

The Symposium will cover the following areas and subjects:

- High density packaging including electronics and opto-electronics packaging, CSP, BGA, Flip-chip, Chip on Board, Surface Mount Technology and other novel emerging technology High density substrate including integrated passives and active devices
- MEMS design, packaging and assembly
- Electronics manufacturing issues including cleaning issues, quality control, logistics, repair, process optimization, statistic process controls, ISO compliance, tooling or equipment, early manufacturing involvement initiatives and yield and test innovations used to enhance manufacturing processes or products related to high density substrates, single chip and multichip packaging, chip bumping and integrated component technologies
- Component failure analysis techniques including non-destructive X-ray, ultrasonic microscopy, IR-microscopy etc
- Simulation and modelling for packaging and electronics manufacturing processes Thermal management
- Environmental design and materials development including life cycle analysis and end of life strategy etc
- Cost reengineering, improvements and analysis for electronics packaging processes and products

Documentation: The documentation from the Symposium will be published in a proceedings with CD ROM with a full length papers (max 12 A4 pages) in English.

Journal publication: In addition, high quality papers will be selection for consideration to be published as special editions of the IEEE CPMT Transactions, "Soldering and Surface Mount Technology" or Journal of Electronics Manufacturing

Location: 865 Changning Road, DaimlerChrysler SIM Technology Co., Ltd. Shanghai, China Languages: First day the spoken language is Chinese, the second one and a half day English will be used. Simultaneous translation into Chinese is made to suit the Chinese delegates. Symposium Chair: Le Luo, DaimlerChrysler SIM Technology Co., Ltd.

Symposium Co-chair: Johan Liu, Chalmers University of Technology, Sweden.

International Advisory Committee

C P Wong, Georgia Institute of Technology, USA, **Co-Chair**

Wilhelm Senske, DaimlerChrysler, Germany, **Co-Chair**

Rolf Aschenbrenner, IZM, Germany

Heiner Bayer, Siemens, Germany

Arun Chaudhuri, Delco Delphi Electronics Systems, USA

Jannick Guinet, Schneider Electric, France

Joakim Anjeby, Saab Ericsson Space, Sweden

Jannes Jagt, Philips, The Netherlands

Jorma Kivilahti, Helsinki University of Technology, Finland

Kare Gustavsson, Ericsson Microelectronics, Sweden

Pontus Lundstrom, Ericsson Microelectronics, Sweden

Wei Koh, Motorola, Asien Manufacturing Research Center, Beijing, China

John Lau, Express Packaging Systems, USA

Y C Lee, University of Colorado, USA Jianhua Wu, Gintic, Singapore

Sheng Liu, Wayne State University, USA

Wei Lu, Shanghai Institute of Technical Physics, China

Jusheng Ma, Tsing Hua University, Beijing, China

Erdogan Madenci, University of Arizona, USA

Bernd Michel, IZM, Germany

James Morris, State University of New York, Binghamton, USA

Koji Nihei, Meisei University, Japan

K W Paik, Korean Advance Institute of Science and Technology, Korea

Yi-Hsin Pao, Ford, USA

Robert Pfall, Motorola, USA

W J Plumbrige, Open University, UK

Patrice Rollet, Promosol, France Petri Savolainen, Nokia, Japan

Frank Stubhan, DaimlerChrysler SIM Technology, China

Ganesh Subarayan, University of Colorado, USA

K. Suganuma, Osaka University, Japan

Ephraim Suhir, Lucent Technologies, USA Kenichi Suzuki, Japan

Osamu Takeda, T & T Ltd, Japan

Andrew Tay, National University of Singapore, Singapore

Rao Tummala, Georgia Institute of Technology, USA

Itsuo Watanabe, Hitachi Chemicals, Japan

David Whalley, Loughborough University, UK

Kin Wong, Semiconductor Equipment and Materials International, USA

Jianming Qu, Georgia Institute of Technology, USA

Anders Tholen, Chalmers University of Technology, Sweden

Liqiang Xu, , DaimlerChrysler SIM Technology, China

Shouwen Yu, Tsing Hua University, Beijing, China

Magnus Willander, Chalmers University of Technology, Sweden

Xiangfu Zong, Fudan University, China

Program committee

Xiaoming Xie, **Chair**, DaimlerChrysler SIM Technology Co., Ltd.

Margareta Ponten, **Co-Chair**, Chalmers University of Technology, Sweden

Tiebing Wang, Program secretary, Chalmers University of Technology, Sweden

Guo Liang Chen, University of Science & Technology, Beijing, China

Liu Chen, Chalmers University of Technology

Yi Lan Kang, Tianjing University, Tianjing, China

Charles Lee, Infineon, Singapore

Jon Nysether, SINTEF, Norway

Xitao Wang, Chalmers University of Technology, Sweden

Piotr Starski, Chalmers University of Technology, Sweden

Arne Tolvgard, Ericsson Radio Systems, Sweden

Yan Li Wang, University of Science & Technology, Beijing, China

You are welcome to submit an abstract with max 300 words that cover the topic, experimental approach, results and conclusions for the paper by October 31, 2000 to Chalmers University of Technology, Division of Electronics Production, Department of Production Engineering, Attn. Dr Tiebing Wang, Se- 431 53 Molndal, Sweden or you can email at tiebing@pe.chalmers.se. Notification of abstracts will be made by November 7, 2000. Final Acceptance of the abstract will be made by November 15, 2000. Final paper is due November 30, 2000. Please send the final paper to Chalmers University of Technology for countries outside of China.

We are also interested to have exhibitors from materials, equipment suppliers to exhibit their products. If you are interested in exhibition, please contact Dr Tiebing Wang, Chalmers University of Technology, Sweden.

Please send abstracts to (for countries outside of China)

Chalmers University of Technology

Division of Electronics Production

Department of Production Engineering

Dr Tiebing Wang

Se-431 53 Molndal Sweden

Telephone: +46-31-706 6291

Fax: +46-31-706 6289

e-mail: tiebing@pe.chalmers.se

KOLEDAR PRIREDITEV - CALENDAR OF EVENTS

NOVEMBER

NOVEMBER 6-10, 2000

MINATEC 2000, GRENOBLE, FRANCE

International meeting on micro and nanotechnologies.

Contact: Regional Agenry for Digital industry

Tel: +33 4 38 12 31 70

email: genevieve.fioraso@numera.org

web: www.minatec.com

NOVEMBER 21-23, 2000

EUROPEAN SURFACE MOUNT CONFERENCE, BRIGHTON, UK

A networking and educational event for the European electronics manufacturing industry;including technical and discussion workshops

Contact: Tony Gordon, Smart Group

Fax: +44 1494 473 975

email: smart@smtuk.demon.co.uk

NOVEMBER 21-24,2000

ELECTRONICA 2000, MUNICH, GERMANY

Electronics fair, expecting to feature over 3,5000 companies amongst its exhibitors. This year's Electronica will feature two new sectors: embedded systems and power supplies.

Contact: Nicole Mundhenk, Messe Munchen

Tel:+498994920671

Fax: +49 89 9 49 2 06 79

email: info@electronica.de

web: www.electronica.de

DECEMBER

DECEMBER 11-13, 2000

IEEE INTERNATIONAL ELECTRON DEVICES MFFTING, SAN FRANCISCO, USA

The conference and forum for reporting the latest breakthroughs in the technology, design and manufacturing of advanced semiconductors and other electron devices.

There will also be a variety of IEDM short courses and evening panel debates. Contact: Erin Peters (Masto PR)

Tel: +1 518 786 6488

Fax: +1 518 786 6497

email: mastopr@cs.com

web: www.ieee.org/conference/iedm

VSEBINA LETNIKA 2000 VOLUME 2000 CONTENT

UDK621.3:(53+54+621+66), ISSN0352-9045 Informacije MIDEM 30(2000)1,Ljubljana

Uvodnik: Revija "Informacije MIDEM" je dobila JCR factor		Editorial: Journal "Informacije MIDEM" gets JCR Impact Factor
ZNANSTVENO STROKOVNI PRISPEVKI		**PROFESSIONAL SCIENTIFIC PAPERS**
K.W. Smith: Polprevodniški detektorji s slikovnimi elementi	**1**	K.W. Smith: Semiconductor Pixel Detectors
G. Pasciak, W. Mielcarek, K. Prociow: Vpliv dodatka Sb_2O_3 na električne parametre in stabilnost ZnO varistorjev	**16**	G. Pasciak, W. Mielcarek, K. Prociow: Influence of Sb_2O_3 Addition on Electric Parameters and Stability of ZnO Varistors
D. Resnik, D. Vrtačnik, U. Aljančič, S. Amon: Direktno bondiranje silicijevih ploščic orientacije (100) in (111)	**20**	D. Resnik, D. Vrtačnik, U. Aljančič, S. Amon: Direct Bonding of (111) and (100) Oriented Silicon Wafers
J. Krč, M. Topič, F. Smole, U.O. Krašovec, U.L. Štangar, B. Orel: Analogni regulator za elektrokromna stekla	**32**	J. Krč, M. Topič, F. Smole, U.O. Krašovec, U.L. Štangar, B. Orel: Analog Regulator for Electrochromic Windows
M. Šalamon, T. Dogša: Nevarnost kaosa v digitalnem situ drugega reda	**37**	M. Šalamon, T. Dogša: Danger of Chaos in a Second-order Digital Filter
PRVO OBVESTILO - KONFERENCA MIDEM 2000	**43**	**ANNOUNCEMENT AND CALL FOR PAPERS - MIDEM 2000 CONFERENCE**
PREDSTAVLJAMO PODJETJE Z NASLOVNICE R L S	**49**	**REPRESENT OF THE COMPANY FROM FRONT PAGE R L S**
PRIKAZI MAGISTRSKIH DEL IN DOKTORATOV, leto 1999	**50**	**M.S. and Ph.D. ABSTRACTS, year 1999**
V SPOMIN Prof. dr. Drago Kolar	**62**	**IN MEMORIAM Prof. Dr. Drago Kolar**
KOLEDAR PRIREDITEV	**64**	**CALENDAR OF EVENTS**
MIDEM prijavnica	**65**	MIDEM Registration Form

UDK621.3:(53+54+621+66), ISSN0352-9045 | Informacije MIDEM 30(2000)2, Ljubljana

ZNANSTVENO STROKOVNI PRISPEVKI		PROFESSIONAL SCIENTIFIC PAPERS
G.W. Herzog, A. Reichmann, K. Reichmann, M. Ruplitsch-Lesnik, K Gatterer: Električne, magnetne in katalitske karakteristike materialov spinelnega in perovskitnega tipa, ki vsebujejo kobalt	71	G.W. Herzog, A. Reichmann, K. Reichmann, M. Ruplitsch-Lesnik, K Gatterer: Electronic, Magnetic and Catalytic Properties of Cobalt Containing Spinel and Perovskite Type Materials
L. Koller, M. Bizjak, B. Praček: Čiščenje tankih pasivacijskih prevlek na Ag kontaktnem materialu z vakuumskim razplinjevanjem	78	L. Koller, M. Bizjak, B. Praček: Cleaning of Thin Passivation Layers on the Ag Contact Material with Vacuum Outgassing
M. Knaipp, F. Unterleitner: Izbira termičnih robnih pogojev pri modeliranju inteligentnih močnostnih vezij	82	M. Knaipp, F. Unterleitner: Thermal Boundary Conditions in Smart Power Devices
D. Korošak, B. Cvikl:Modelski izračun odvisnosti induciranega naboja na vmesni plasti od zunanje napetosti na polprevodniških strukturah narejenih z metodo curka ioniziranih skupkov atomov	89	D. Korošak, B. Cvikl: Model Calculation of Ionized Cluster Beam Induced Bias Dependent Interface Charge
M. Milanovič, A. Roškarič, M. Auda: Polnilnik baterij zasnovan na dvojnem pretvorniku navzdol in pretvorniku navzgor	98	M. Milanovič, A. Roškarič, M. Auda: Battery Charger Based on Double-buck and Boost Converter
M. Komac: Tehnološko predvidevanje: instrument nabora družbeno in gospodarsko releventnih vsebin raziskovanja	105	M. Komac: Technology Foresight: a Convenient Tool for the Prioritization of Scientific Research
R. Osredkar, B. Gspan: Študija planarizacijskih lastnosti tankih BPSG plasti	110	R. Osredkar, B. Gspan: A Study of Planarizing Properties of Thin BPSG Films
KONFERENCE, POSVETOVANJA, SEMINARJI, POROČILA		**CONFERENCES, COLLOQUYUMS, SEMINARS, REPORTS**
L. Trontelj: Tridesetletnica Laboratorija za mikroelektroniko na Fakulteti za elektrotehniko v Ljubljani	113	L. Trontelj: Thirty Years of Laboratory of Microelectronics on Faculty of Electrical Engineering in Ljubljana
M. Hrovat: Šesti Groveov simpozij o gorivnih celicah	114	M. Hrovat: Sixth Grove Fuel Cell Symposium
M.Hrovat: Konferenca Micro Technologies 2000	118	M.Hrovat: Conference Micro Technologies 2000
I. Pompe: Kdor pride pozno, dobi kosti	121	I. Pompe: Who comes too late gets the bones
Pozdravni govor ob odprtju analitskega elektronskega mikroskopa JEM-2010 F, dne 22. junija 2000 na Institutu Jožef Stefan v Ljubljani	122	Speech at the Occasion of Inauguration of the Electronic Microscope JEM-2010 F on 22. June 2000 at the Jožef Stefan Institute
VESTI	123	**NEWS**
KOLEDAR PRIREDITEV	128	**CALENDAR OF EVENTS**
MIDEM prijavnica	129	MIDEM Registration Form
Slika na naslovnici: Učinkovite rešitve za izzive dereguliranega trga električne energije		Front page: Effective solutions for challenges for deregulated market of electric energy

UDK621.3:(53+54+621+66), ISSN0352-9045 Informacije MIDEM 30(2000)3,Ljubljana

ZNANSTVENO STROKOVNI PRISPEVKI		PROFESSIONAL SCIENTIFIC PAPERS
D. Belavič: Trendi na področju hibridne debeloplastne tehnologije	133	D. Belavič: Technology Trends Within the Thick-film Hybrid Microelectronics
M. Lamot, B. Žalik: Programsko orodje za podporo sprotnemu nadzoru temperature v mikroelektronskih sistemih	144	M. Lamot, B. Žalik: Software Tool for the Support of On-line Thermal Monitoring of Microelectronics Systems
A. Hanžič, J. Voršič: Izdelava modela sončne celice s programom za analizo vezij - SPICE	148	A. Hanžič, J. Voršič: Development of a Solar Cell Model with a Programme for Circuit Analysis - SPICE
A. Časar, Z. Brezočnik, T. Kapus: Formalna verifikacija digitalnih vezij s simboličnim preverjanjem modelov	153	A. Časar, Z. Brezočnik, T. Kapus: Formal Verification of Digital Circuits Using Symbolic Model Checking
Ž. Čučej, T. Romih, J. Mohorko: Adaptiven tokovni merilnik za števce električne moči	161	Ž. Čučej, T. Romih, J. Mohorko: Adaptive Current Measuring Circuit for Electric Power Meters
M. Bunc, J. Rozman: Način merjenja pretoka tekočin s posebno turbino	165	M. Bunc, J. Rozman: Another Way of a Liquid Flow Measurements by Using a Specially Designed Turbine
PREDSTAVLJAMO INSTITUCIJO Z NASLOVNICE		**REPRESENT OF THE INSTITUTION FROM FRONT PAGE**
Novi analitski elektronski mikroskop JEM-2010F na Odseku za keramiko IJS	168	New Analytical Electron Microscope JEM-2010F at Ceramics Department, Jožef Stefan Institute
KONFERENCE, POSVETOVANJA, SEMINARJI, POROČILA		**CONFERENCES, COLLOQUYUMS, SEMINARS, REPORTS**
M. Hrovat: 23.Mednarodni spomladanski seminar o elektonski tehnologiji ISSE'2000	172	M. Hrovat: 23rd International Spring Seminar on Electronic Technology SSE'2000
Naši strokovnjaki dobivajo priznanja za svoje prispevke na konferencah v tujini	175	Our Experts Are Receiving Awards for Their Contributions Presented in the Conferences Abroad
VESTI	176	NEWS
KOLEDAR PRIREDITEV	182	CALENDAR OF EVENTS
MIDEM prijavnica	185	MIDEM Registration Form
Slika na naslovnici: Novi analitski elektronski mikroskop JEM-2010F na Odseku za keramiko IJS		Front page: New analytical electron microscope JEM-2010F at Ceramics department, Jožef Stefan Institute

UDK621.3:(53+54+621+66), ISSN0352-9045

Informacije MIDEM 30(2000)4,Ljubljana

ZNANSTVENO STROKOVNI PRISPEVKI		PROFESSIONAL SCIENTIFIC PAPERS
G.U. Pignatel, M. Boscardin, G.-F. Dalla Betta: Najnovejša dognanja pri razvoju silicijevih detektorjev sevanja v IRST	191	G.U. Pignatel, M. Boscardin, G.-F. Dalla Betta: Recent Developments in Silicon Radiation Detectors at IRST
P. Mach: Diagnosticiranje nelinearnosti tokovno-napetostne karakteristike - teorija in uporaba	199	P. Mach: Diagnostics of Nonlinearity of Current vs. Voltage Characteristics - Theory and Application
A.Zalar: Karakterizacija materialov z Augerjevo elektronsko spektroskopsko (AES) profilno analizo	203	A.Zalar: Materials Characterisation by Auger Electron Spectroscopy Sputter Depth Profiling
J.J. Hren, V.V. Zhirnov, Z. Sitar, G. Wojak: Vrednotenje dielektričnih materialov na merilnih konicah	210	J.J. Hren, V.V. Zhirnov, Z. Sitar, G. Wojak: Characterisation of Dielectrics on the "tips of needles"
H. Bender: Uporaba fokusiranega curka ionov pri analizi adpovedi	216	H. Bender: Application of Focused Ion Beam for Failure Analysis
I. Muševič: Mikroskopija na atomsko silo	223	I. Muševič: Atomic Force Microscopy
N. Daneu, A. Rečnik, S. Bernik: Uporaba metod elektronske mikroskopije za študij inverznih meja v varistorski keramiki na osnovi ZnO	228	N. Daneu, A. Rečnik, S. Bernik: The Application of Electron Microscopy methods in the Study of Inversion Boundaries in ZnO-Based Varistors
KONFERENCA MIDEM 2000 – POROČILO	233	MIDEM 2000 CONFERENCE REPORT
ZOISOVA PRIZNANJA		ZOIS PRIZES
MED LETOŠNJIMI PREJEMNIKI ZOISOVIH PRIZNANJ STA DVA ČLANA DRUŠTVA MIDEM	235	THIS YEAR'S ZOIS PRIZES WERE AWARDED TO TWO MIDEM MEMBERS
VESTI	237	NEWS
KOLEDAR PRIREDITEV	244	CALENDAR OF EVENTS
VSEBINA LETNIKA 2000	245	VOLUME 2000 CONTENT
MIDEM prijavnica	249	MIDEM Registration Form

Slika na naslovnici: Letošnja konferenca MIDEM 2000 se je odvijala v hotelu Jama v Postojni. Udeleženci konference so ob priložnosti lahko občudovali lepote Postojnske jame.

Front page: MIDEM 2000 Conference was held in hotel Jama, Postojna. One of the evenings, the participants were able to admire beauties of Postojna caves.